Elettra
Sincrotrone
Trieste

Infrared Spectroscopy and Microscopy

Lisa Vaccari
SISSI beamline manager

Elettra
Sincrotrone
Trieste

Outlines

- Infrared Spectroscopy: Basic Concepts
- FTIR Spectromicroscopy: Instrumentation
- A brief history of IR spectroscopy at SR facilities
- IRSR: Generation and properties
- SR FTIR Microscopy: Selected application for life Sciences
- New trends for IRSR
    - FTIR Imaging and tomography
    - IR nanoscopy: beyond diffraction limit with near-field IR
    - Plasmonic for ultrasensitive SR FTIR microscopy

Elettra
Sincrotrone
Trieste

Infrared Spectroscopy: Basic Concepts

Elettra Sincrotrone Trieste

Electromagnetic Spectrum: a closer view into the IR spectral range

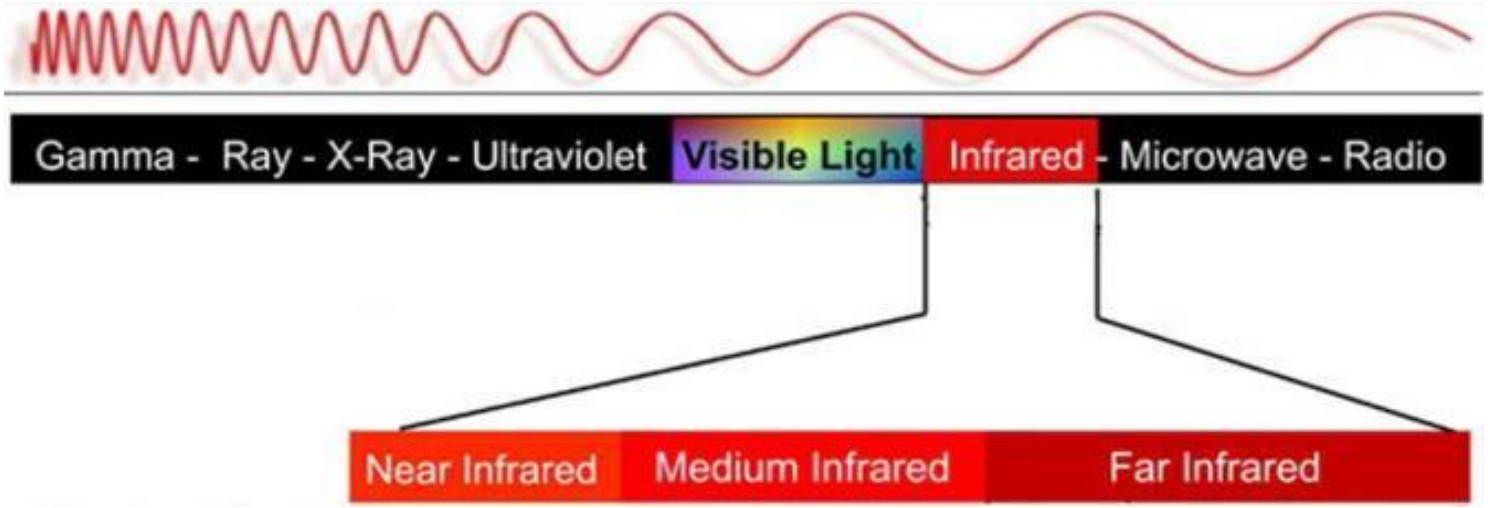

	NIR	MIR		FIR
λ (μm)	0.74	3	30	300
ν (THz)	400	100	10	1
$\overline{\nu}$ (cm^{-1})	~13000	~3333	~333	~33
E (eV)	1.65	0.413	0.041	0.004
E (Kcal/mol)	37	10	1	0.1

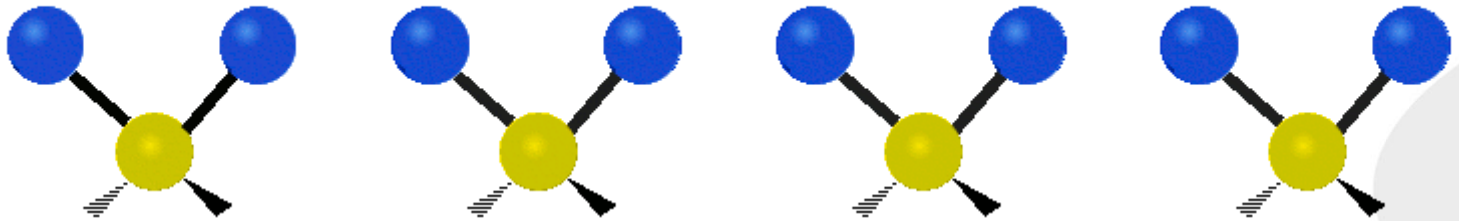

Infrared Spectroscopy: Basic concepts

IR spectroscopy is an absorption spectroscopy that probes molecular vibrations

The classical description of vibrational motion

The Hooke's law

F(restoring force) = $-k \cdot x$, k = *Force constant* $[Nm^{-1}]$

Stronger the bond is, higher the value of k is

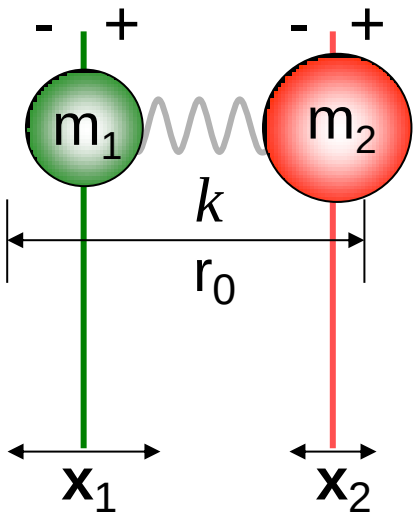

$$\nu = \frac{1}{2\pi}\sqrt{\frac{k}{\mu}}$$

$$\mu = \frac{m_1 m_2}{m_1 + m_2}$$

$$E_{\text{Total Energy}} = \frac{1}{2}kx^2$$

Any vibrational energy value is allowed by the classical solution as well as null vibrational energy

Elettra Sincrotrone Trieste

Infrared Spectroscopy: Basic concepts

The anharmonic oscillator in quantum mechanics

$$E_{vib} = h\nu_e[(n+1/2) - x_o(n+1/2)^2 + higher\ terms]$$

ν_e = harmonic frequency x_0 = anharmonic constant

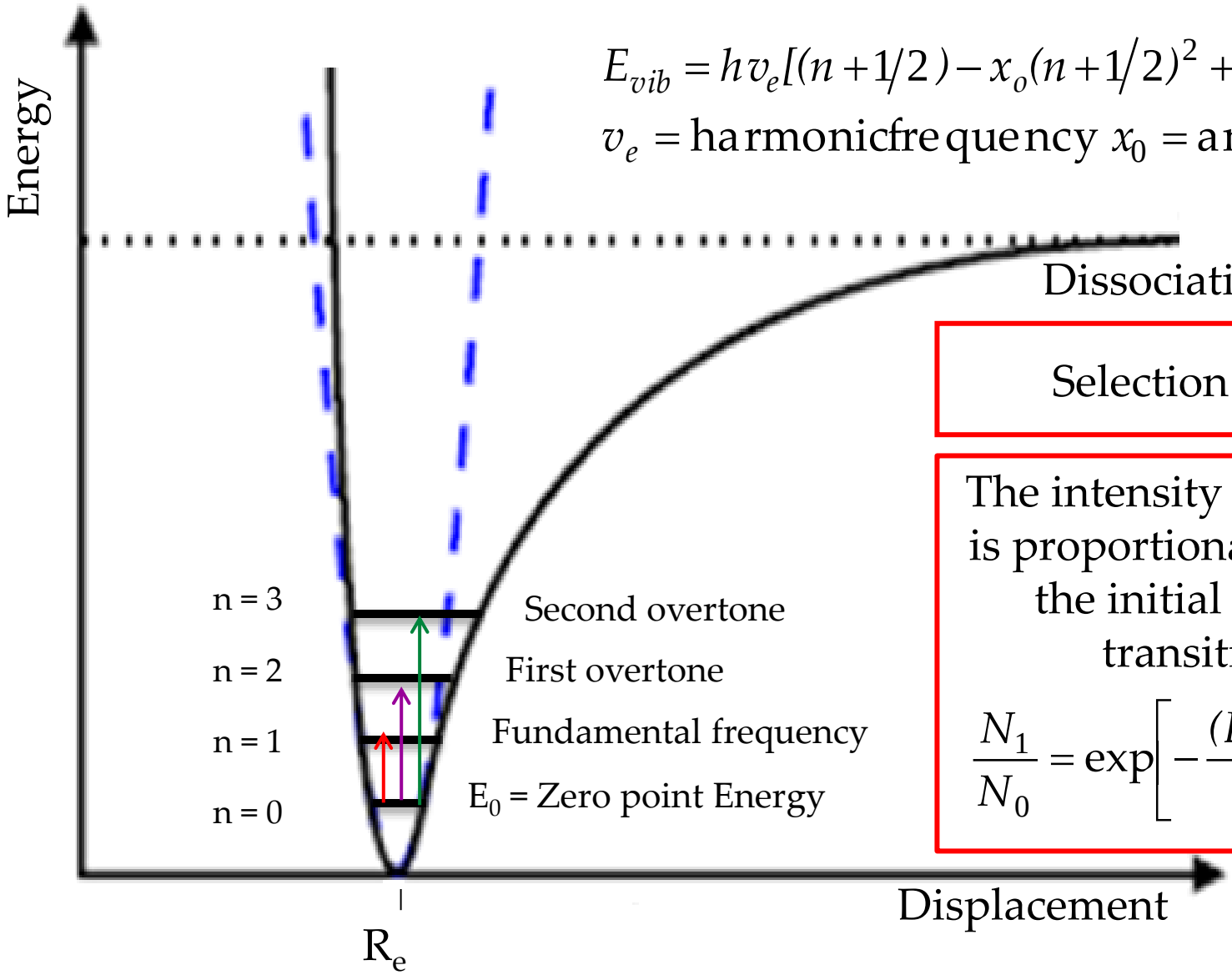

Selection rule $\Delta n = \pm integer$

The intensity of an absorption band is proportional to the population of the initial state from which a transition takes place.

$$\frac{N_1}{N_0} = \exp\left[-\frac{(E_1 - E_0)}{k_B T}\right] = \exp\left(-\frac{\Delta E}{k_B T}\right)$$

Elettra Sincrotrone Trieste

Infrared Spectroscopy: Basic concepts

Allowed and Forbidden vibrational Transitions

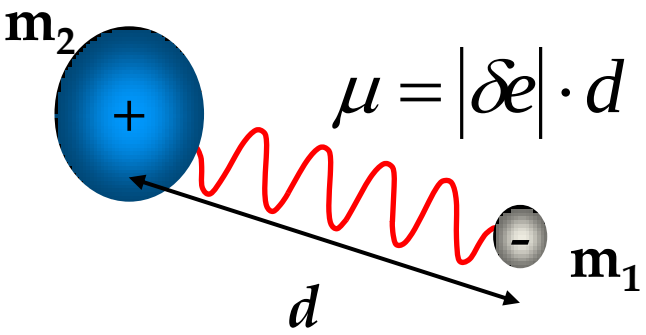

A vibrating molecule is a dipole oscillator that produces a stationary alternating electric field. The electric dipole moment oscillates at its fundamental vibrational frequency, and hence EMR of this frequency can be absorbed and induces vibrational transitions

Vibrations that do not induce variation of the dipole moment of the molecule are forbidden

How many vibrational transitions?

By exploiting molecular symmetries, it can be demonstrated that any vibration of a molecule constituted by N atoms can be described by the suitable combinations of 3N-6 (3N-5 for linear molecules) simple harmonic vibrations, the so called NORMAL MODES of vibration.

Normal modes of vibration are characterized by all the atoms moving in phase (they pass thorough their equilibrium position at the same time), at the same frequency but with different amplitudes.

Elettra
Sincrotrone
Trieste

Infrared Spectroscopy: Basic concepts

Stretching modes (ν)

Symmetric Stretching

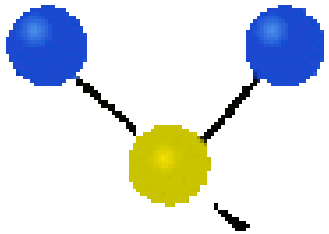

Antisymmetric Stretching

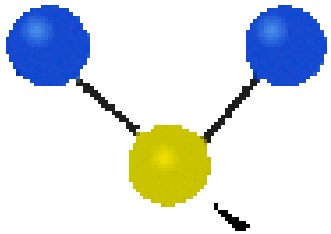

Deformation modes

Scissoring (δ)

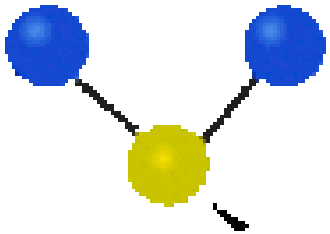

Rocking (r or ϱ)

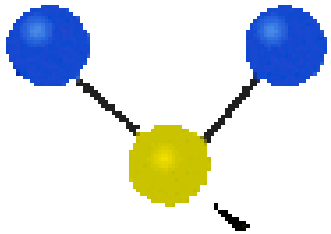

Wagging (ω)

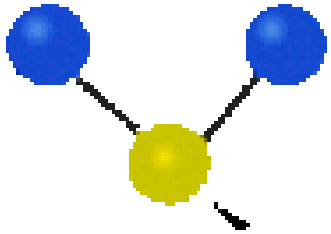

Twisting (τ)

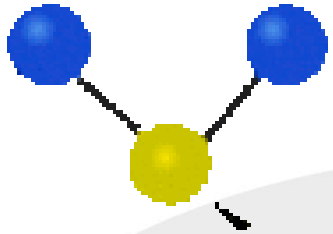

In plane deformations

Out plane deformations

Infrared Spectroscopy: Basic concepts

Elettra Sincrotrone Trieste

An example: Vibrational Spectrum of liquid water

Overtones and combination bands

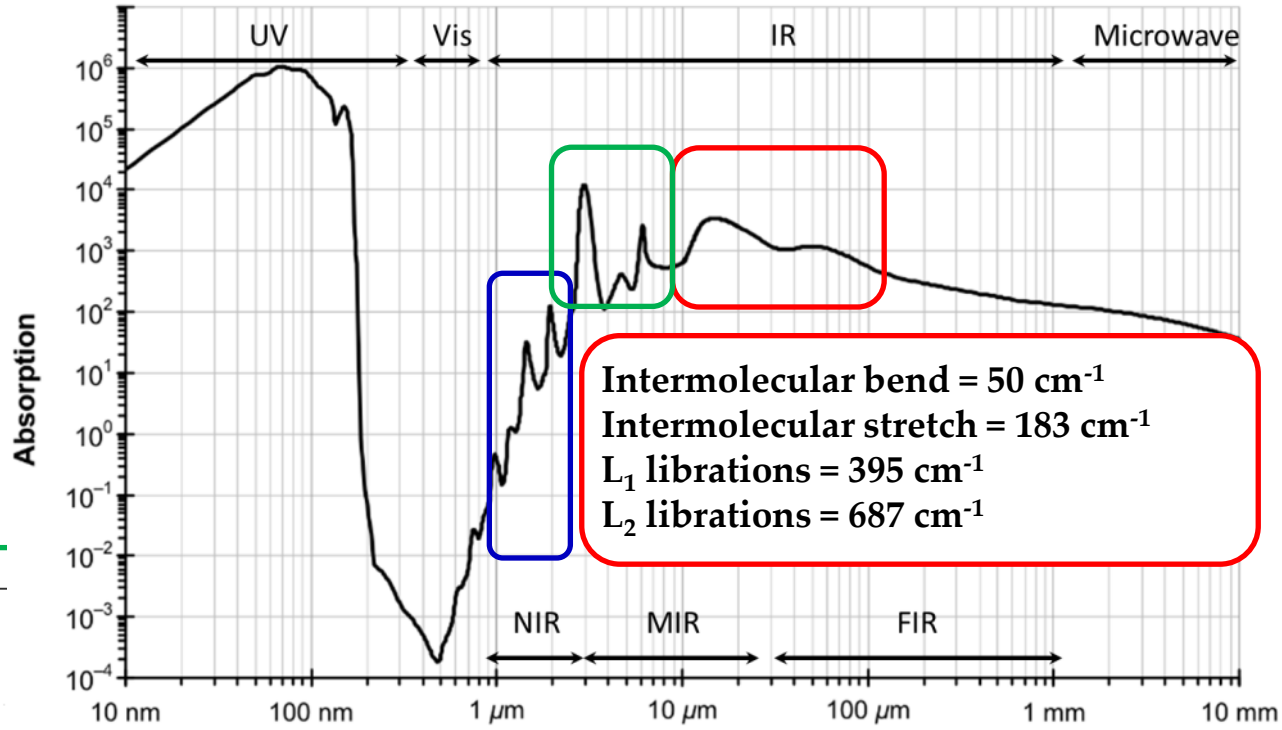

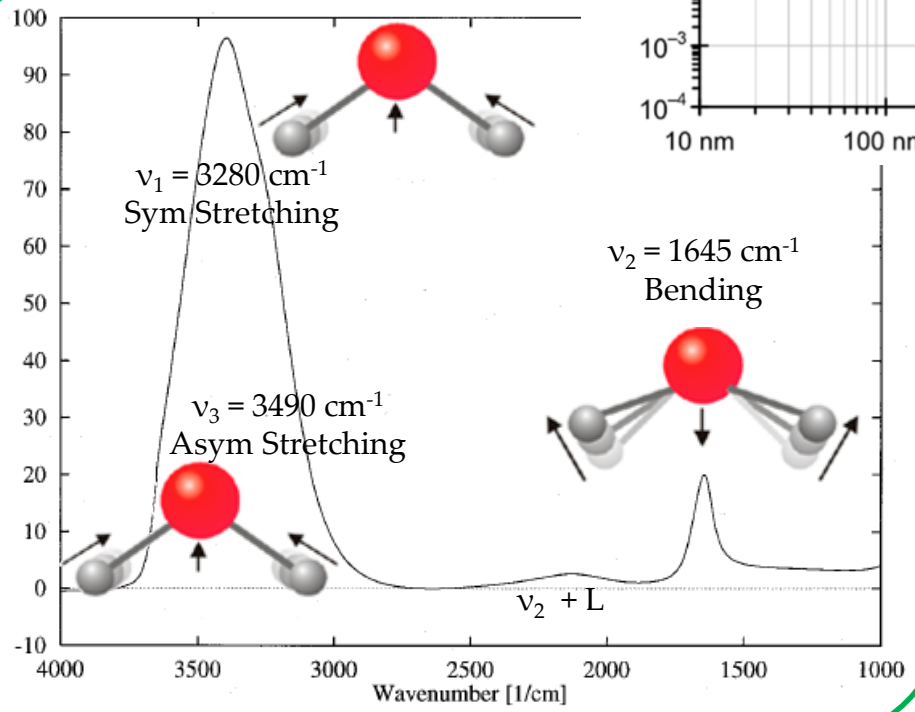

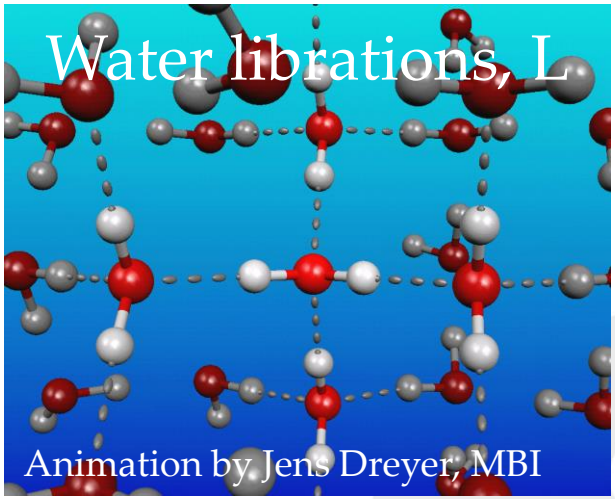

Elettra Sincrotrone Trieste

Infrared Spectroscopy: Basic concepts

FROM PEAK POSITION, INTENSITY AND WIDTH

NATURE OF ATOMS INVOLVED IN THE SPECIFIC VIBRATION
PARAMETERS OF THE ATOMIC BOND : BOND STRENGTH AND LENGHT
BOND CONFORMATION: DOUBLE BOND CIS/TRANS, PROTEINS' CONFORMATION,….
CHEMICAL ENVIRONMENT (THROUGH MODULATION OF THE DIPOLE MOMENT)
ROTATIONAL MODES IN THE FIR REGION

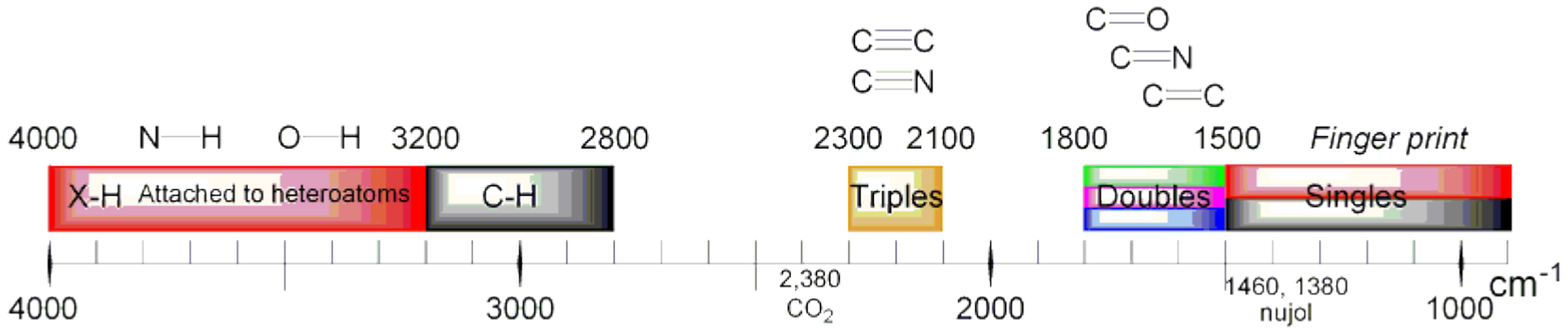

FROM WHOLE SPECTRUM

NATURE OF THE MOLECULE: SPECTRAL FINGERPRINT=> MOLECULAR IDENTIFICATION
SAMPLE INTERACTIONS: FREE/BOUND WATER …
SAMPLE EVOLUTION: REACTION KINETIC, AGING, PHYSICO CHEMICAL TREATMENT,
CONSTRAINTS (PRESSURE, TEMPERATURE, pH) …
ATOMIC BOND ORIENTATION: POLARIZATION MEASURMENT

QUANTITATIVE or SEMI-QUANTITATIVE ANALYSIS

SIMPLE MIXTURES: BEER LAMBERT BOUGUER LAW
COMPLEX MIXTURE : PLS, CLS, ALS, MCR, PCR …

Elettra
Sincrotrone
Trieste

FTIR Spectromicroscopy: Instrumentation

FTIR Spectromicroscopy: Instrumentation

When dealing with molecular species (normal modes of vibration 3N-6), the absorption profile at a single frequency (or limited spectral range) is scarcely useful. Only a multi-frequency profile can account for the system complexity and its interaction with the environment

↓

An FTIR spectrum needs to be energy resolved over a large spectral range

The past instrumentation: Dispersive Interferometers

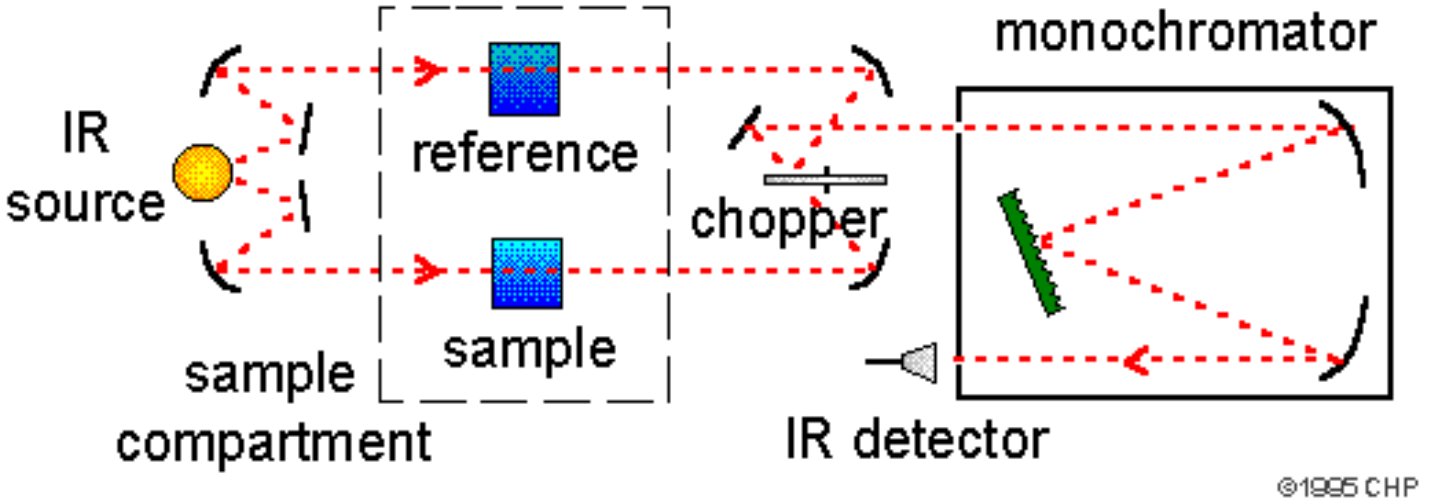

http://www.chemicool.com/definition/fourier_transform_infrared_spectrometer_ftir.htm

This slow acquisition time limited the wide spreading of infrared spectroscopy until 1960s', when Fourier Transform Interferometer have been first proposed.

Elettra Sincrotrone Trieste

FTIR Spectromicroscopy: Instrumentation

The present instrumentation: Fourier Transform InfraRed Interferometers

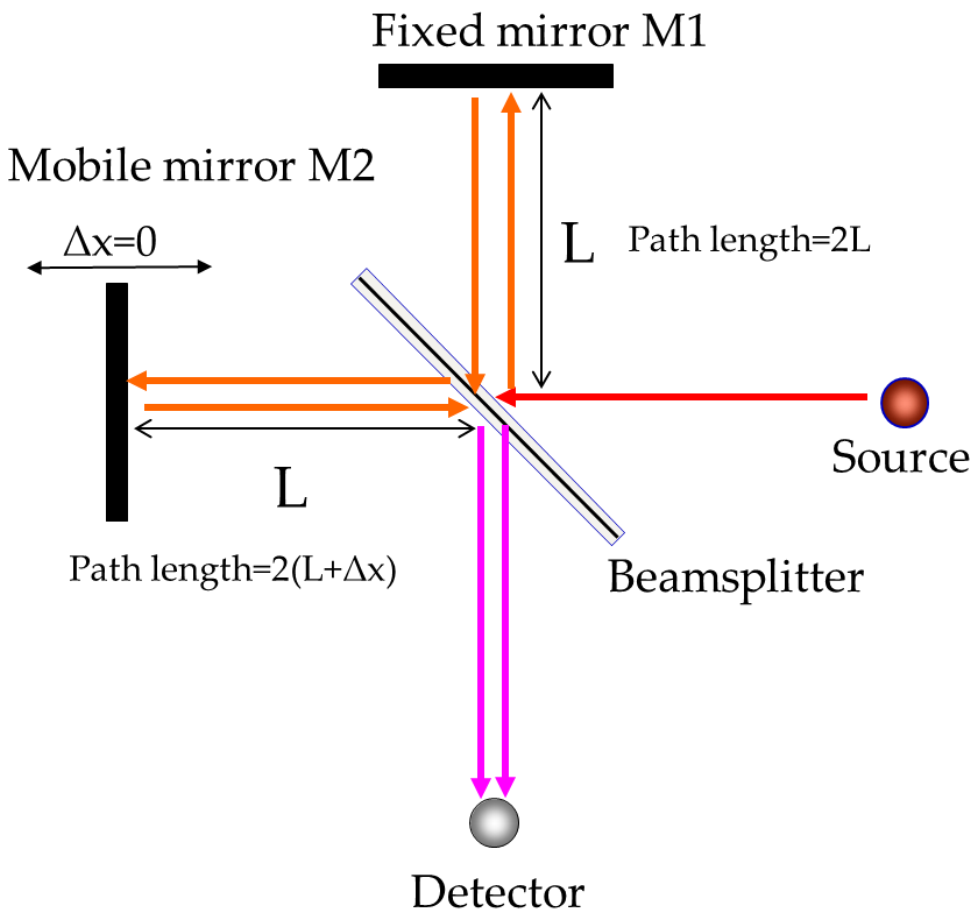

Optical Path Difference _ OPD

$2\Delta x = 2vt$ ***v = mirror velocity***

- Conventional sources
  - NIR: Tungsten lamp
  - MIR: Glow bar (SiC)
  - FIR: Hg-Arc
- Beamsplitters
  - NIR: CaF_2
  - MIR: KBr
  - FIR: Mylar, Silicon
- Detectors
  - NIR – InGaAs, InSb, Ge, Si room temperature detectors
  - MIR: Room temperature DLaTGS Nitrogen cooled MCT
  - FIR – He Cooled Silicon Bolometer Room temperature DLaTGS

Elettra
Sincrotrone
Trieste

FTIR Spectromicroscopy: Instrumentation

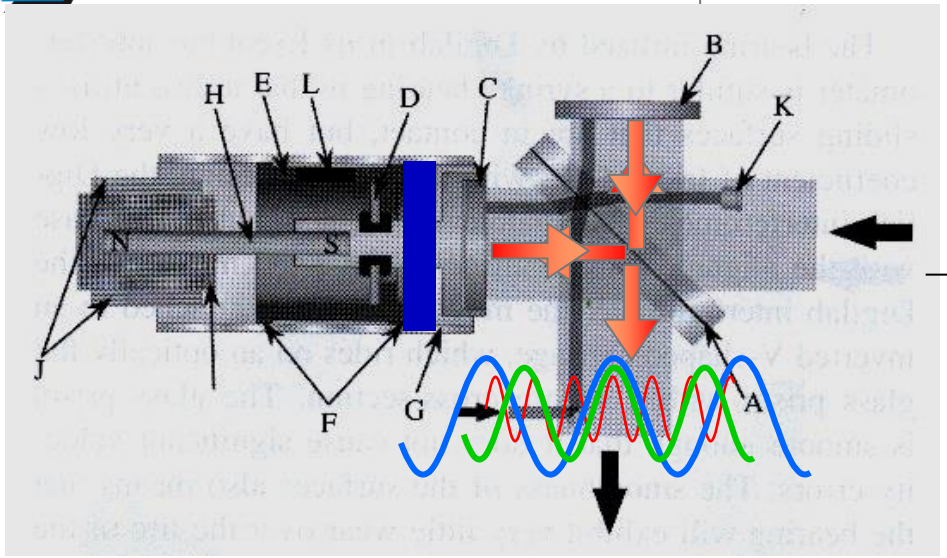

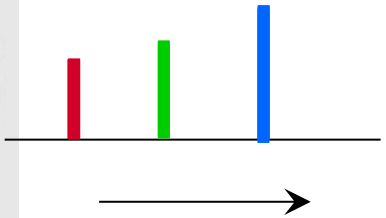

For a single wavelength

$$I(x) = I(\tilde{\nu})[1 + \cos(2\pi x \tilde{\nu})]$$

For a polychromatic source

$$I(x) = \int I(\tilde{\nu}) d\tilde{\nu} + \int I(\tilde{\nu}) \cos(2\pi x \tilde{\nu}) d\tilde{\nu}$$

$$I(ZPD) = 2\int I(\tilde{\nu}) d\tilde{\nu} = I_0$$

$$I(x) = \frac{1}{2} I_0 + \int I(\tilde{\nu}) \cos(2\pi x \tilde{\nu}) d\tilde{\nu}$$

$$I(x) - \frac{1}{2} I_0 = I'(x) = \int I(\tilde{\nu}) \cos(2\pi x \tilde{\nu}) d\tilde{\nu}$$

Fourier Transform (FT) →

$$I(\tilde{\nu}) \propto \int_{-\infty}^{+\infty} I'(x) \cos(2\pi x \tilde{\nu}) dx$$

Elettra
Sincrotrone
Trieste

FTIR Spectromicroscopy: Instrumentation

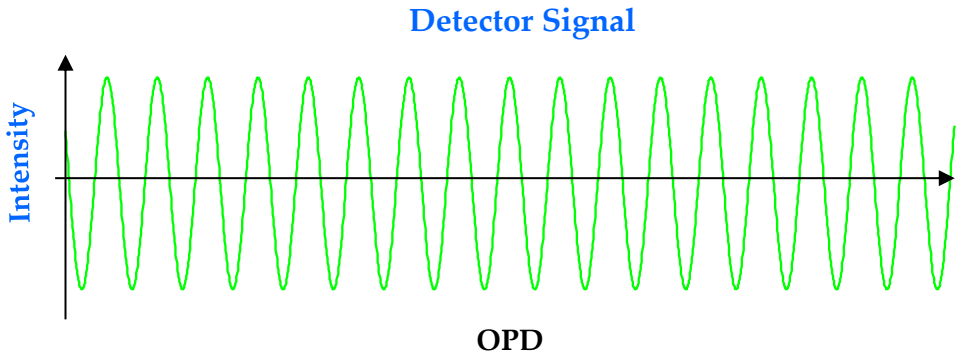

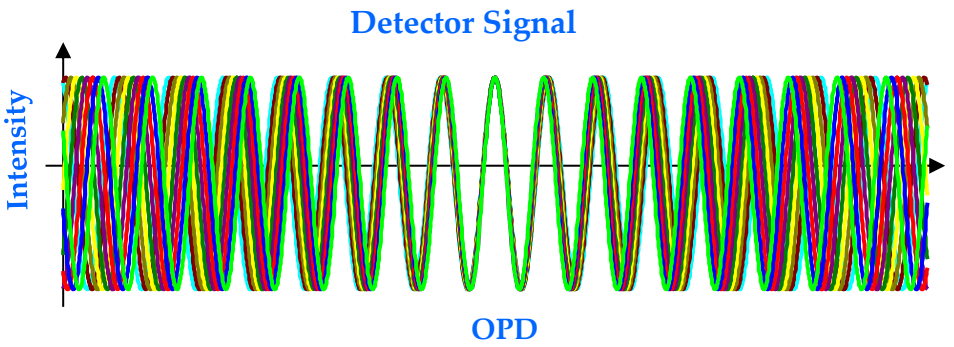

$$\lambda_i = v_0 t_i = \frac{v_0}{f_i}$$

V_0 speed of change of OPD
V_M mirror velocity
f_i frequency
t_i period

$$v_0 \propto v_M$$

V_M has to be KNOWN and CONSTANT
He-Ne laser (632,80 nm)

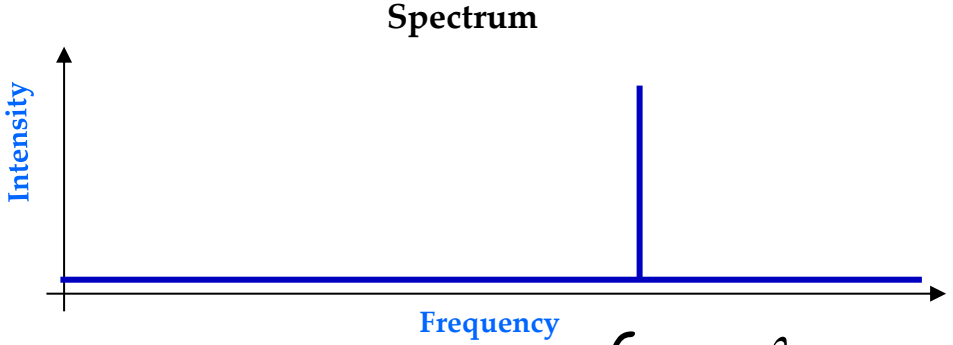

$$f_i = v_0 \lambda_i$$

FT ↓

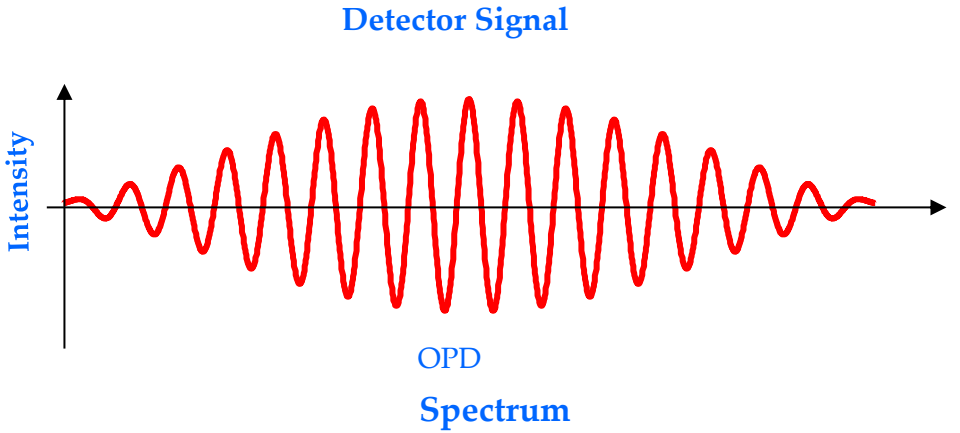

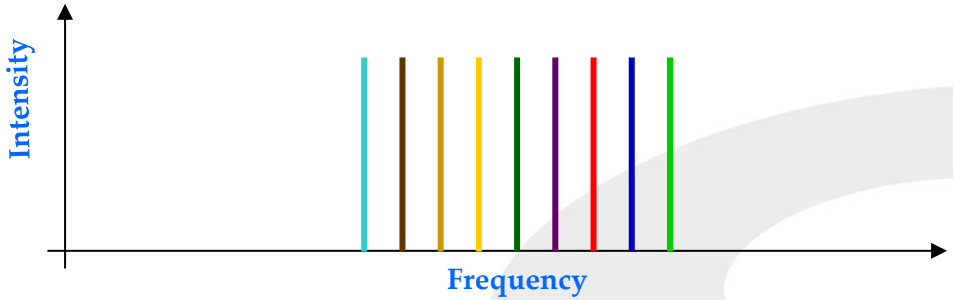

Elettra
Sincrotrone
Trieste

FTIR Spectromicroscopy: Instrumentation

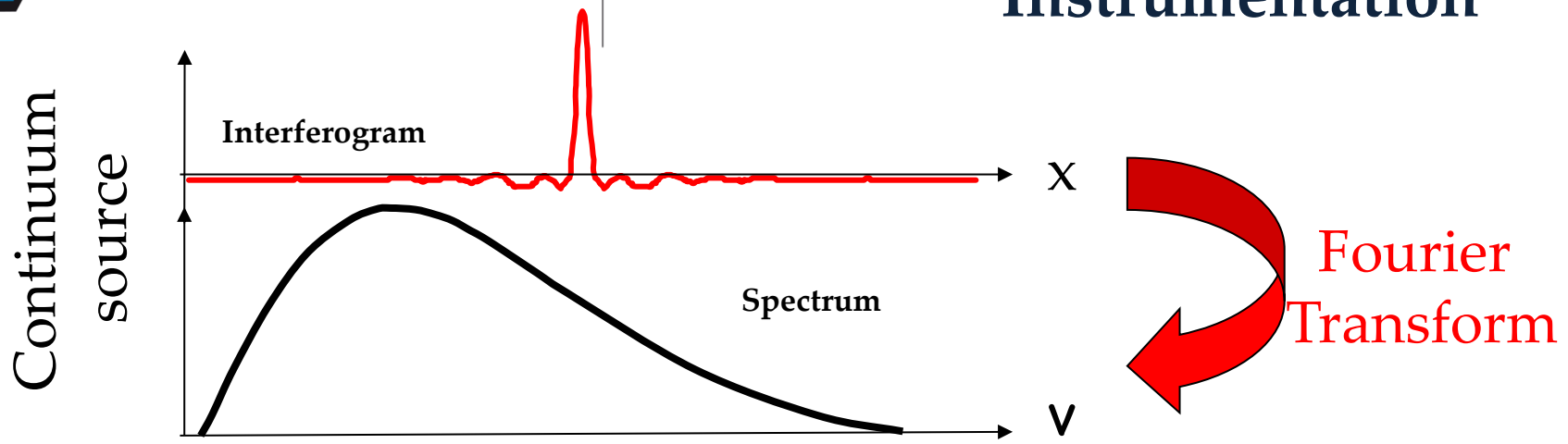

Apodization function

$$I(\tilde{\nu}) \propto \int_{-L\max}^{+L\max} I'(x)\cos(2\pi x\tilde{\nu})dx = \int_{-\infty}^{+\infty} D(x)I'(x)\cos(2\pi x\tilde{\nu})dx$$

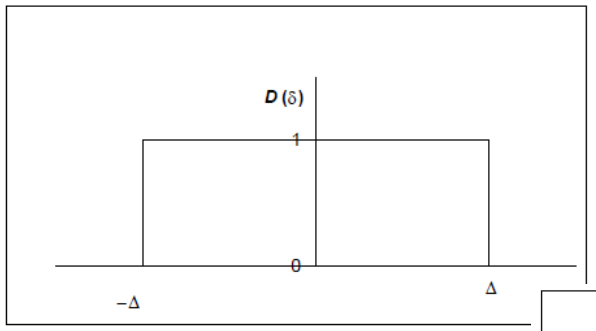

Box-car waveform

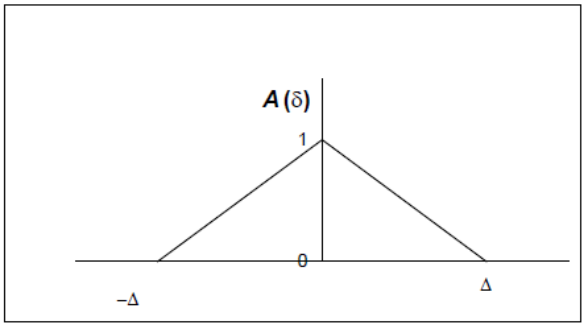

Triangular waveform

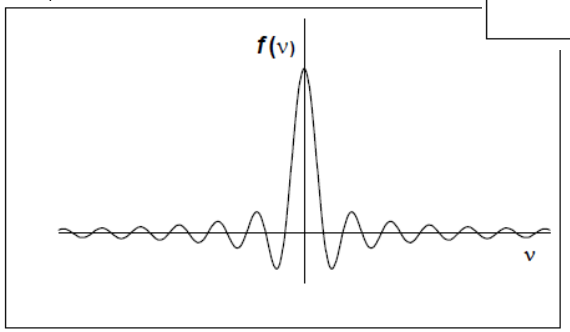

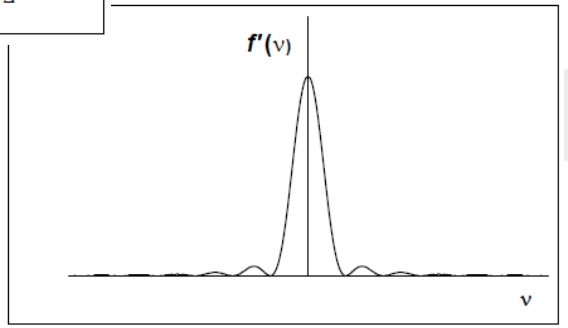

Elettra
Sincrotrone
Trieste

FTIR Spectromicroscopy: Instrumentation

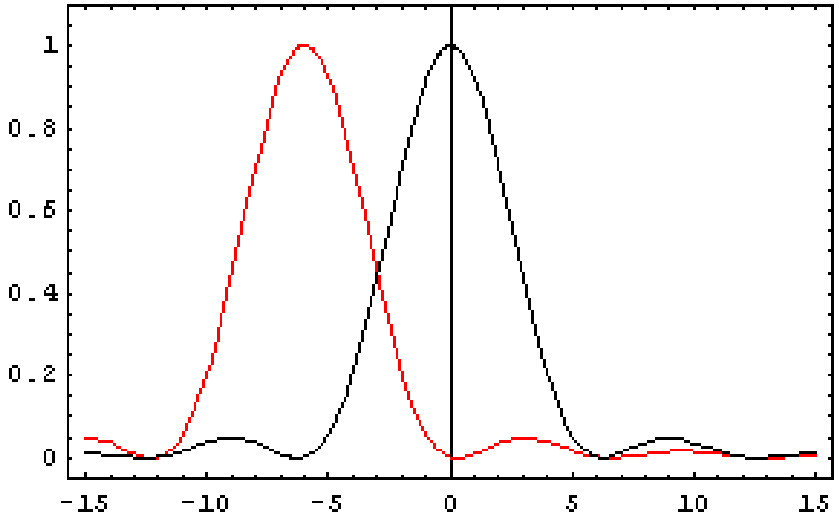

The spectral resolution or resolving power ($\Delta\tilde{\nu}$) of a spectrograph is a measure of its ability to resolve features in the electromagnetic spectrum.

$$\Delta\tilde{\nu}_{\max} \propto \frac{1}{(OPD)_{\max}}$$

Elettra
Sincrotrone
Trieste

FTIR Spectromicroscopy: Instrumentation

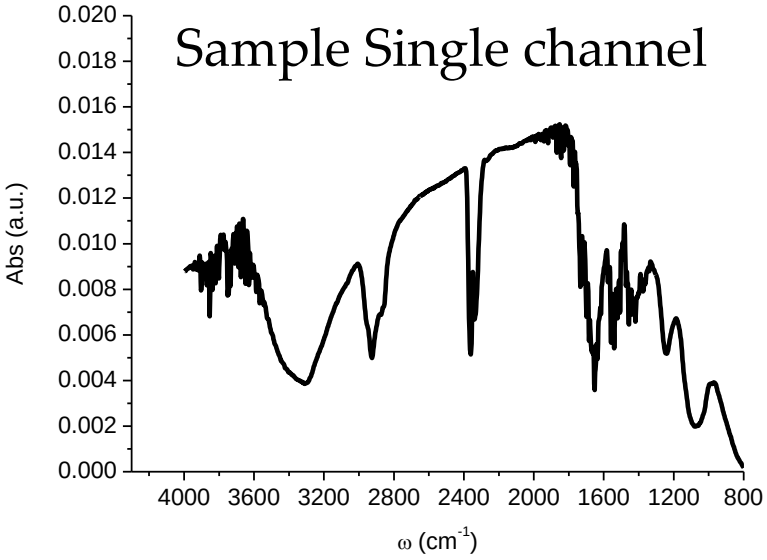

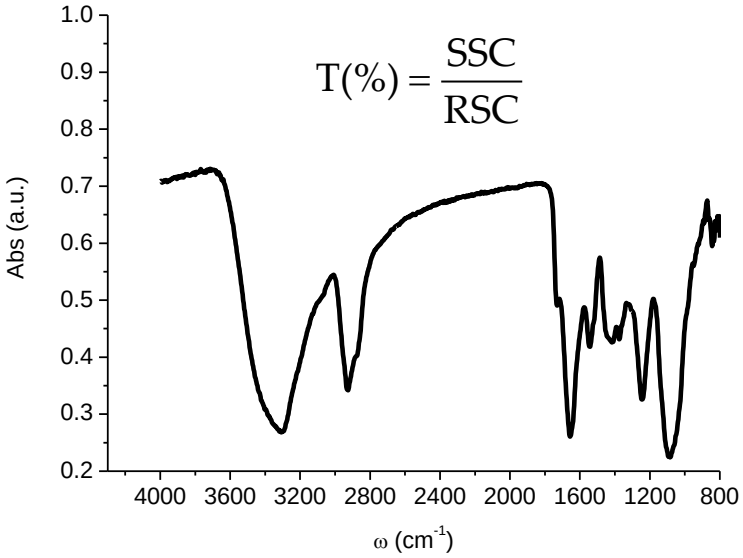

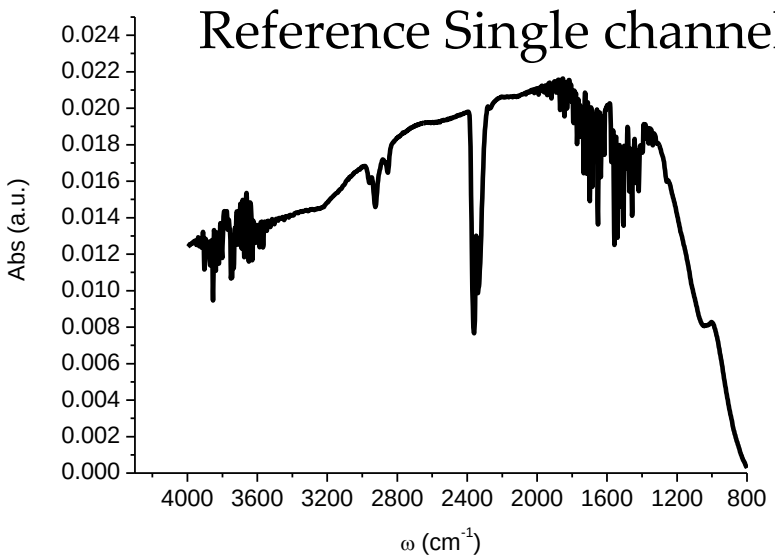

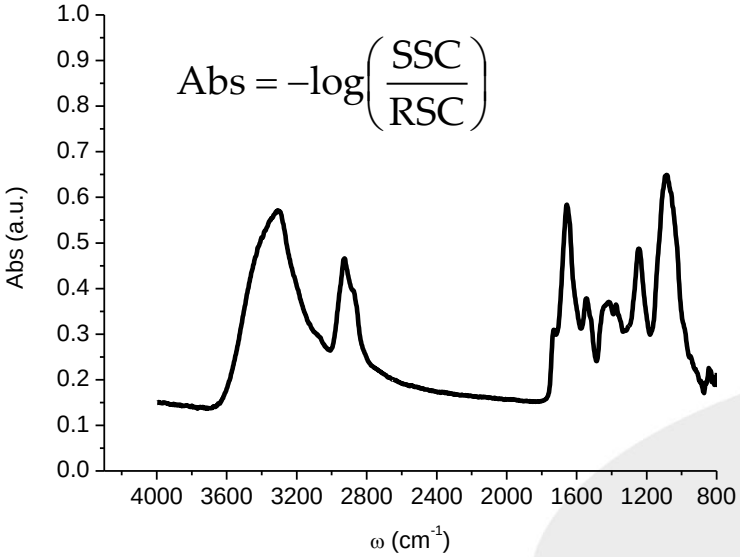

Elettra
Sincrotrone
Trieste

FTIR Spectromicroscopy: Instrumentation

Spatially resolved chemical information on heterogeneous samples are obtained by coupling FTIR spectrometers with specially designed Vis-IR microscopes

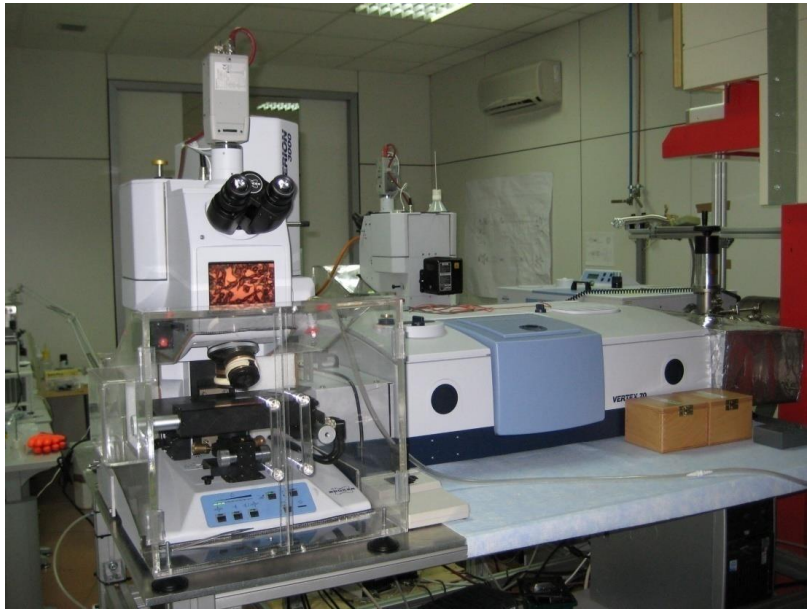

Schwarzschild objective

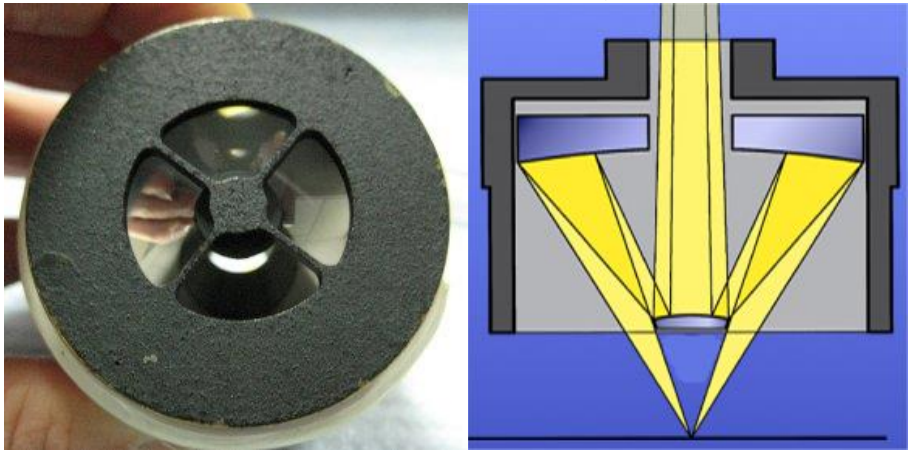

$$NA = n \cdot \sin 2\theta$$

2θ = angular aperture

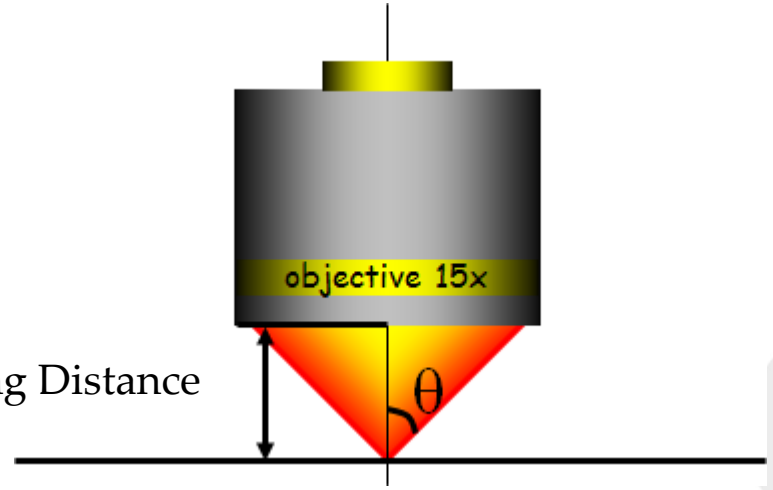

Elettra Sincrotrone Trieste

FTIR Spectromicroscopy: Instrumentation

In far-filed microscopies, and FTIR microscopy as well, lateral resolution, δ, is diffraction limited

$$\delta \approx 0.66 \frac{\lambda}{nNA}$$

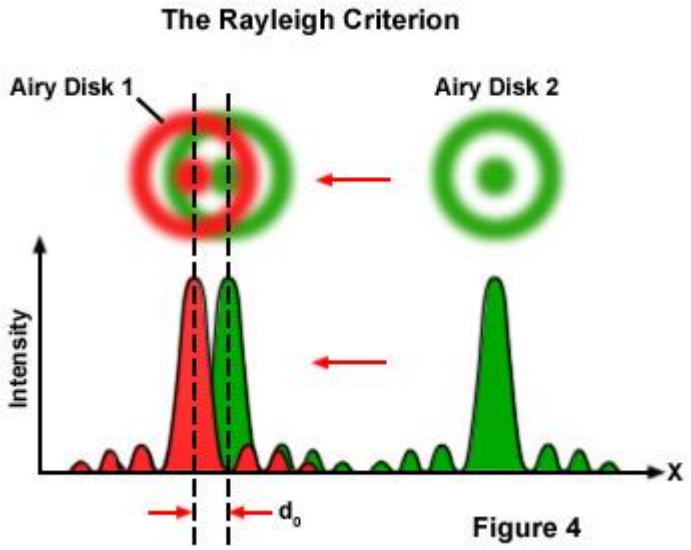

Figure 4

Objective NA	Wavelength	δ
0.4	10 μm (1000cm^{-1})	~15 μm
	2.5 μm (4000cm^{-1})	~ 4 μm
0.65	10 μm (1000cm^{-1})	~ 9.5 μm
	2.5 μm (4000cm^{-1})	~ 2.5 μm

$$\delta \approx \lambda$$

Elettra
Sincrotrone
Trieste

A brief history of IR spectroscopy at SR facilities

Elettra
Sincrotrone
Trieste

Once upon a time…..

Volume I. *July–August, 1893.* *Number 1.*

THE

PHYSICAL REVIEW.

A STUDY OF THE TRANSMISSION SPECTRA OF CERTAIN SUBSTANCES IN THE INFRA-RED.

By Ernest F. Nichols.

WITHIN a few years the study of obscure radiation has been greatly advanced by systematic inquiry into the laws of dispersion of the infra-red rays by Langley,[1] Rubens,[2] Rubens and Snow,[3] and others. Along with this advancement has come the more extended study of absorption in this region. The absorption of atmospheric gases has been studied by Langley[1] and by Ångstrom.[4] Ångstrom[5] has made a study of the absorption of certain vapors in relation to the absorption of the same substances in the liquid state, and the absorption of a number of liquids and solids has been investigated by Rubens.[6]

In the present investigation, the object of which was to extend this line of research, the substances studied were: plate glass, hard rubber, quartz, lamp-black, cobalt glass, alcohol, chlorophyll, water, oxyhæmoglobin, potassium alum, ammonium alum, and ammonium-iron alum.

[1] Report on Mt. Whitney Expedition, Profess. Papers, U. S. Signal Service, XV.
[2] Annalen der Physik und Chemie, N. F. XLV., p. 238.
[3] Annalen der Physik und Chemie, N. F. XLVI., p. 529.
[4] Bihang till K. Svenska Vet.-Akad. Handlingar, Band 15, Afd. 1, No. 9.
[5] Ofversigt af Kongl. Vetenskaps-Academiens Forhandlingar, 1890, No. 7, Stockholm.
[6] Annalen der Physik und Chemie, N. F. XLV., p. 258.

Elettra
Sincrotrone
Trieste

IR beamlines

The Cinderella Story

1976 Meyer and Lagarde (LURE, Orsay) published the first paper on IRSR

1981 Duncan and Yarwood observed at Daresbury the first IRSR emission

1985 The first IRSR spectrum (on N_2O) is collected at Bessy (Berlin)

1986 The first beamline was opened to users at UVSOR (Japan)

1987 Started the brilliant story of IR-beamlines at NSLS Brookhaven (USA)

1992 In Europe: Orsay (France), Lund (Sweden), Daresbury (GB)

1995 First international workshop on IRSR, Rome (Italy)

2001 First IR beamline in Italy (SINBAD@DAΦNE)

2006 Second beamline in Italy (SISSI@Elettra)

Opening of the IR1 beamline at LNLS (Brazil)

New IR beamlines are under construction

Elettra
Sincrotrone
Trieste

SR-IR beamlines

More than 40 IRSR beamlines worldwide

Elettra
Sincrotrone
Trieste

IRSR: Generation and properties

Elettra
Sincrotrone
Trieste

IRSR Generation

Bending Magnet IRSR

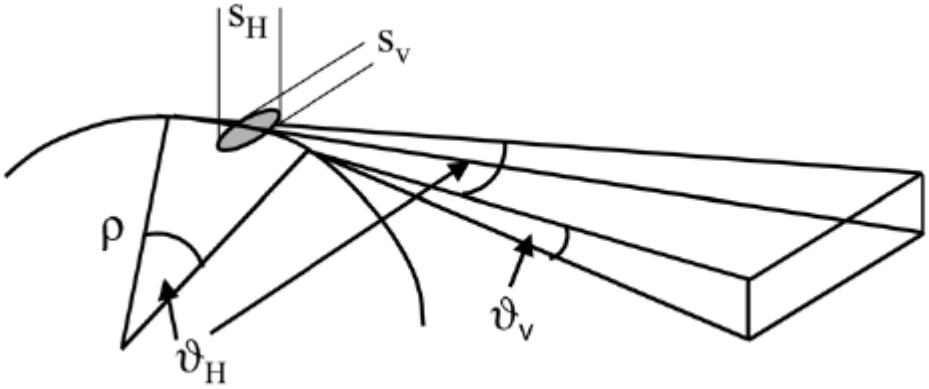

Extrapolation of the Schwinger equations (1949) by WD Ducan and GP William (1980s)

Infrared synchrotron radiation from electron storage rings; Appl Opt. 1983 22(18):2914.

$$P_{BM}(\lambda) = 4.38\times10^{14}\times I\times\theta_H\times bw\times\left(\frac{\rho}{\lambda}\right)^{1/3} \quad \text{photons}\cdot\text{s}^{-1} \quad [1]$$

$I =$ Current(A)

$\theta_H =$ HorizontalCollectionAngle (rads)

$bw =$ Bandwidth(%)

$\rho, \lambda =$ Radiusof the ring, Wavelength(sameunits)

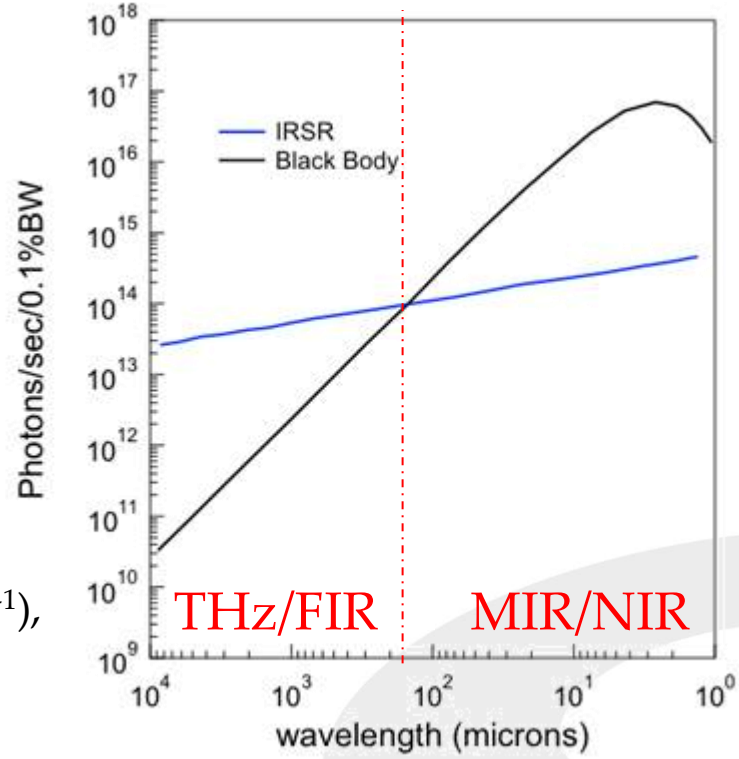

P(λ) as obtained in [1], in the spectral range 1 to 10^4 μm (10^4 to 1 cm^{-1}), for a current of **1 A**, a horizontal angle θ_H **= 100 mrads** and ρ **= 5 m**. Comparison with the emission for a BB source at 2000K.

IRSR Generation

Bending Magnet IRSR

Constant Field Emission

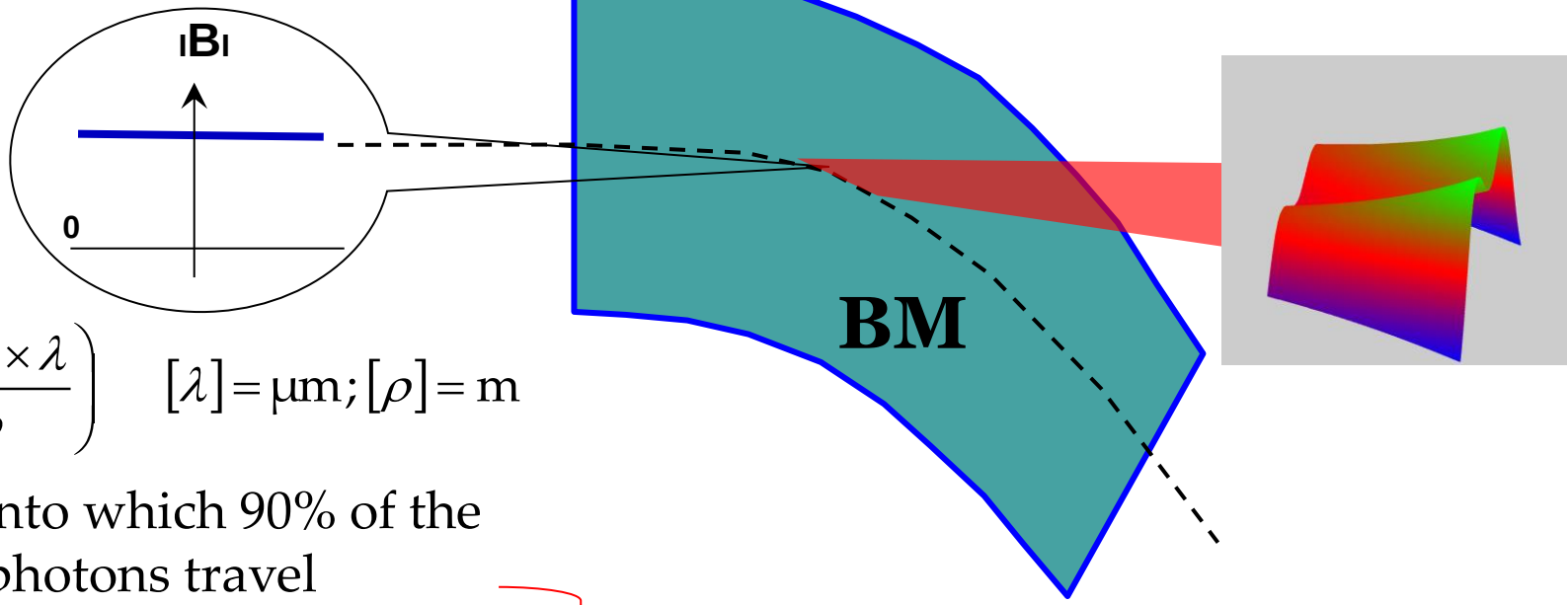

$$\theta_{V-Nat} = 1.66\left(\frac{1000\times\lambda}{\rho}\right) \qquad [\lambda]=\mu m;[\rho]=m$$

Angular range into which 90% of the emitted photons travel

λ [μm]	υ [cm^{-1}]	THz	$\theta_{V\text{-}Nat}$
1	10000	300	9.2
10	1000	30	19.8
100	100	3	42.2
1000	10	0.3	90.3

Calculated for Elettra ρ = 5.5 m.

Very large extraction apertures are needed for IR beamlines for:

- Maximizing the flux (θ_H)
- Allowing efficient extraction of lower energy components of IR synchrotron emission (θv)

Elettra
Sincrotrone
Trieste

IRSR Generation

Bending Magnet IRSR

Vertical opening angle depends on the electron energy (through bending magnet radius)

INDUS
0.45 GeV
45 mrad H X 30 mrad V
BM

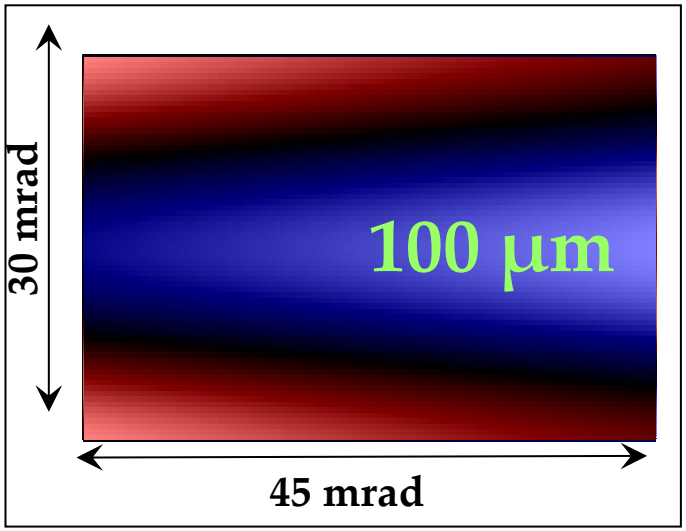

DIAMOND
3.0 GeV
45 mrad H X 30 mrad V
BM

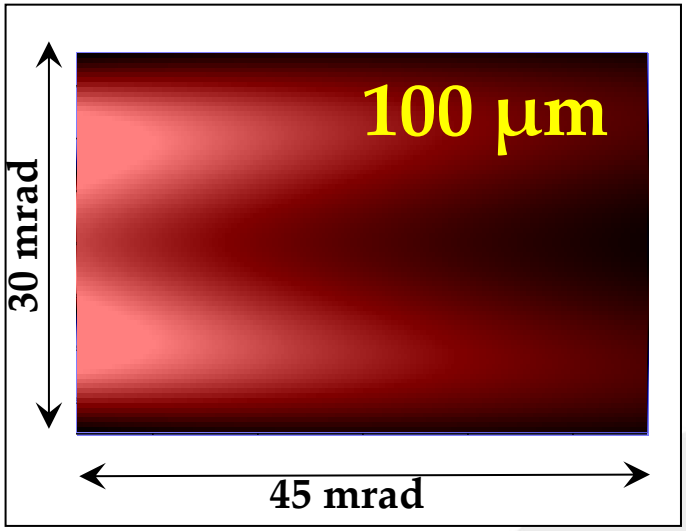

By courtesy of Paul Dumas, SOLEIL

Elettra Sincrotrone Trieste

IRSR Generation

Edge Radiation

Edge radiation is produced when electrons experience a changing magnetic field (entering or exit a BM, where B is constant).

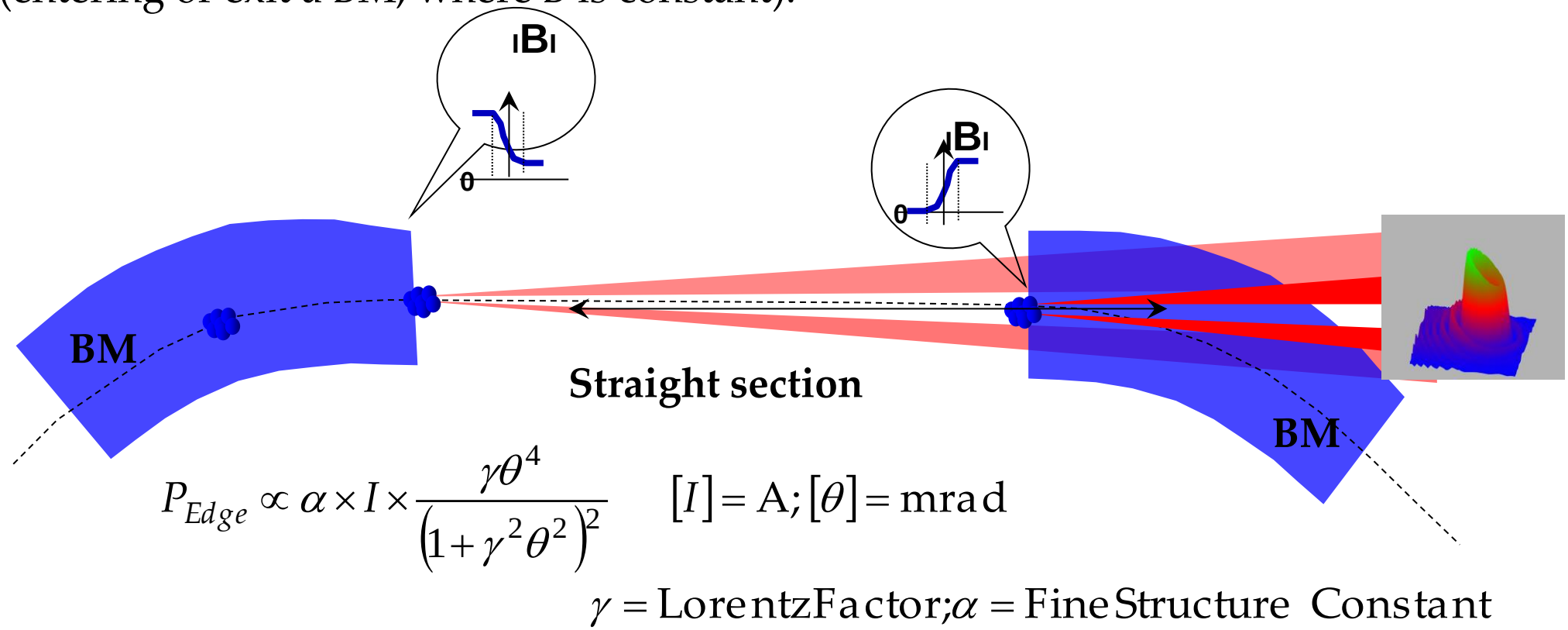

$$P_{Edge} \propto \alpha \times I \times \frac{\gamma\theta^4}{\left(1+\gamma^2\theta^2\right)^2} \qquad [I]=\mathrm{A};[\theta]=\mathrm{mrad}$$

$$\gamma = \mathrm{LorentzFactor};\alpha = \mathrm{FineStructure\ Constant}$$

- Edge radiation has a ring structure characterized by interference pattern
- Being $\Theta_{max} \sim 1/\gamma \sim 10$ mrads, it is spatially confined and intrisically bright
- It is radially polarized

By courtesy of Paul Dumas, SOLEIL

Elettra
Sincrotrone
Trieste

IRSR Generation

Edge Radiation

SOLEIL
2.75 GeV
45 mrad H X 30 mrad V
BM

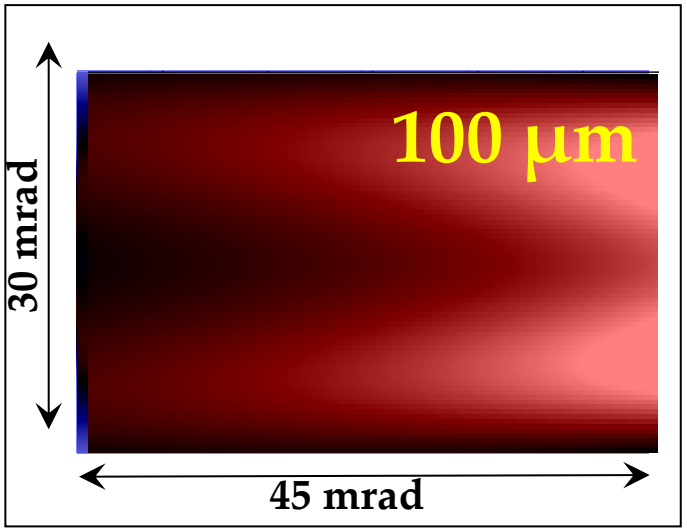

SOLEIL
2.75 GeV
30 mrad H X 30 mrad V
BM

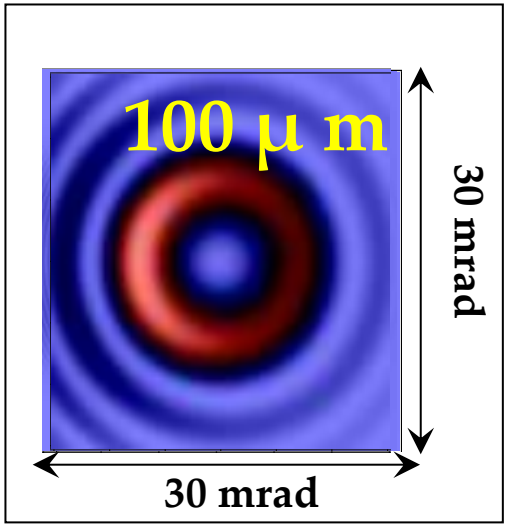

By courtesy of Paul Dumas, SOLEIL

Elettra Sincrotrone Trieste

IRSR

The brightness advantage

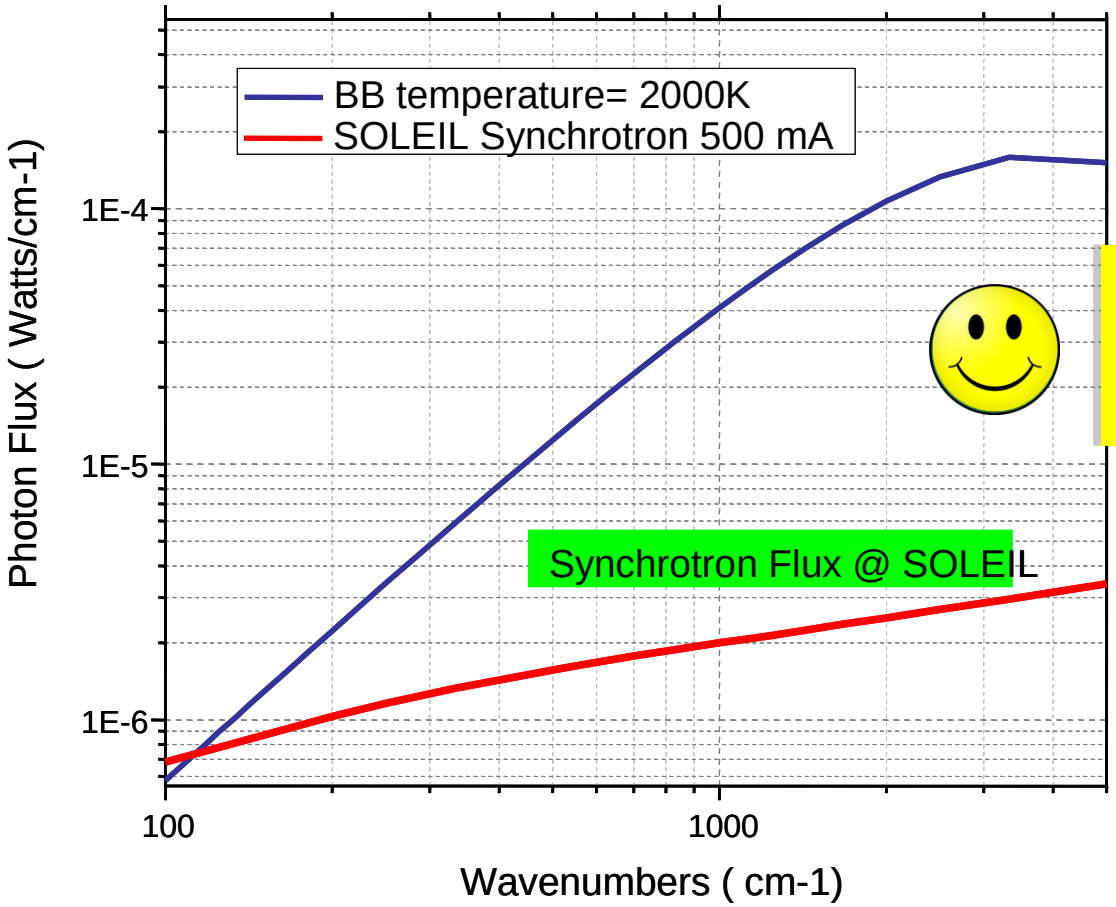

Synchrotron IR is much brighter !

$$B(\lambda) \approx \frac{3.8\times10^{20}\times bw\times I}{\lambda^2} \qquad [\lambda]=\mu\text{m};[I]=\text{A};[bw]=\%$$

By courtesy of Paul Dumas, SOLEIL

Elettra Sincrotrone Trieste

IRSR

The brightness advantage

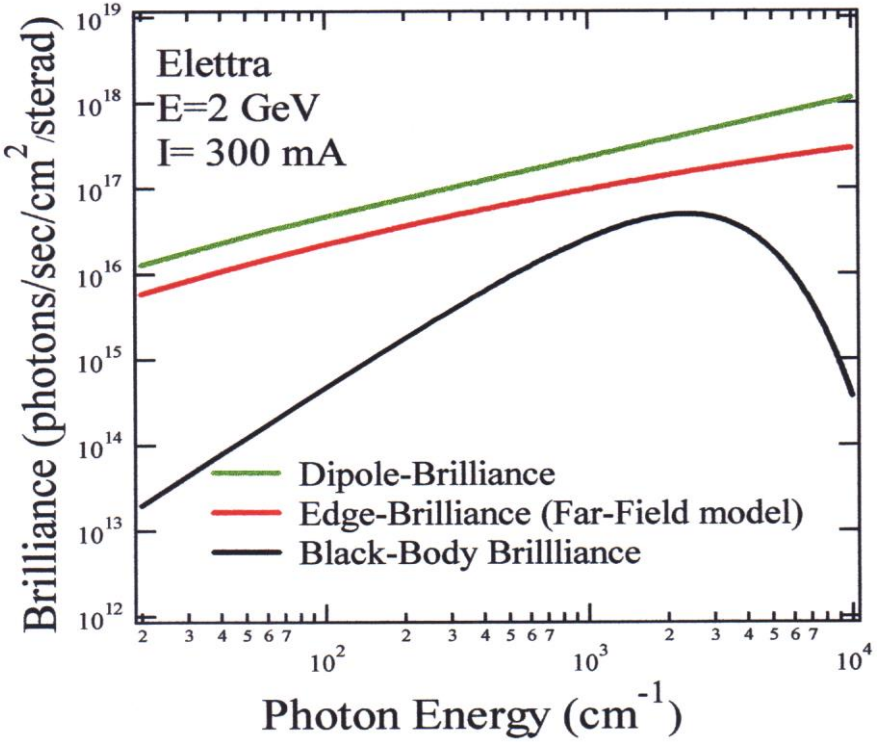

It is the brightness, *B*, that determines the signal to noise ratio, S/N, in a infrared experiment via the formula

$$\%N(Noise\%) = \frac{100A^{1/2}}{B(\nu)\Delta\nu\varepsilon t^{1/2}\xi D^*}$$

→ Particularly useful for microscopy and spectroscopy of small sample/diluted systems

Elettra Sincrotrone Trieste

Exploitation of IRSR advantages

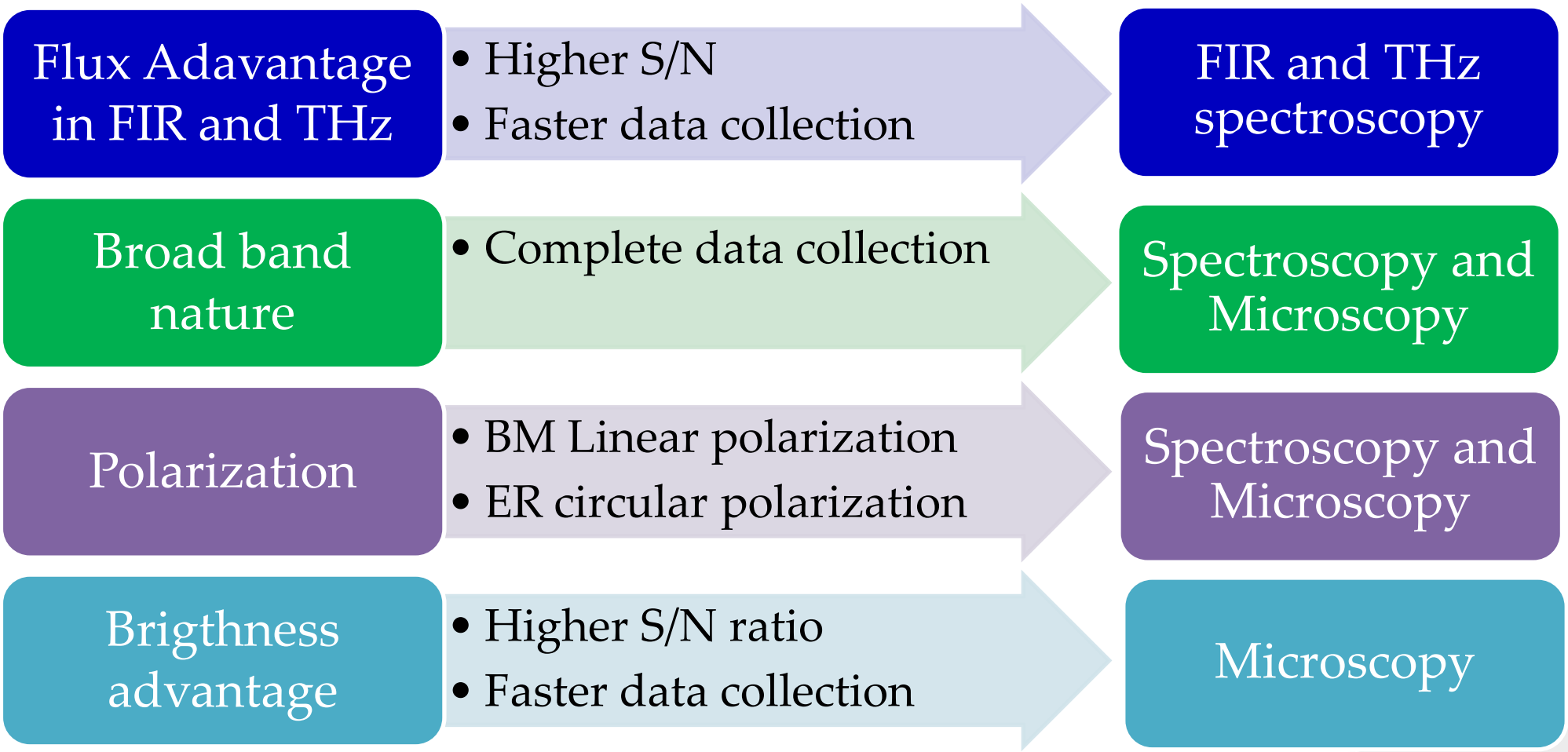

Elettra
Sincrotrone
Trieste

IR beamlines: A special design

SISSI beamline layout
Synchrotron Infrared Source for Spectroscopy and Imaging

Radiation is collected over a large solid 65 mrad (H) x 25 mrad (V)

M1 Plane mirror
M2 Ellipsoidal mirror
M3 Plane mirror
M4 Ellipsoidal mirror

a=3.5 m	**d=1.5m**
b=1.0m	**e=1.0m**
c=11.5m	**f=2.5m**

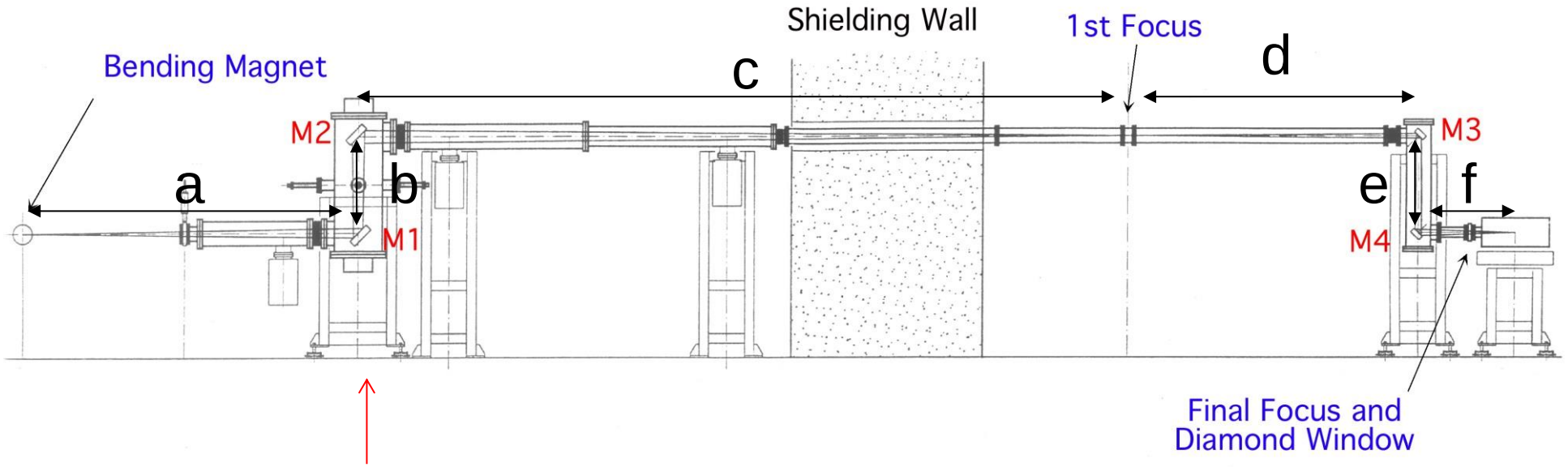

First Chamber in the Ring Tunnel

Elettra
Sincrotrone
Trieste

IR beamlines: A special design

The air-cooled
extraction mirror (M1)

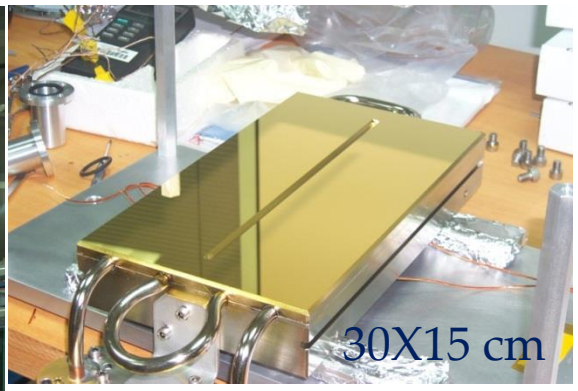

The focusing
Ellipsoidal mirror (M2)

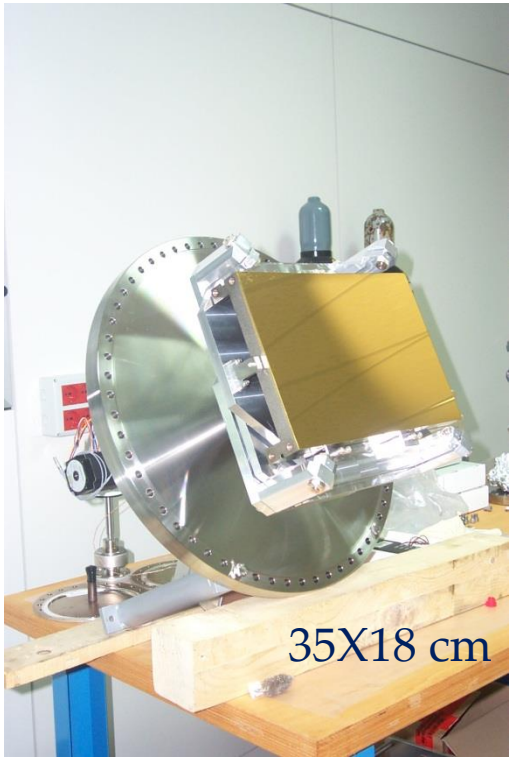

IRSR intensity distribution at the
extraction mirror

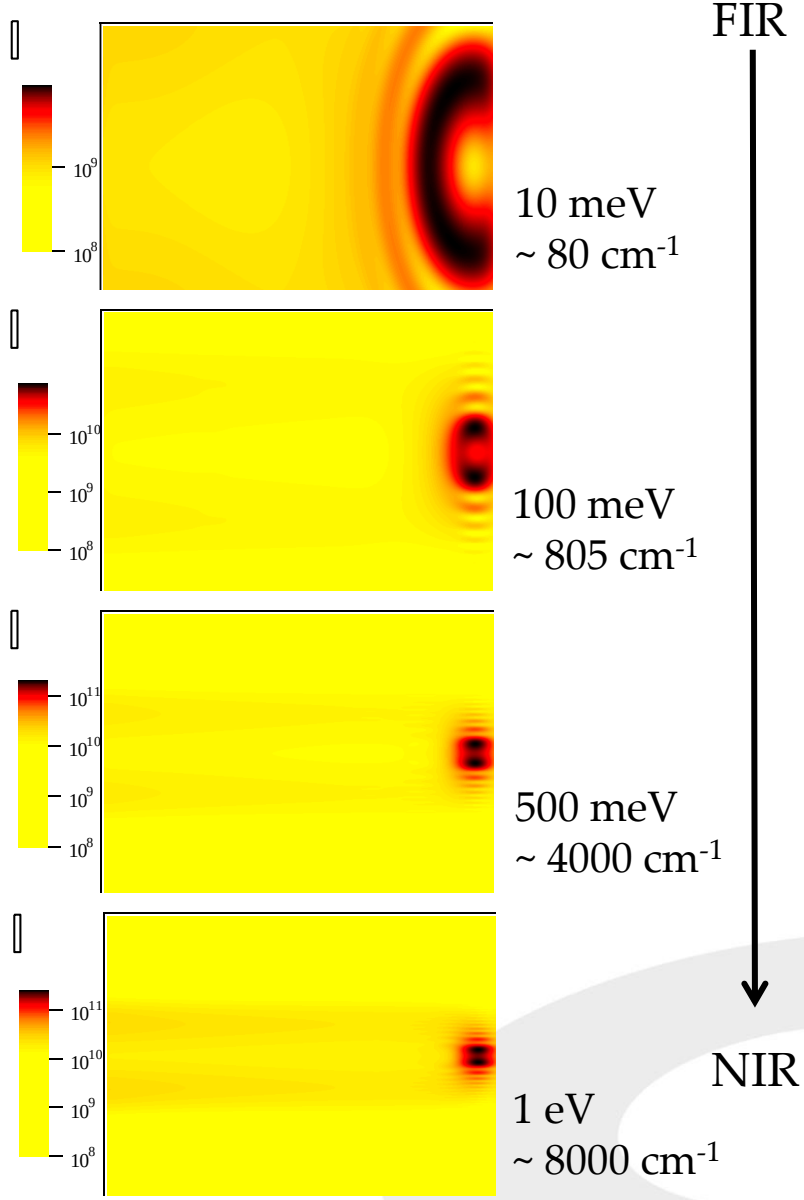

Elettra
Sincrotrone
Trieste

IR beamlines: A special design

@ Australian Synchrotron

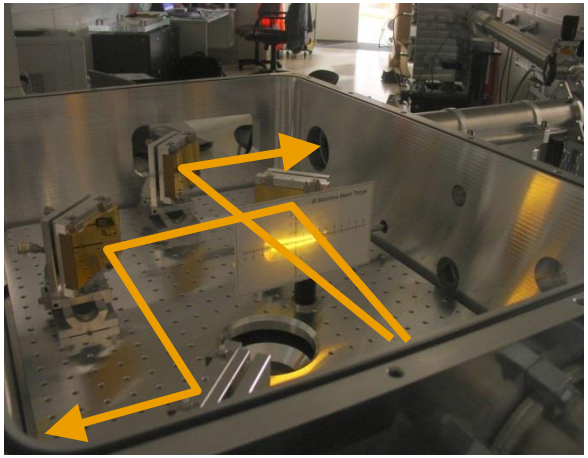

Edge radiation to "high resolution" spectrometer

Bending magnet radiation to "microscope"

@ Soleil

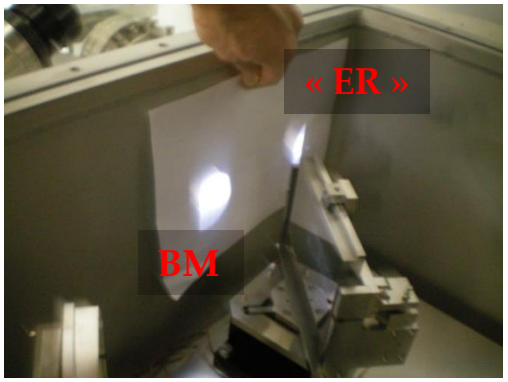

Microscope 2
Branche ER

Microscope 1
Branche BM

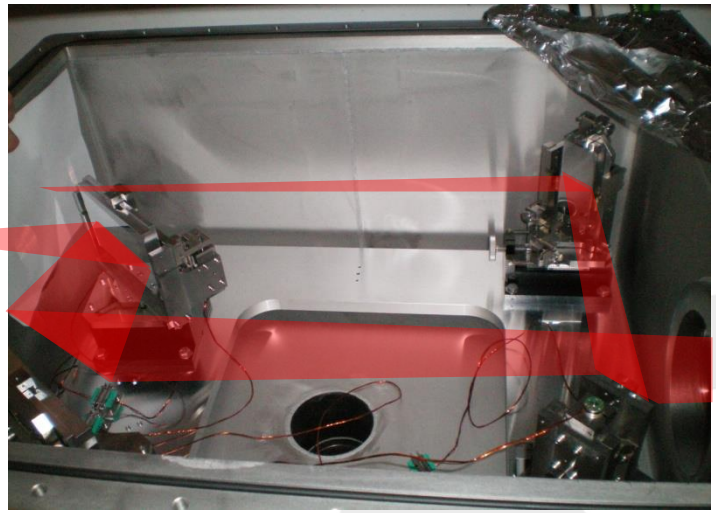

Elettra
Sincrotrone
Trieste

Performance of SISSI beamline

Conventional Source

Diffraction Limited FTIR Microscopy is practically achievable only with IRSR

IRSR

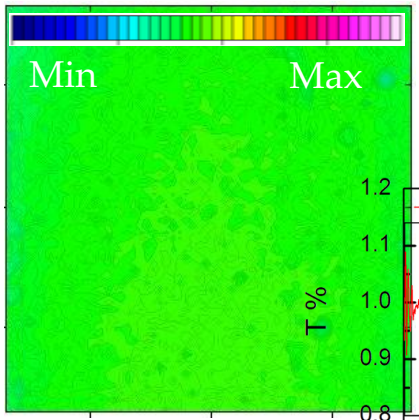

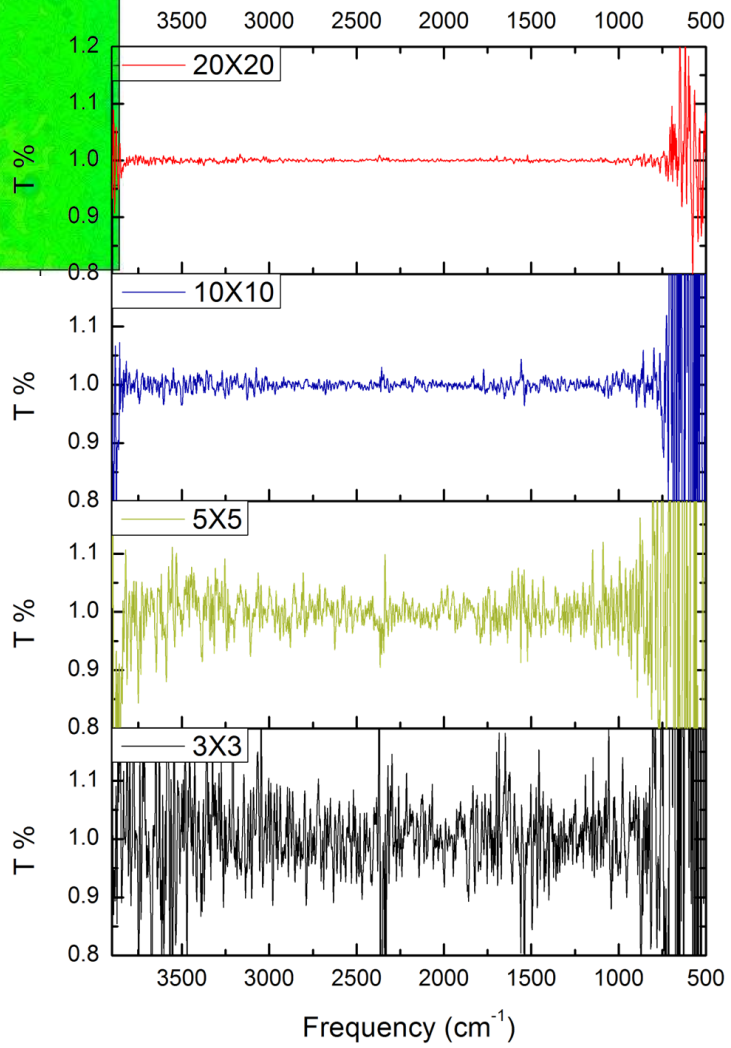

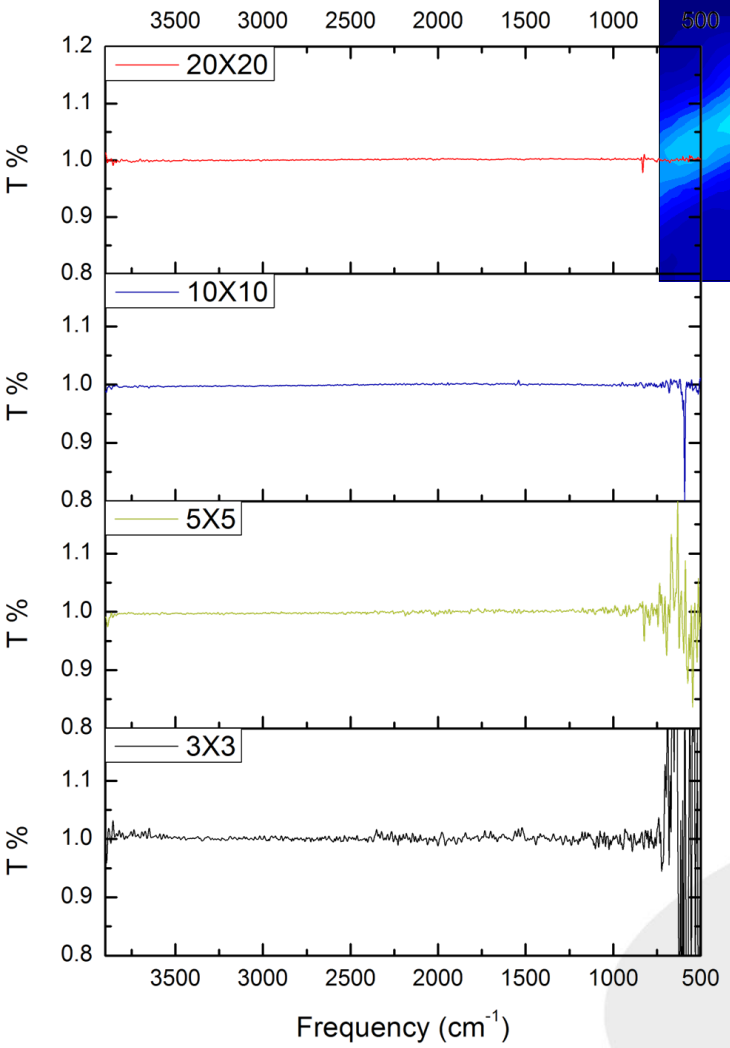

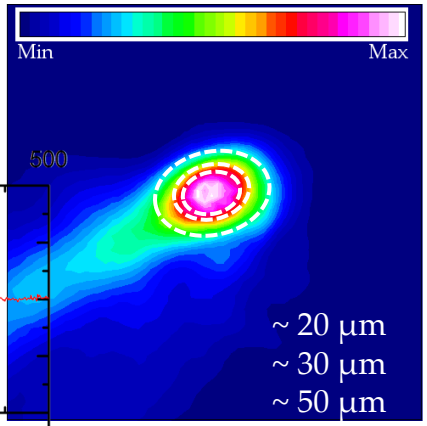

SISSI branchlines

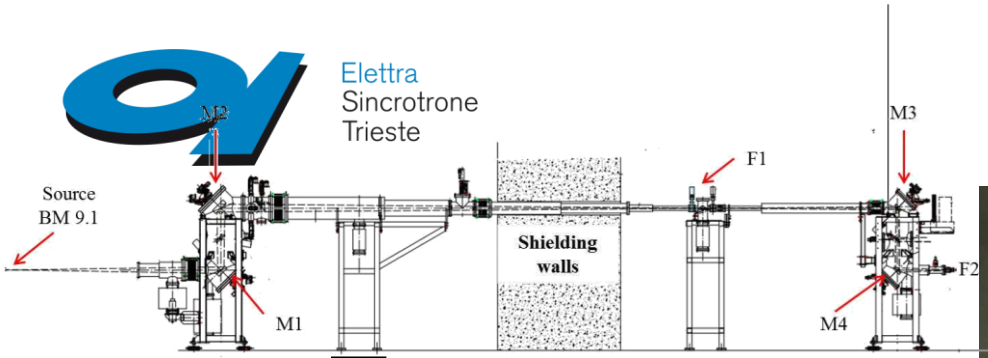

Elettra
Sincrotrone
Trieste

Vertex 70

Vertex 70v

Hyperion 2000

Consiglio Nazionale Ricerche

Elettra
Sincrotrone
Trieste

SR-FTIR Mapping

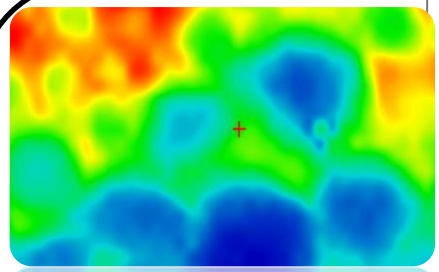

Chemical map of the Sample

The spatial resolution is achieved by beam confinement

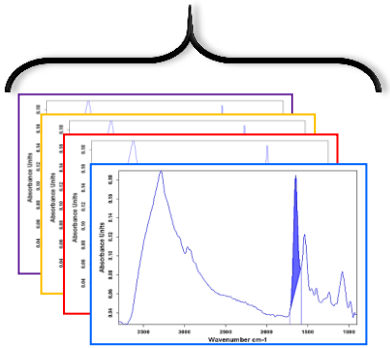

Integration of a Specific Band

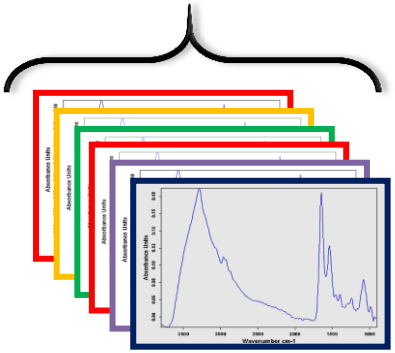

Acquired Spectra

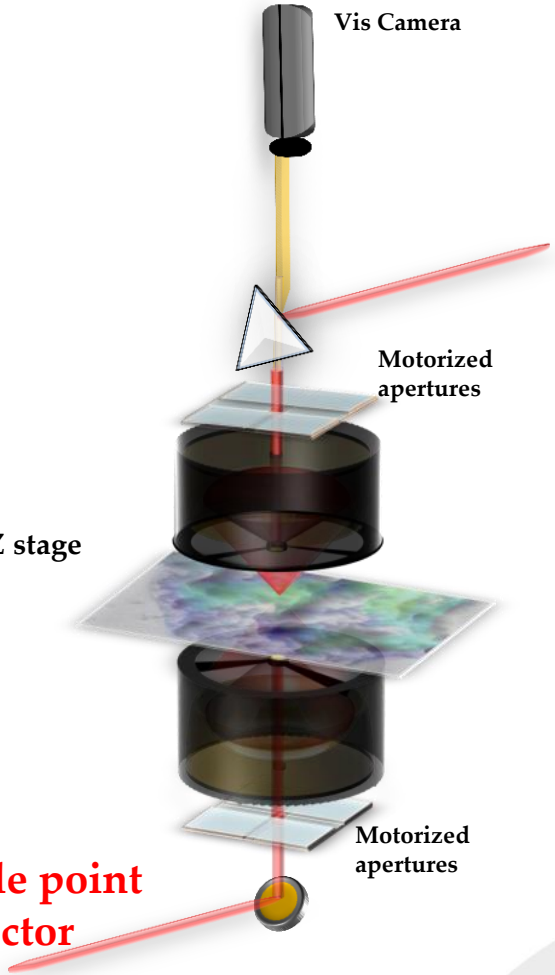

To Single point Detector

Elettra
Sincrotrone
Trieste

SR FTIR Microscopy: Selected application for life Sciences

Elettra
Sincrotrone
Trieste

Biology and life sciences: The spectroscopic point of view

FTIR Spectroscopy

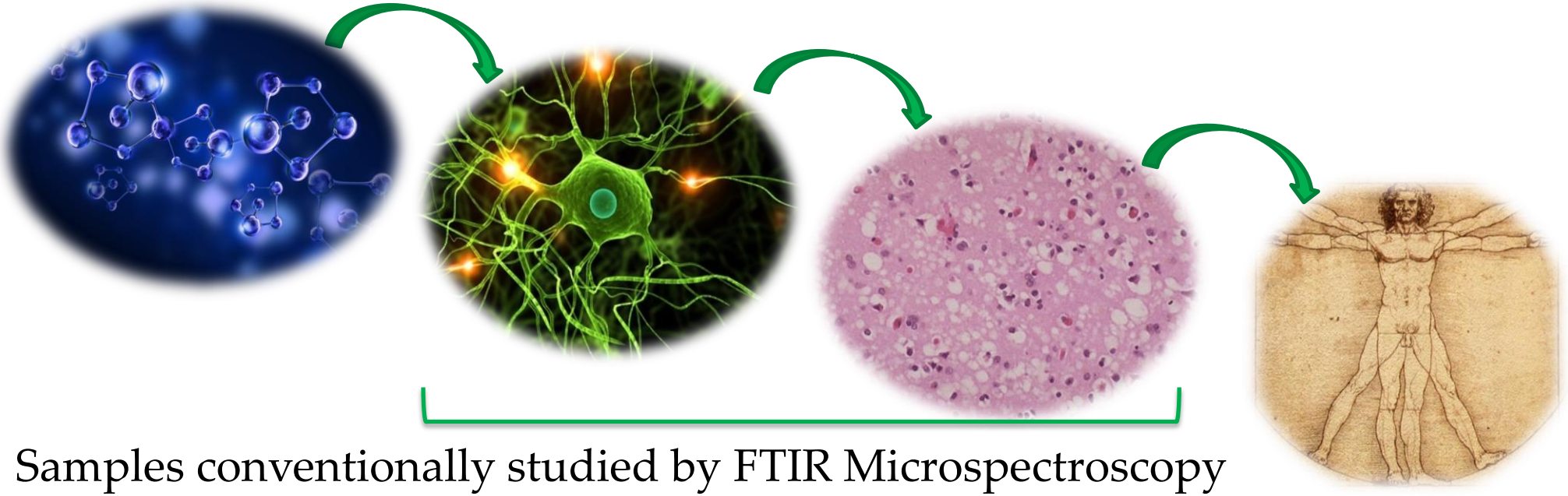

Samples conventionally studied by FTIR Microspectroscopy

FTIR Microscopy allows to investigate several aspects of the **biochemistry** of cells and tissues

Elettra
Sincrotrone
Trieste

Biology and life sciences: The spectroscopic point of view

Lipids

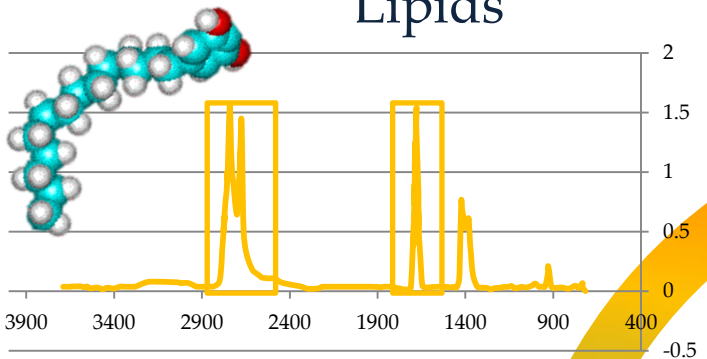

Carbohydrates

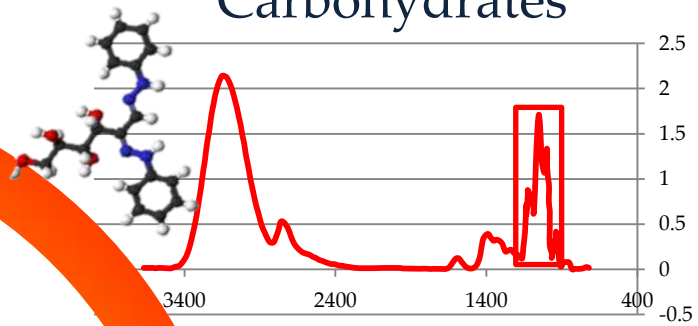

Nucleic Acids

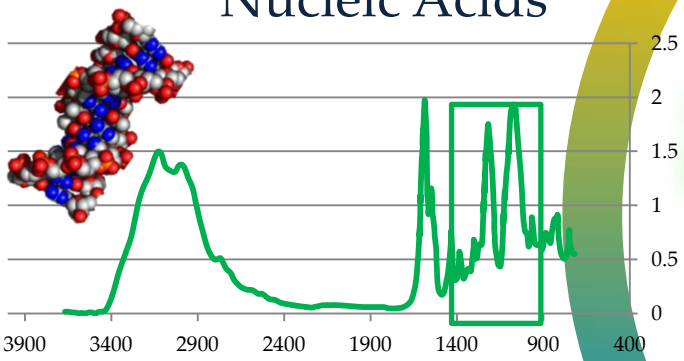

Proteins

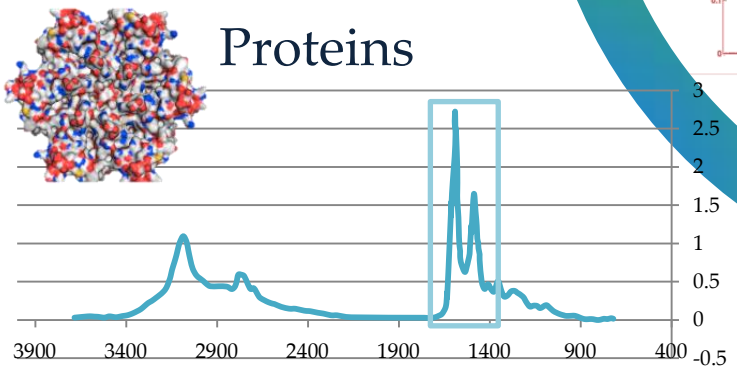

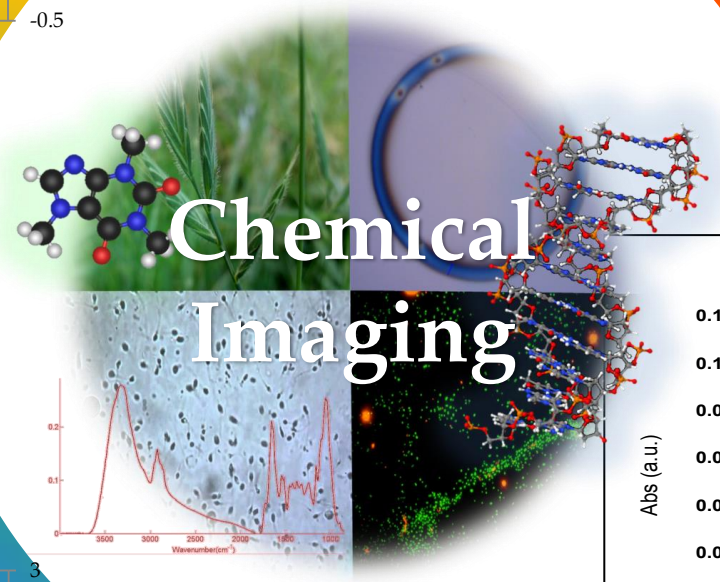

SINGLE CELL SPECTRUM

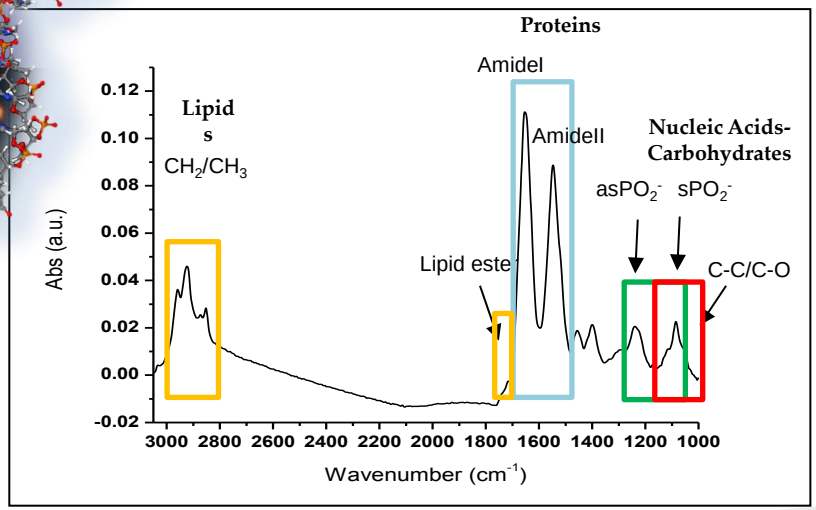

Band intensity, position, width and shape (band components) are sensitive to subtle biochemical changes of bio-specimens

Compositional and structural information at tissue, cellular and sub-cellular level can be achieved by exploiting SR brightness advantage

Soft X-Ray Radiation Damage On Fixed Cells Investigated with SR FTIRM, AFM and XRM

TwinMic Beamline at Elettra

Functionality and toxicity of Zn in wheat

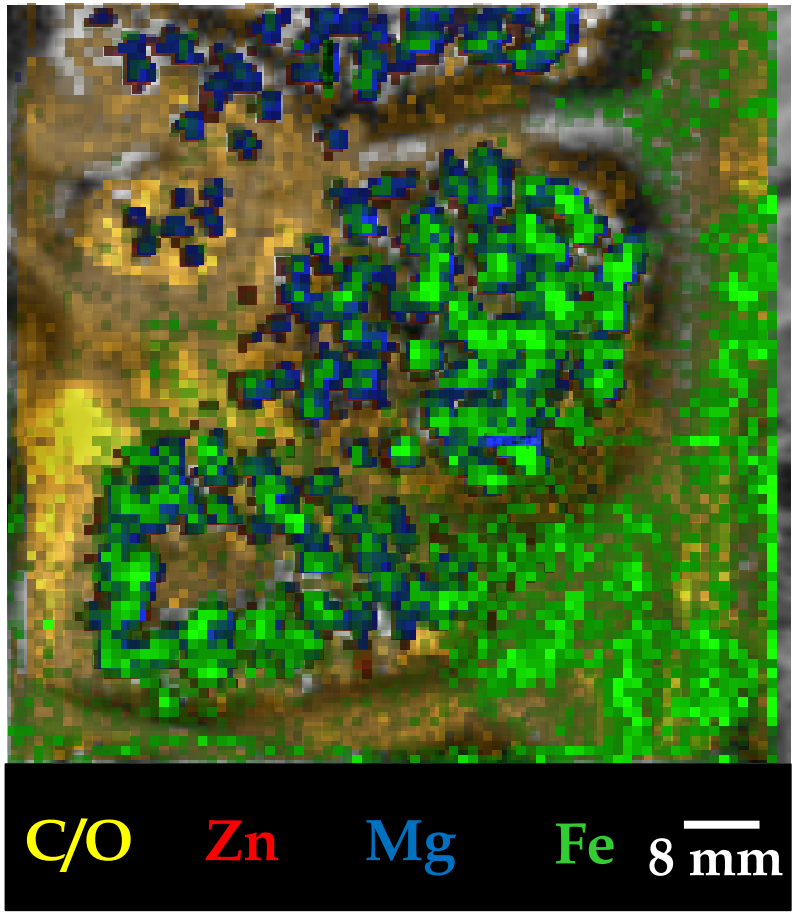

- Radiation damage induced by X-rays on biological samples is one of the remaining bottlenecks for their ultrastructural characterization by X-ray microscopy techniques
- X-ray nanofocusing is a today reality but the extent to which the lateral resolution can be pushed without unacceptable bio-sample degradation is still an open question

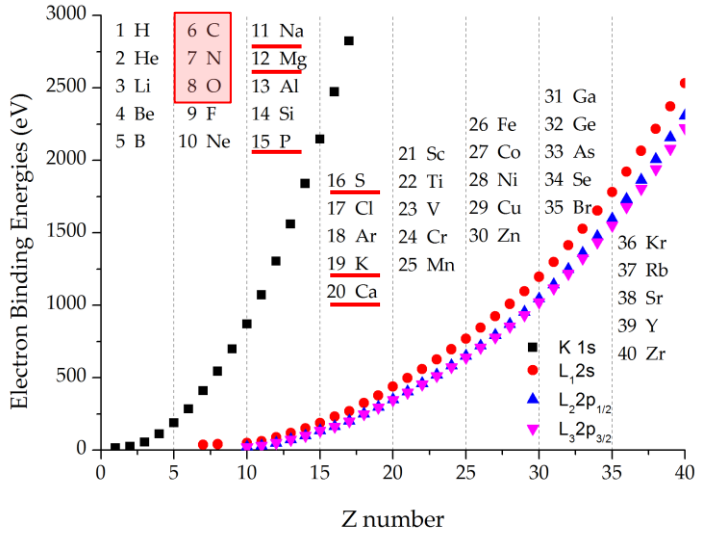

M. Regvar, D. Eichert, B. Kaulich, A. Gianoncelli, P. Pongrac, K. Vogel-Mikus, I. Kreft, New insights into globoids of protein storage vacuoles in wheat aleurone using synchrotron soft X-ray microscopy, Journal of Experimental Botany, Vol. 62, No. 11, 3929–3939, 2011.

Soft X-Ray Radiation Damage On Fixed Cells Investigated with SR FTIRM, AFM and XRM

Elettra Sincrotrone Trieste

The very same radiation that induces damage is exploited for probing it

Literature Survey

Radiation damage is dose dependent

Radiation damage depends on sample preparation

Hydrated samples undergo more relevant changes with respect to fixed ones

Cryo-XRM better preserves the structural integrity of bio-samples

Radiolytic effects undergone by a specific molecule strongly depend on the sample architecture

Genetic material is extremely sensitive to ionizing radiation

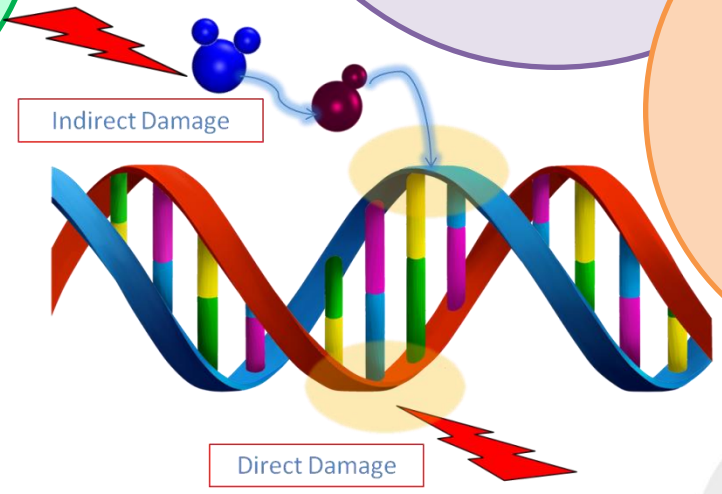

Soft X-Ray Radiation Damage On Fixed Cells Investigated with SR FTIRM, AFM and XRM

Elettra Sincrotrone Trieste

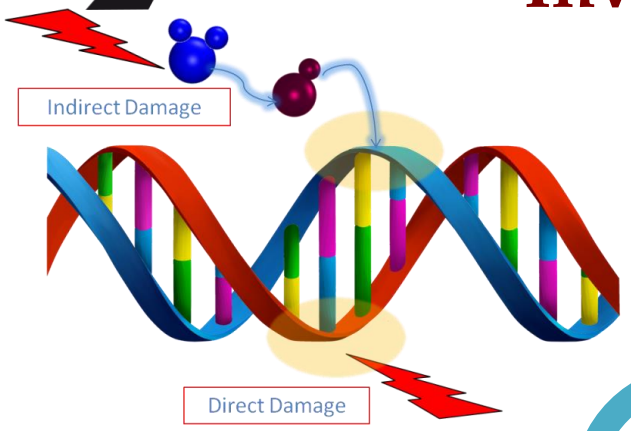

Hek293T cells (human embryonic kidney)

Step 0
Cell growth on 100 nm Si_3N_4 membranes
Cell fixation with PFA 3.7% and overnight air drying

Step 1
Cell drying in vacuum @ TwinMic
($p < 10^{-5}$ mbar) for 1:30 hour

Step 2
Low Dose STXM mapping @ TwinMic 1 keV
Estimated dose: $2*10^6$ Gy

Step 3
High Dose STXM mapping @ TwinMic 1 keV Estimated dose: $2*10^7$ Gy
Cumulative estimated dose: $2.2*10^7$ Gy

Step 4
Very high dose STXM mapping @ TwinMic 1 keV
Estimated dose: $6*10^8$ Gy
Cumulative estimated dose: $6.2*10^8$ Gy

A. Gianoncelli, L. Vaccari, G. Kourousias, D. Cassese, DE Bedolla, S. Kenig, P. Storici,. M. Lazzarino and M. Kiskinova. **Soft X-Ray Microscopy Radiation Damage On Fixed Cells Investigated With Synchrotron Radiation FTIR Microscopy.** *Scientific Reports* **2015** *5*, article number 10250

Elettra
Sincrotrone
Trieste

Outcomes of AFM

- Minimal cell shrinkage
- Evident degradation/thinning of pseudopodia terminations
- Appreciable thickness variations, especially on the nuclear region at Step 4
- Outstanding topographical changes: nanometric pits and bulges increase in number and size when increasing dose

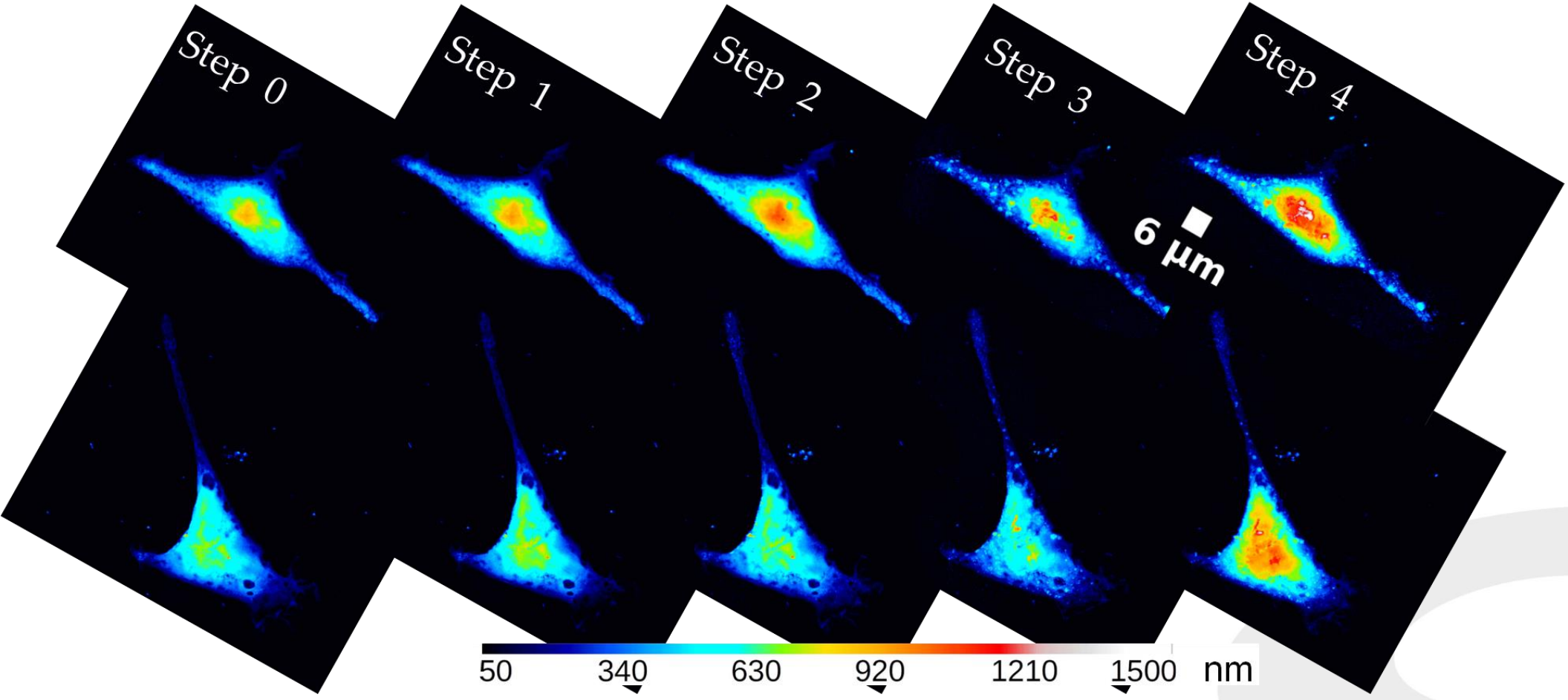

Elettra Sincrotrone Trieste

Outcomes of XRM

Mass Thickness $\rho t = -\ln \frac{(I/I_0)}{\mu^*}$

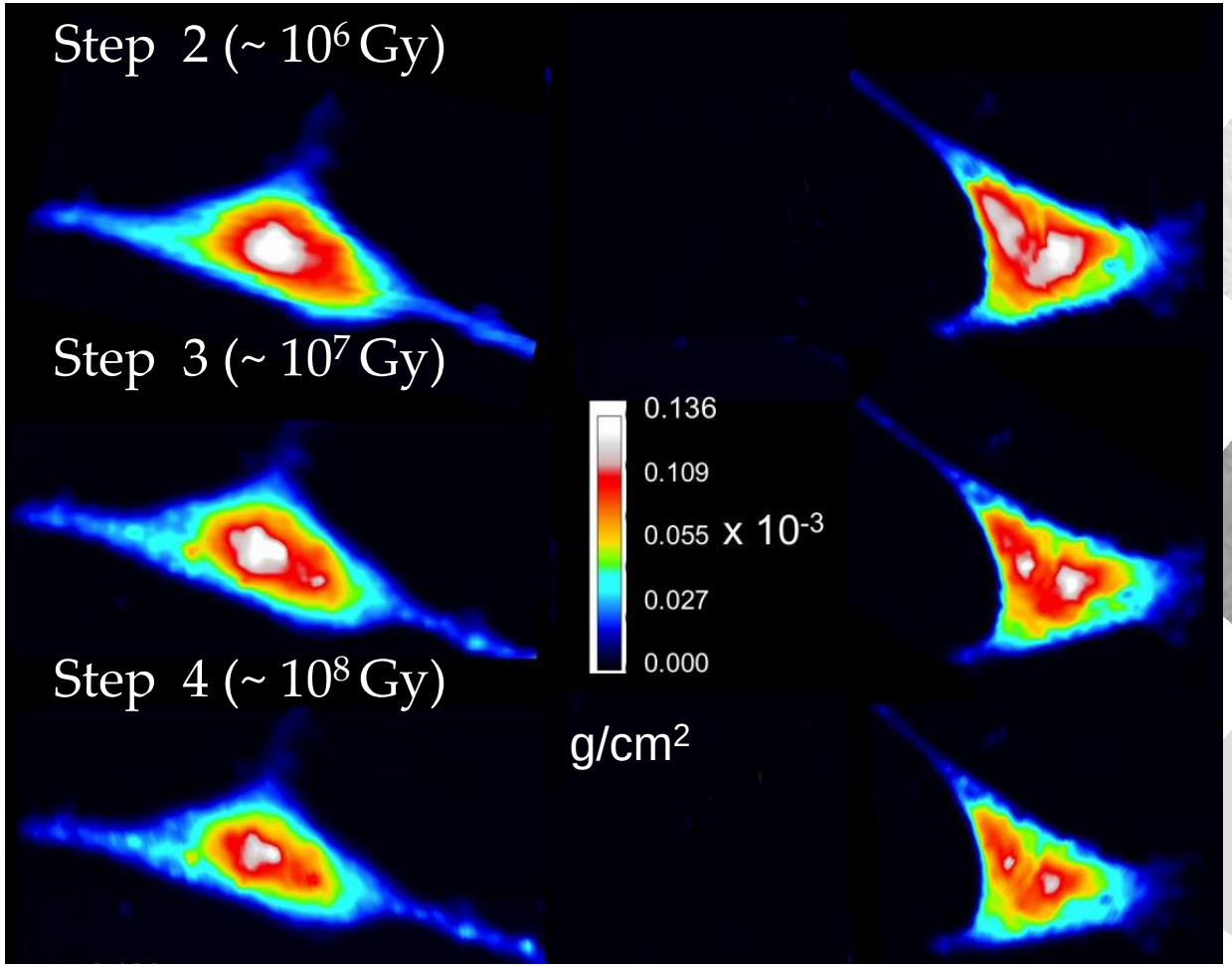

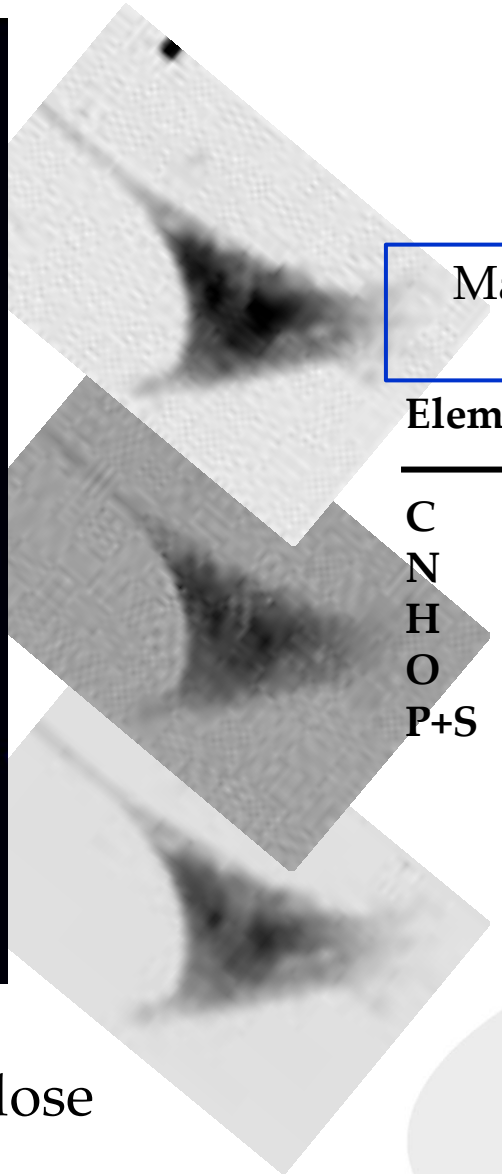

Mass absorption coefficient

Element	Mass fraction
C	0.5
N	0.16
H	0.07
O	0.25
P+S	0.02

- Mass Thickness decreases with increasing dose

Elettra
Sincrotrone
Trieste

Combining XRM and AFM

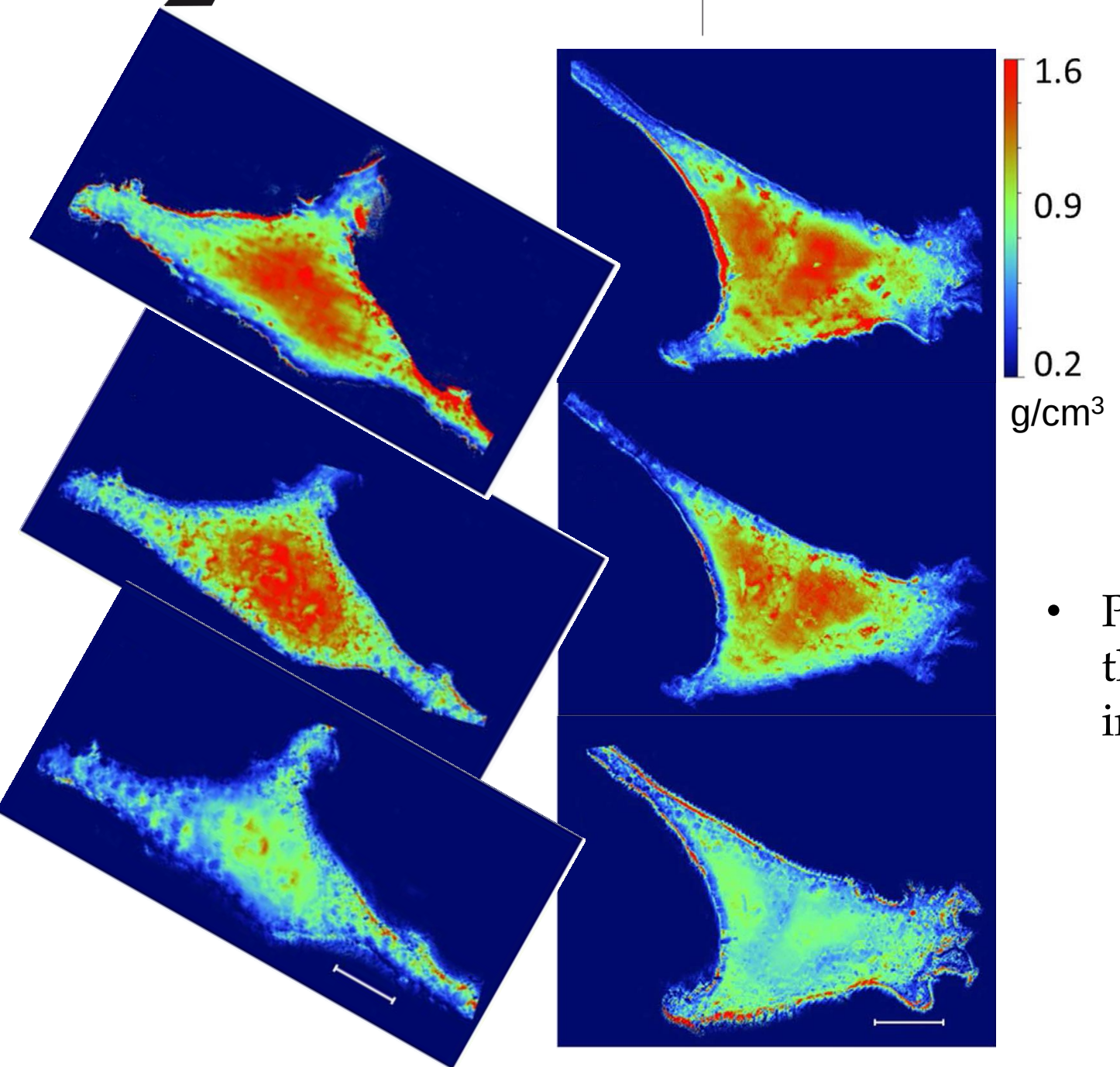

XRM cell images normalized over AFM cell thickness

$$\rho = -\ln \frac{(I/I_0)}{\mu * t}$$

- Progressive reduction of the cell density with increasing X-ray dose

Elettra
Sincrotrone
Trieste

FTIRM Outcomes

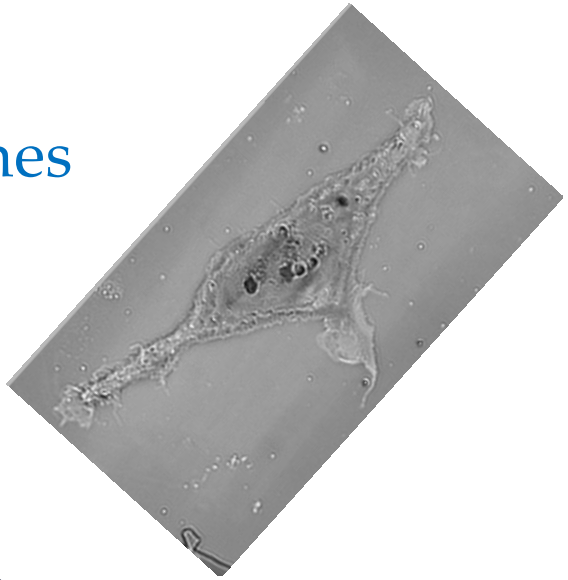

Step 0

Step 1

Step 2

Step 3

Step 4

Lipids

2988-2830 cm^{-1}

Proteins

1702-1480 cm^{-1}

Nucleic acids

1270-1190 cm^{-1}

0 1

Min Max

Elettra
Sincrotrone
Trieste

FTIRM Outcomes

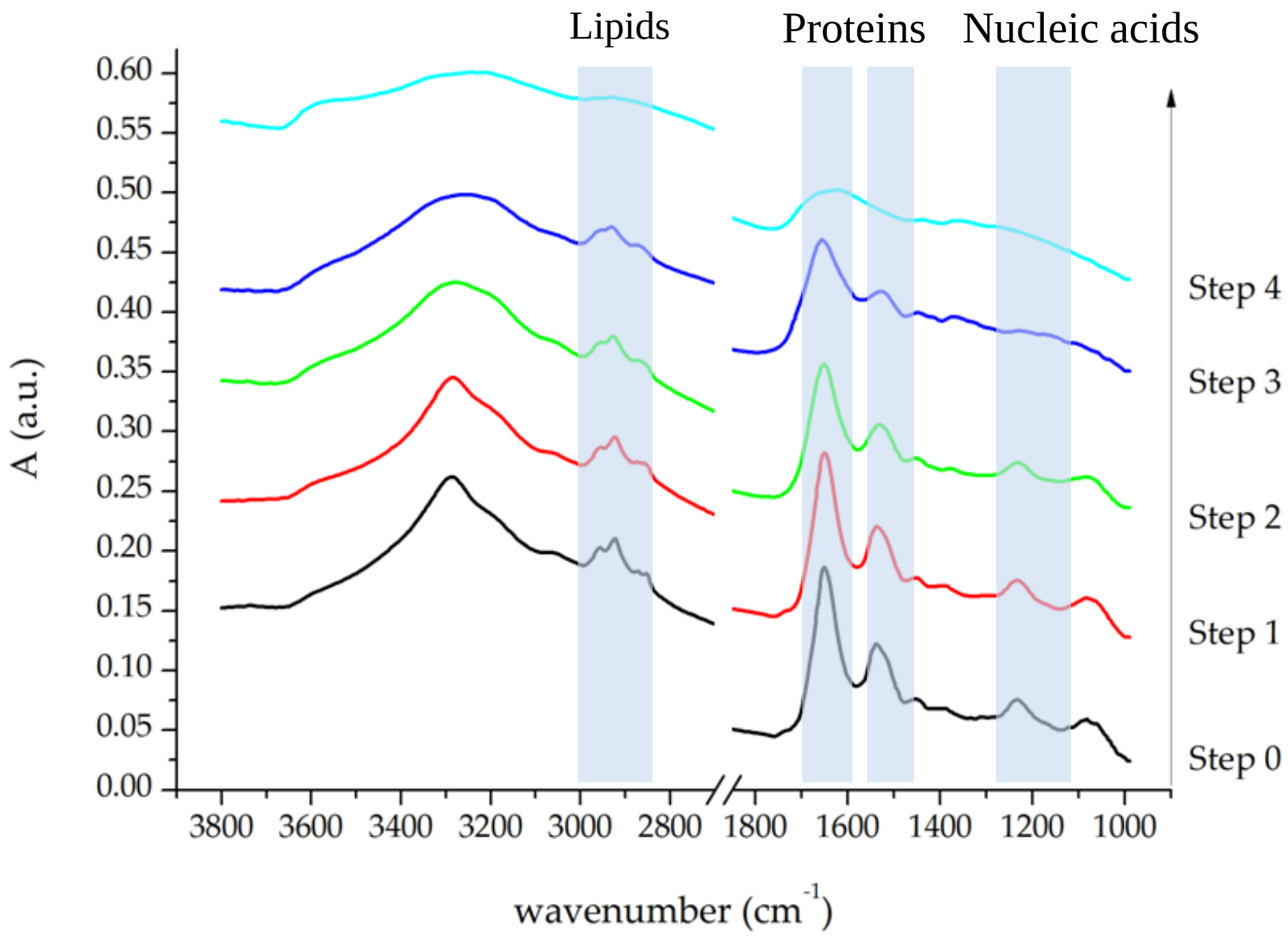

Elettra
Sincrotrone
Trieste

FTIRM Outcomes

Dehydration → Low-Dose → Medium-Dose → High-Dose

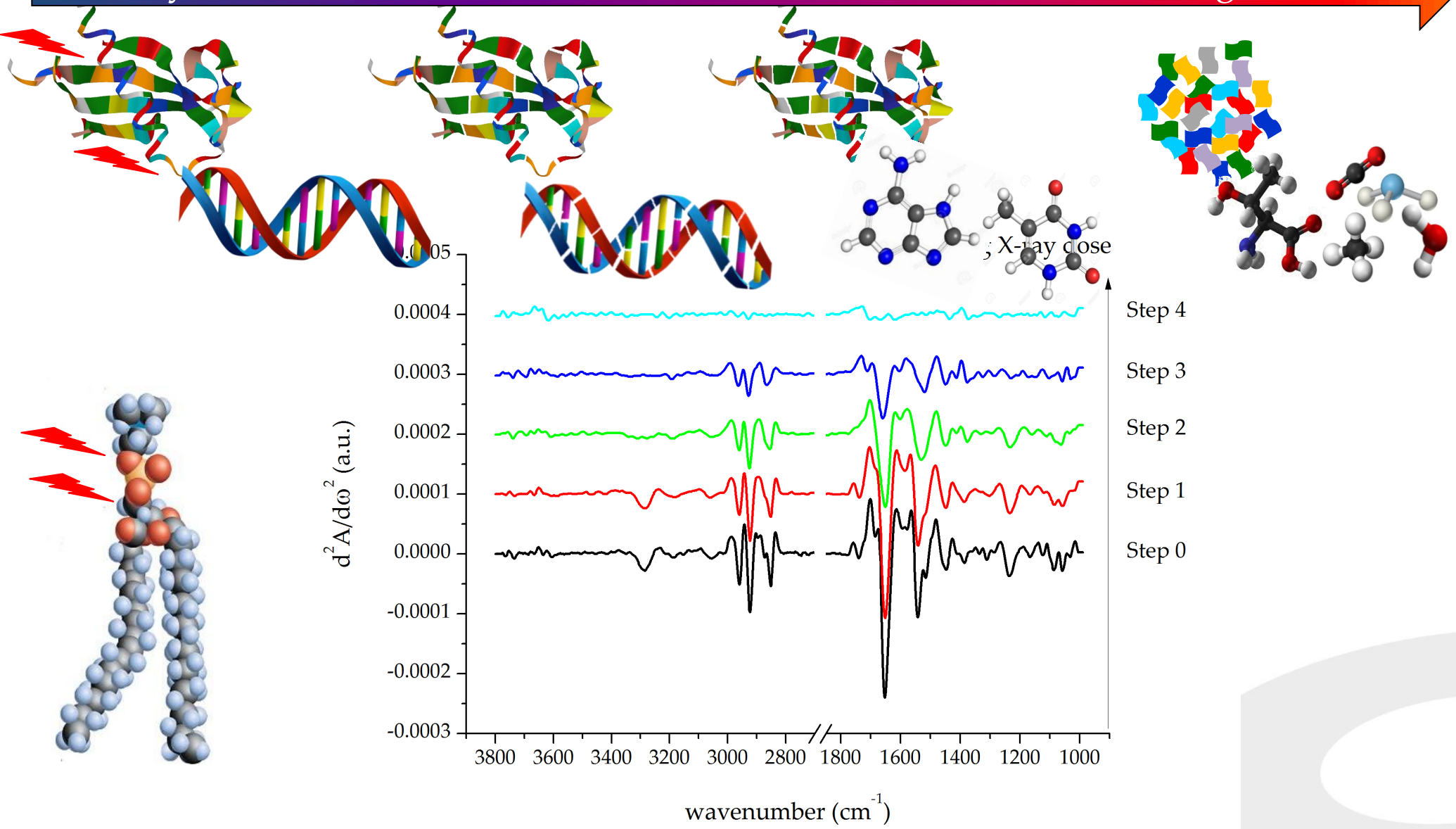

Elettra
Sincrotrone
Trieste

General Conclusions

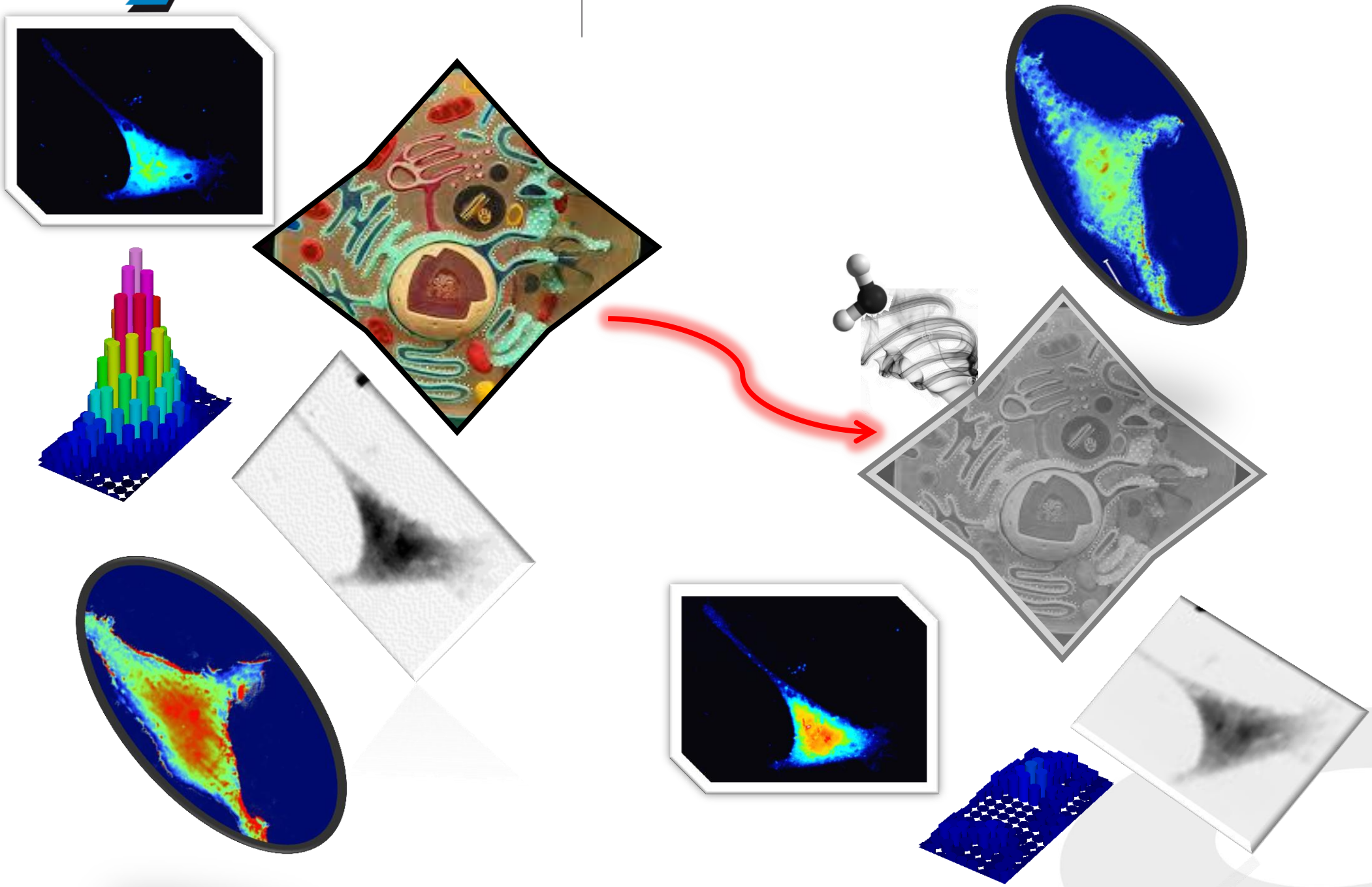

Elettra Sincrotrone Trieste

FTIR Microscopy and Prion Research

Aberrant metabolism of the Prion Protein (PrP)

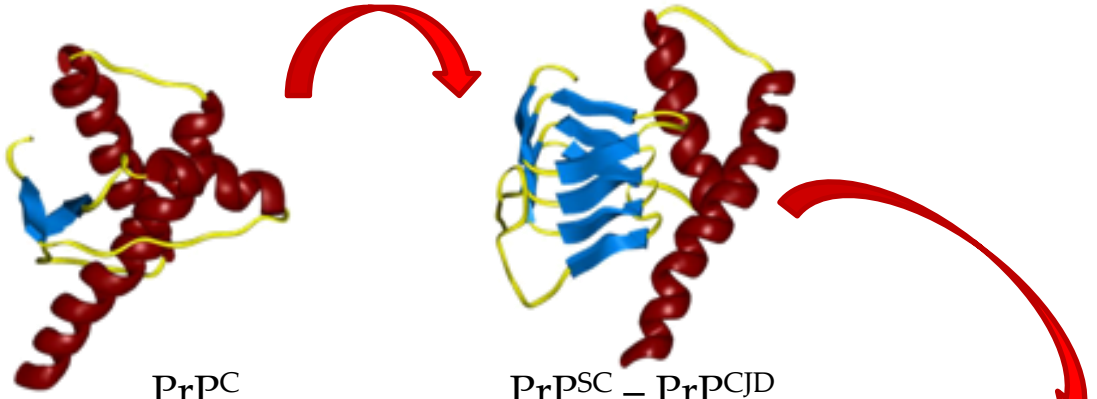

PrP^{C}
Alpha-helical
Protease sensitive

PrP^{SC} – PrP^{CJD}
beta- plated sheet
Protease resistant

As revealed by FTIR spectroscopy

PrP^{C} 42% α-helix; 3% β-sheet

PrP^{Sc} < α-helix; > β-sheet Phenotype dependent

Amide I band – 1700-1600 cm^{-1}	
1695-1675	Antiparallel β-sheet/ Aggregated strands
1670-1660	3_{10} - Helix
1660-1648	α-helix
1648-1640	Random coil
1640-1625	β-sheet
1628-1610	Aggregated strands

As revealed by FTIRM

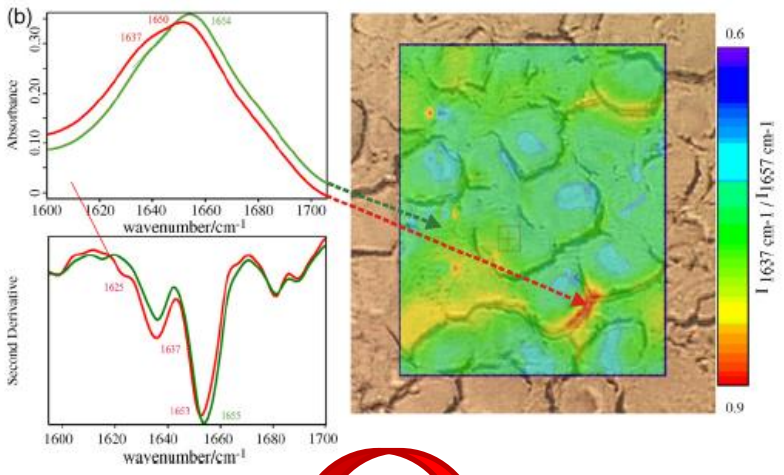

Prion rods

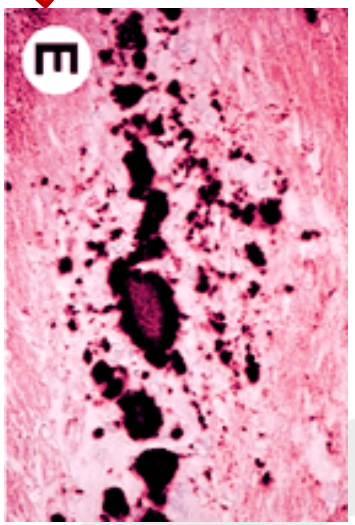

PrP amyloid plaques

PNAS 1999 vol. 96 no. 26 15137-15142

PNAS 1998 vol. 95 no. 23 13363-13383

Ariane Kretlow, Qi Wang, Janina Kneipp, Peter Lasch, Michael Beekes, Lisa Miller, Dieter Naumann. **FTIR-microspectroscopy of prion-infected nervous tissue**. Biochimica et Biophysica Acta (BBA) - Biomembranes, **2006**, 1758 (7), 948-959

Elettra
Sincrotrone
Trieste

A multi-technique approach for cellular analysis

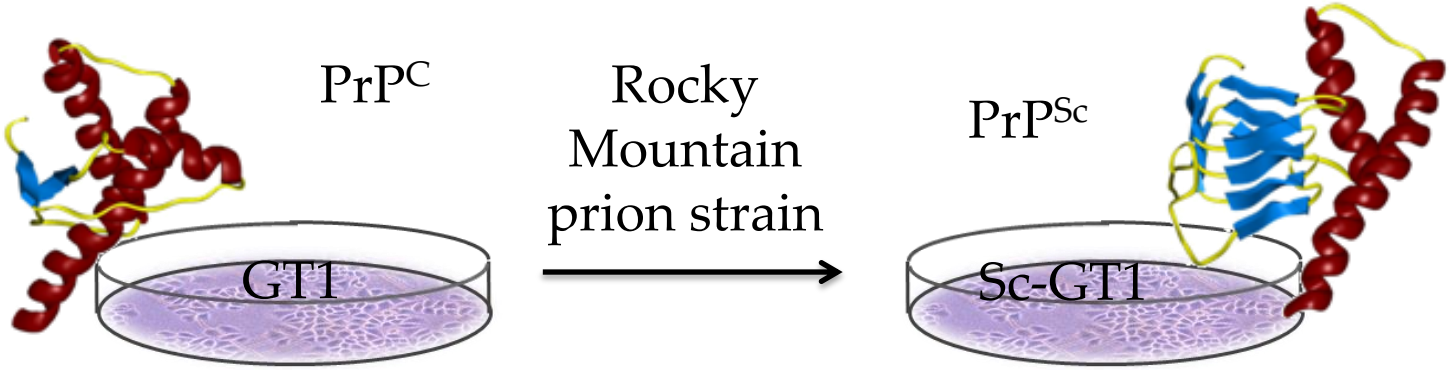

AFM outcomes

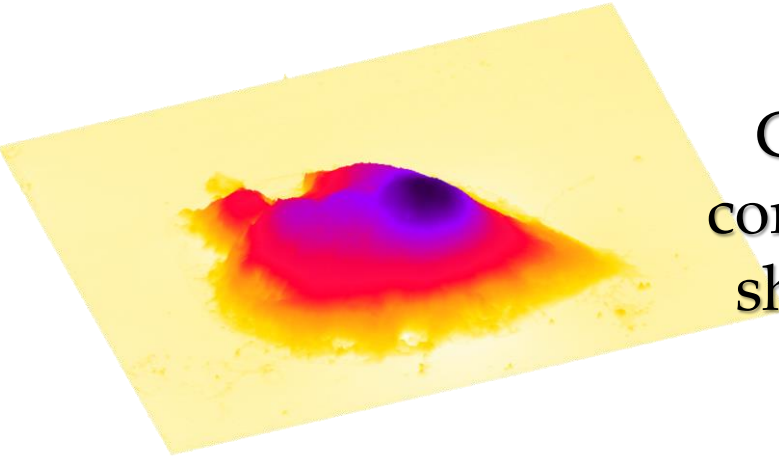

GT1 and Sc-GT1 have comparable pyramid like shape and effective cell height

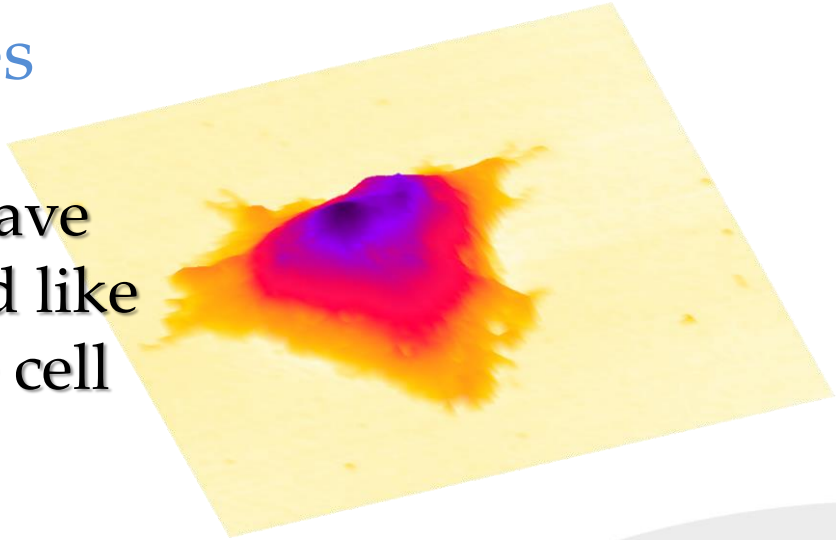

Prion Laboratory , Neurobiology Sector, SISSA Prof. G. Legname, A. Didonna

Alessandro Didonna, Lisa Vaccari, Alpan Bek, and Giuseppe Legname. **Infrared Microspectroscopy: A Multiple-Screening Platform for Investigating Single-Cell Biochemical Perturbations upon Prion Infection.** *ACS Chemical Neuroscience* **2011** *2* (3), 160-174

Elettra
Sincrotrone
Trieste

Outcomes of FTIRM on individual single cells_1

Proteinase K Western blot assay
Chronic infection of the neural cell line

FTIR Microscopy on whole cells
Healthy and Infected cells can be discerned

▪Multiple cell sensitivity
▪Execution time: many hours

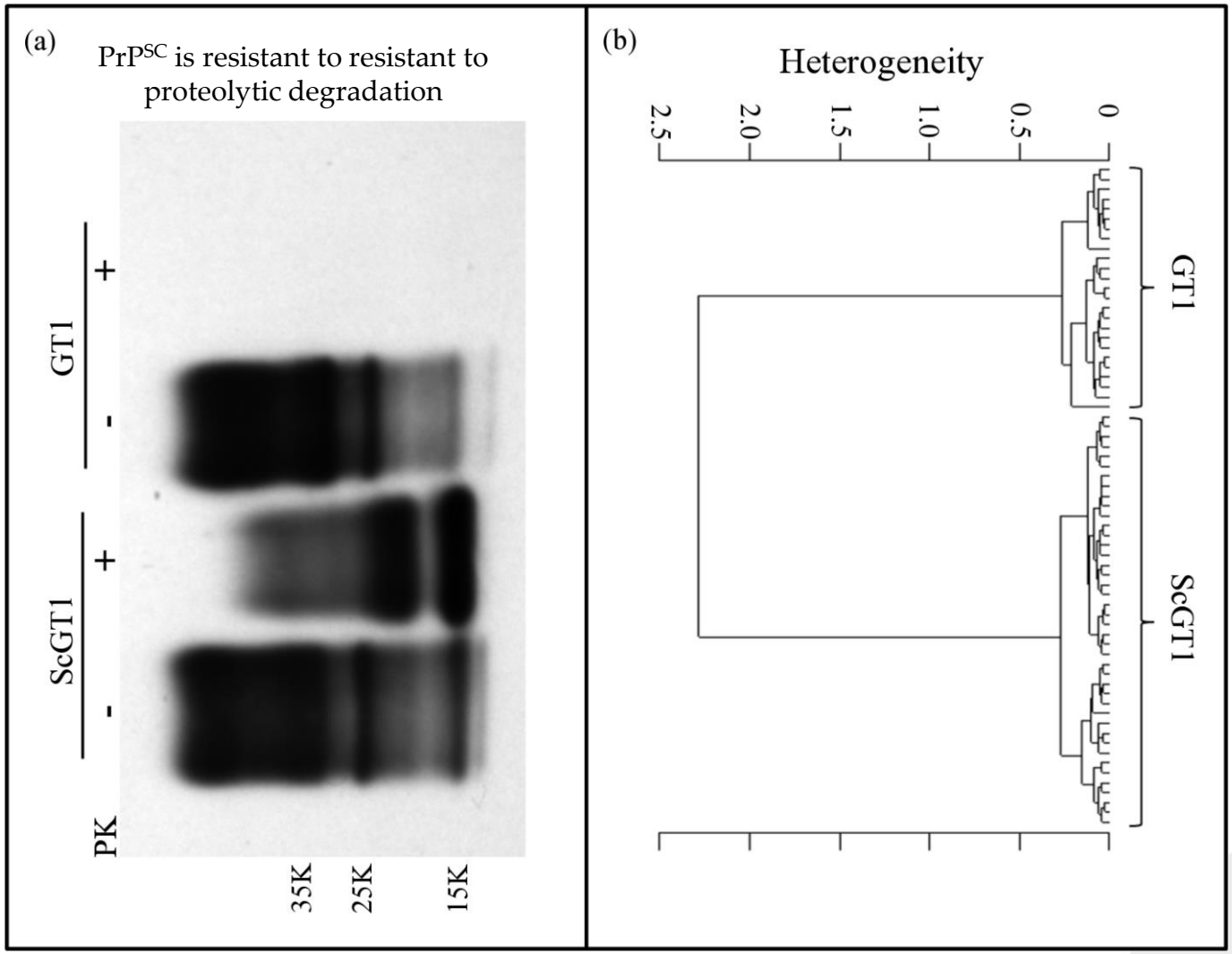

▪Single cell sensitivity
▪Execution time: few minutes

HCA on SVN 1st derivatives of IR cell microspectra
[1800-1150 cm^{-1}, Euclidean distances, Ward's algorithm]

Elettra Sincrotrone Trieste

Multivariate statistical analysis: Cluster Analysis

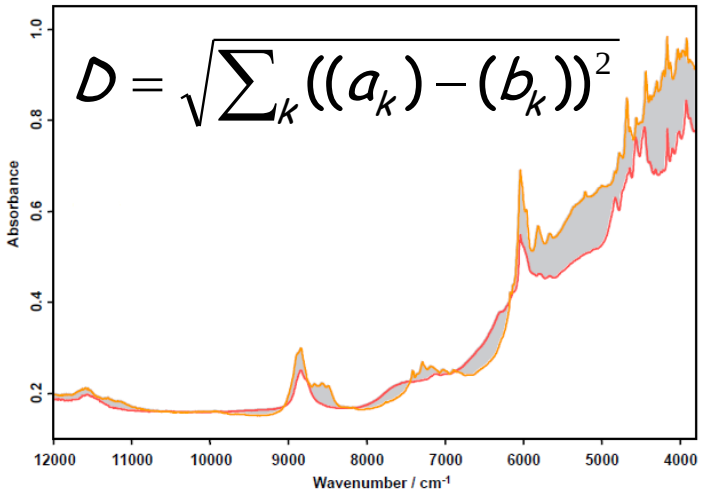

1. Spectral distance calculation

Distance between spectra *a* and *b* can be calculated with many algorithms. Euclidean spectral distance between a and b spectra is calculated over the all sampled k points (or within specific intervals).

2. Spectral distance matrix

	a	b	c	d	e
a	0				
b	44	0			
c	11	54	0		
d	100	68	97	0	
e	120	92	115	21	0

There are many methods available to calculate spectral distances between a newly-created cluster and all the other spectra or clusters.

N	Clusters
1	a-b-c-d-e
2	ac-b-d-e
3	ac-b-de
4	abc-de
5	abcde

3. Spectra clustering

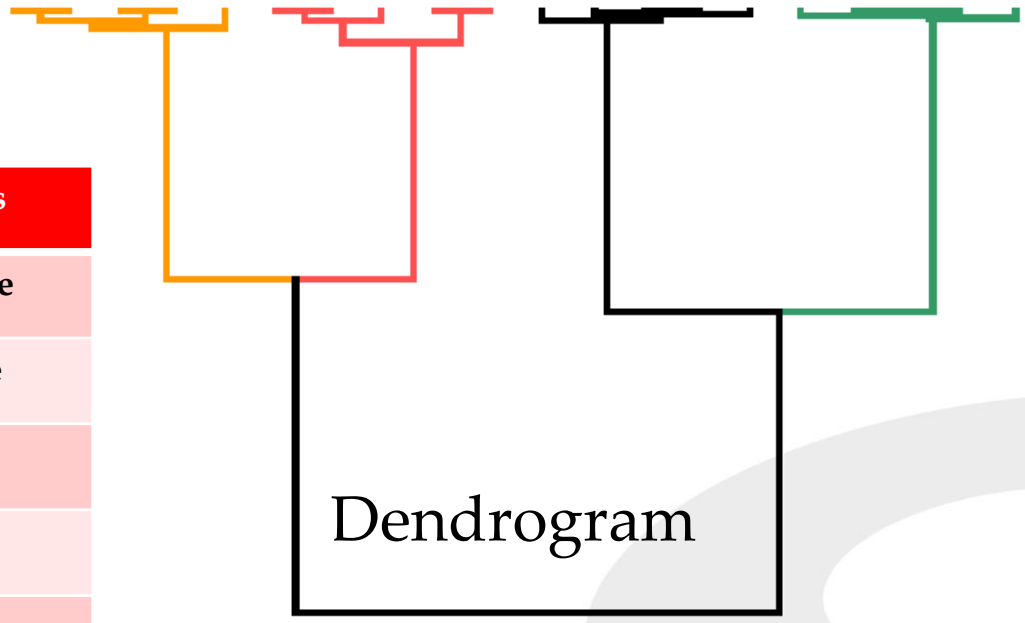

Elettra Sincrotrone Trieste

Multivariate statistical analysis: PCA

Principal component Analysis

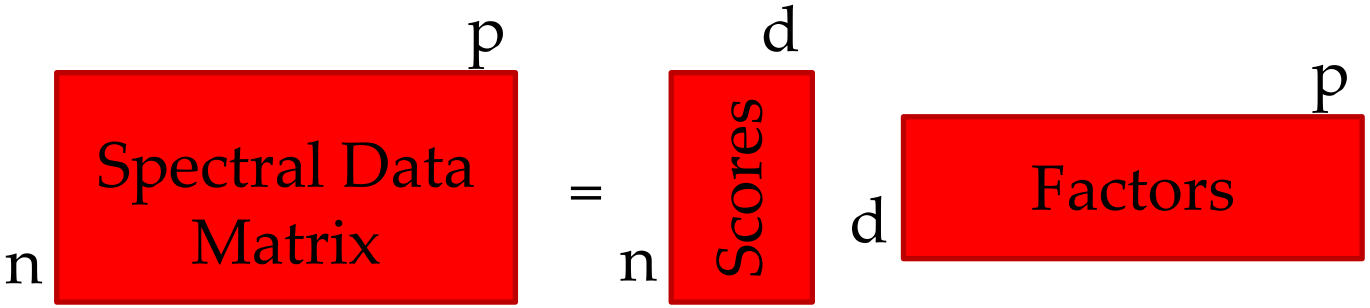

n spectra with p data points; d scores for each spectrum (d<n); d factors with p data points (d<n)

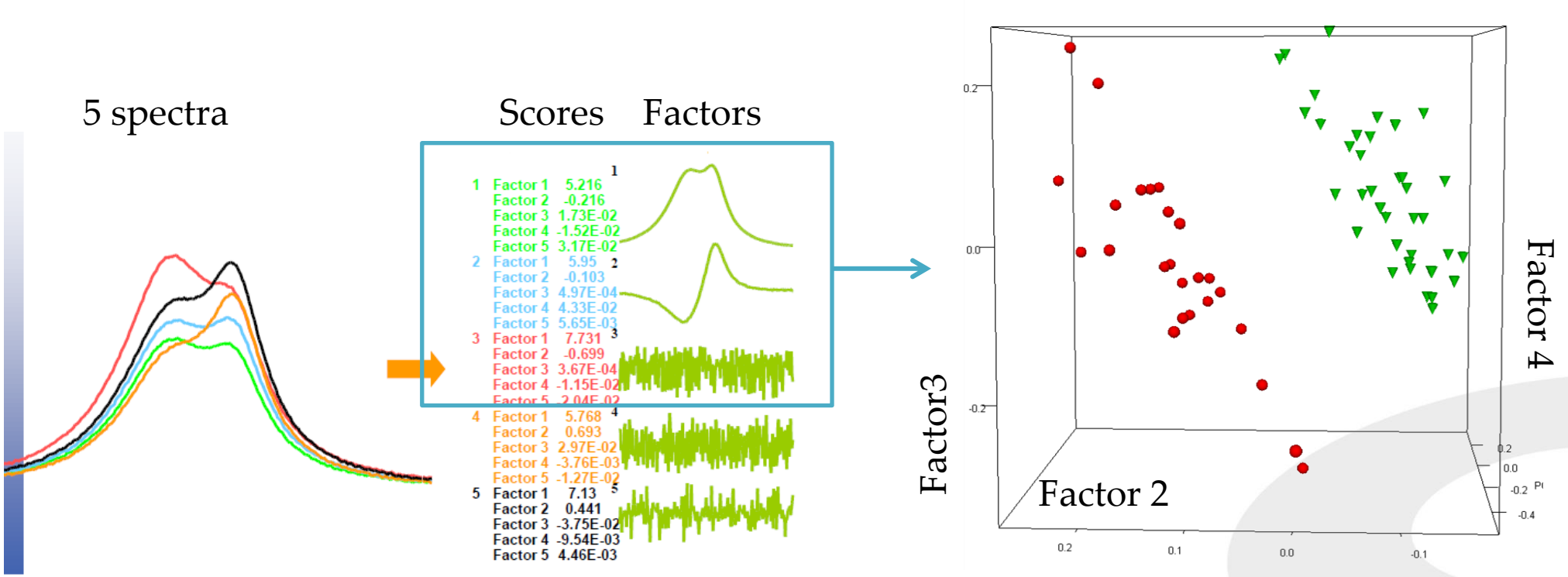

Elettra
Sincrotrone
Trieste

Outcomes of FTIRM on individual single cells_2

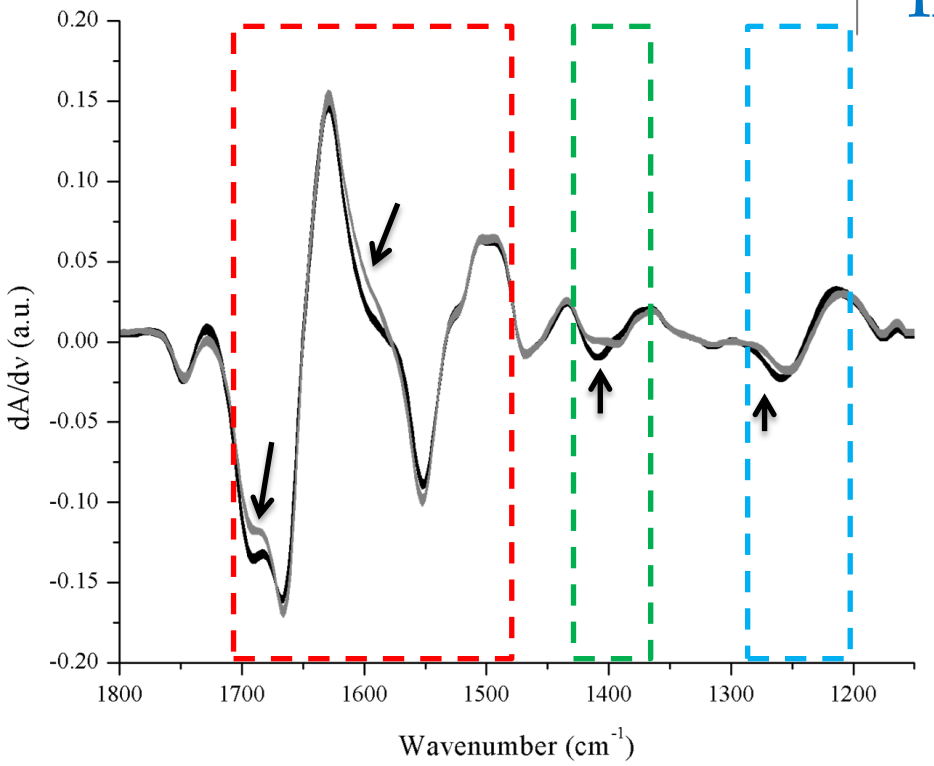

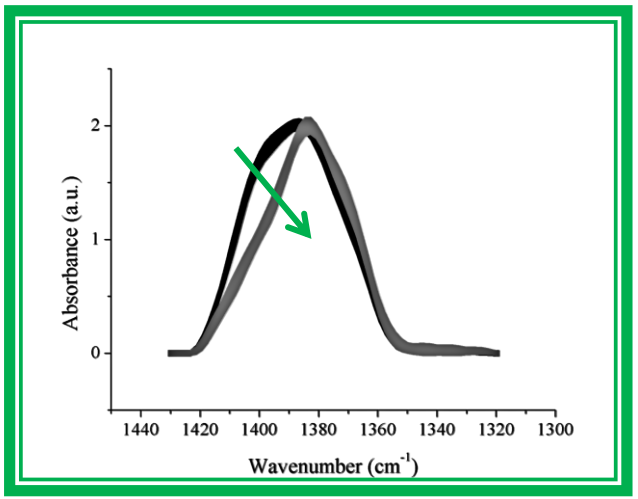

Aspartate → Aspartic acid
Glutamate → Glutamic acid

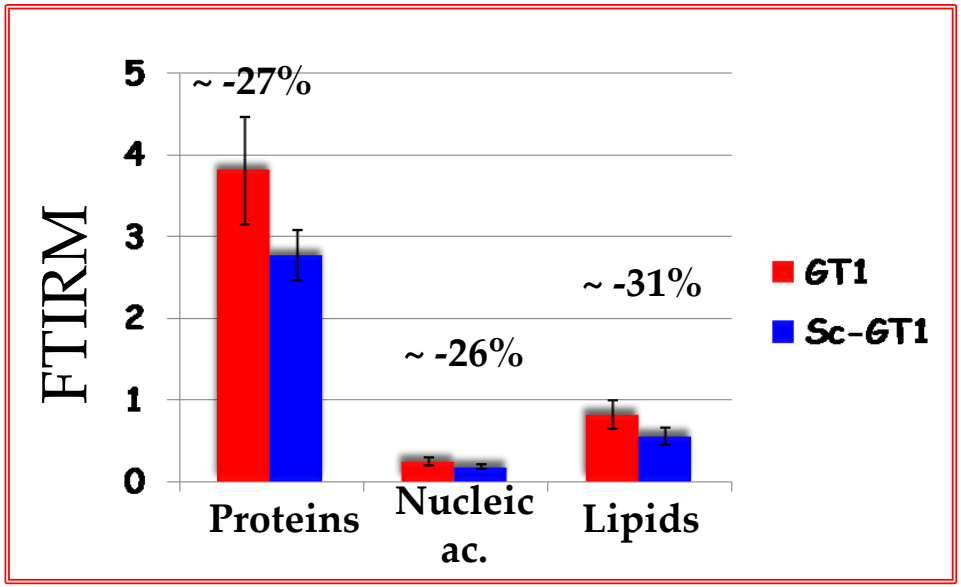

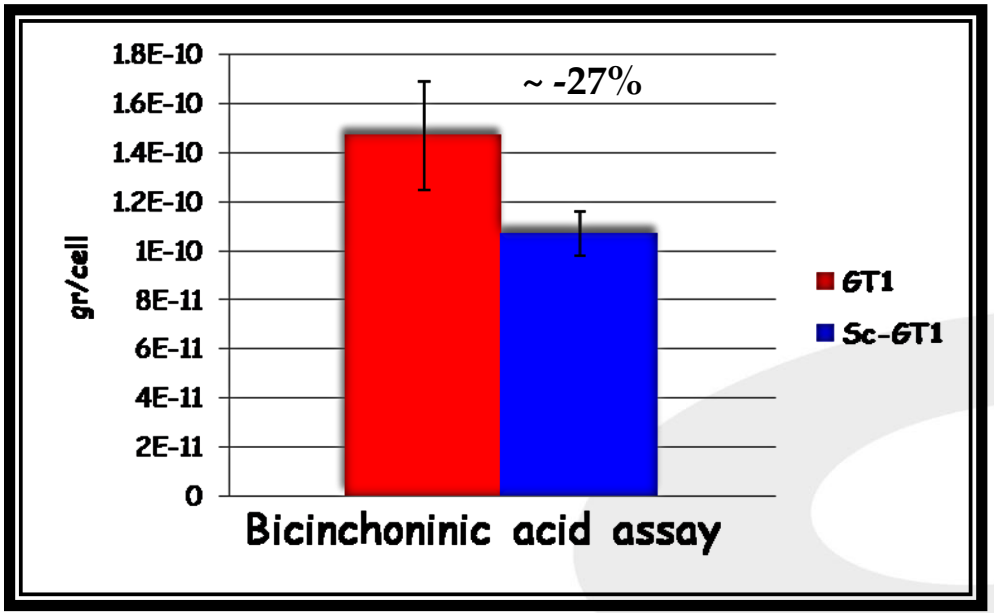

Elettra
Sincrotrone
Trieste

Outcomes of FTIRM at subcellular level: GT1

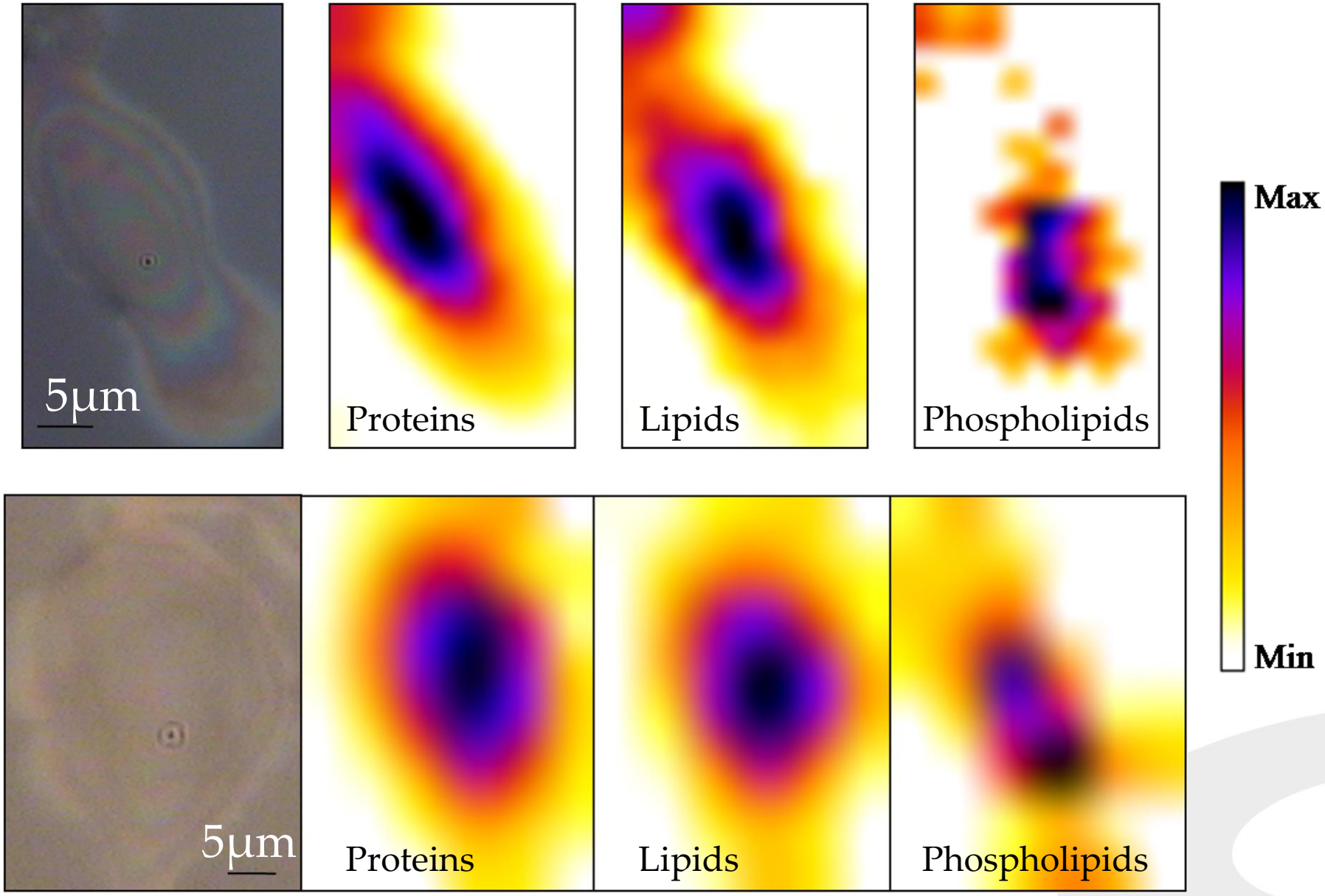

Elettra
Sincrotrone
Trieste

Outcomes of FTIRM at subcellular level: ScGT1

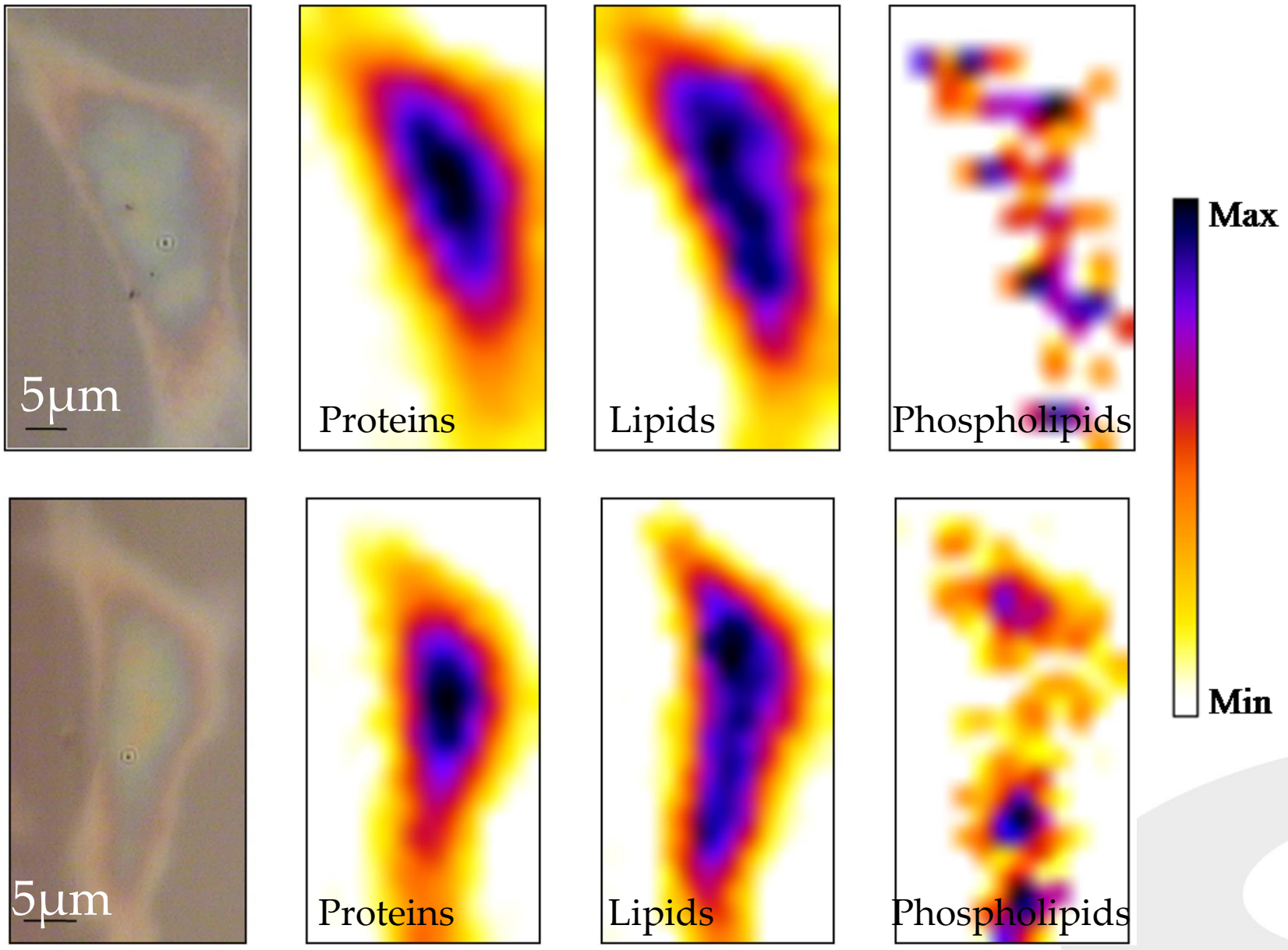

Elettra Sincrotrone Trieste

Conclusions

- Down-regulation of Lipid and Protein metabolism
- The lower concentration of cellular proteins and lipids is not related to variations in shape and volume of the infected cells

One of the distinctive histophatological hallmarks of prion disease is spongiosis
→ GT1 cell line seems to undergo *in vitro* the same alterations experienced *in vivo*

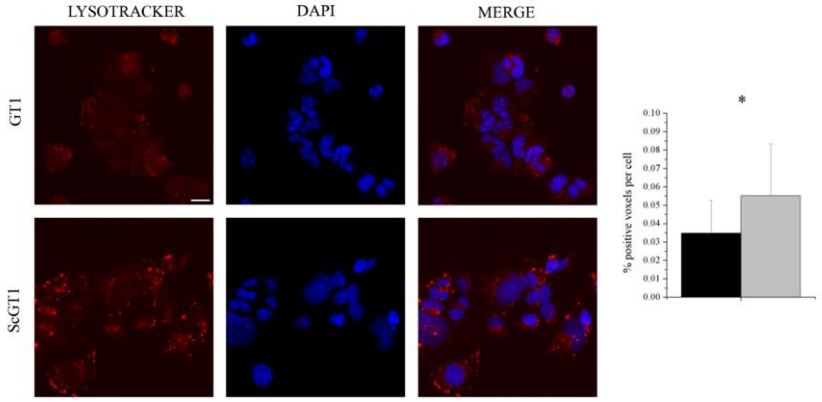

Extended cytosolic vesicles and discrete vesicular foci characterize prion infection
→ Direct Involvement of the lysosomal compartment in prion propagation

Subcellular compartment/s where the PrP^{C} to PrP^{SC} conversion takes place is still the subject of intense debate
Our results may reflect the role of lysosomal compartment as conversion sites

FTIR Microscopy and Cancer Research
Glioblastomas

Elettra Sincrotrone Trieste

AZIENDA OSPEDALIERO UNIVERSITARIA
Santa Maria della Misericordia di Udine

Gliomas are an heterogeneous group of primary brain tumors
Glioblastoma is the most malignant one (only 5% 5-years survival)

Cancer Stem Cells Theory

Only a small subpopulation of cancer stem cells is able to initiate tumor growth and drive development

CSCs not removed by surgery are responsible for tumor recurrence

CSCs are resistant to standard radio- and chemo-therapies

Inducing differentiation of stem cells is the most promising therapeutic approach nowadays under investigation

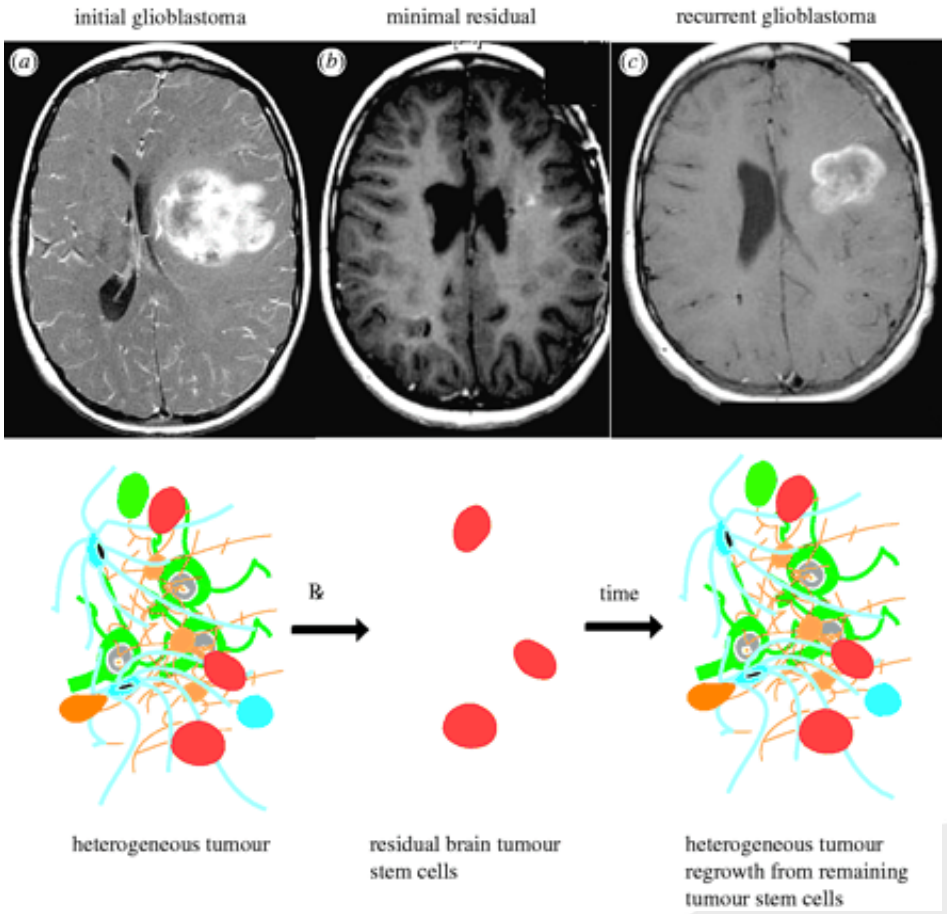

Fast methods for monitor the presence/abundance of stem cells and the efficiency of stem-differentiating agent are needed

Elettra
Sincrotrone
Trieste

Stem cell differentiation as revealed by FTIRM

CONTROL STEM CELLS

NCH421K Human Stem Cell Like Gliomblastoma cell line

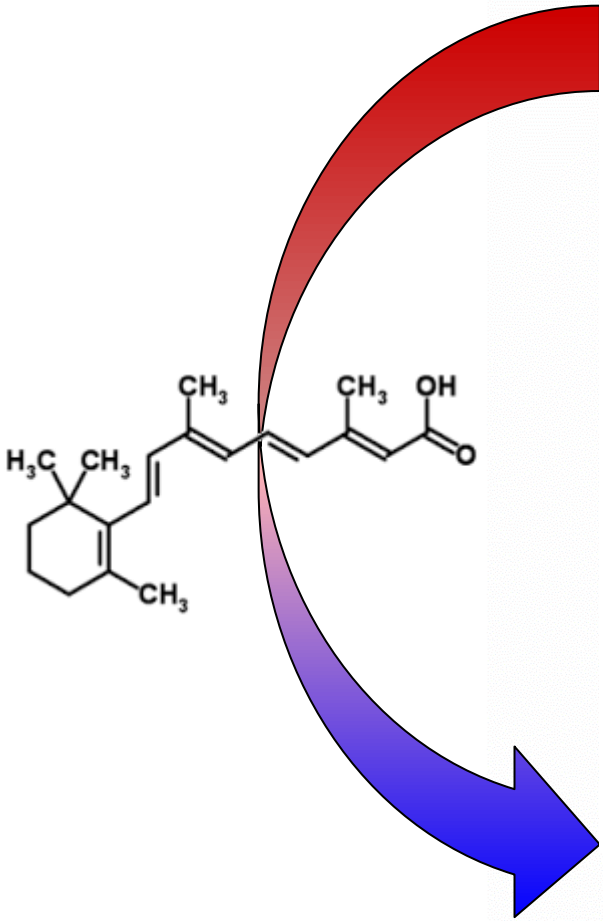

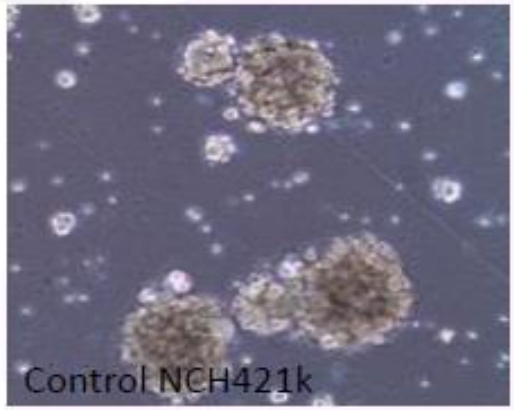

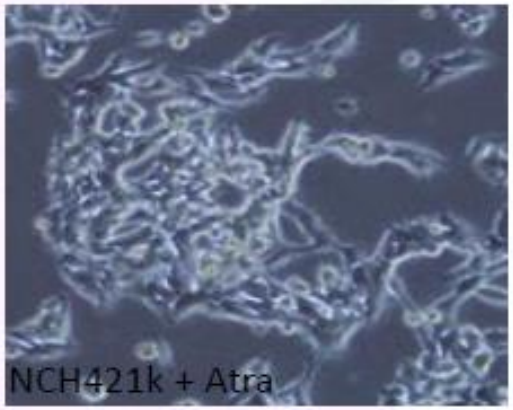

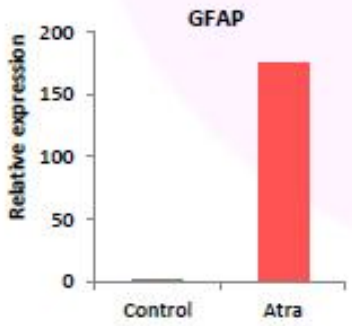

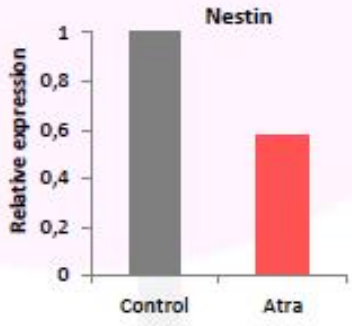

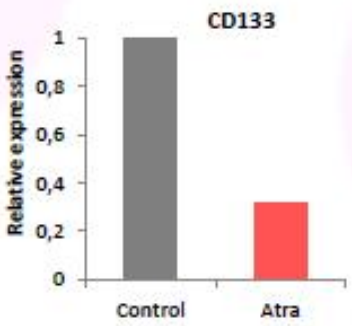

Astrocytes differentiation marker

Stemness markers

ATRA-DIFFERENTIATED CELLS

Saša Kenig, Diana Bedolla, Giovanni Birarda, Valentina Faoro, Elisa Mitri, Alessandro Vindigni, Paola Storici, Lisa Vaccari. **Fourier transform infrared microspectroscopy reveals biochemical changes associated with glioma stem cell differentiation.** *Biophysical Chemitry* **2015** *207*, 90-96

Elettra
Sincrotrone
Trieste

Stem cell differentiation as revealed by FTIRM

ATRA-DIFFERENTIATED – STEM CELLS

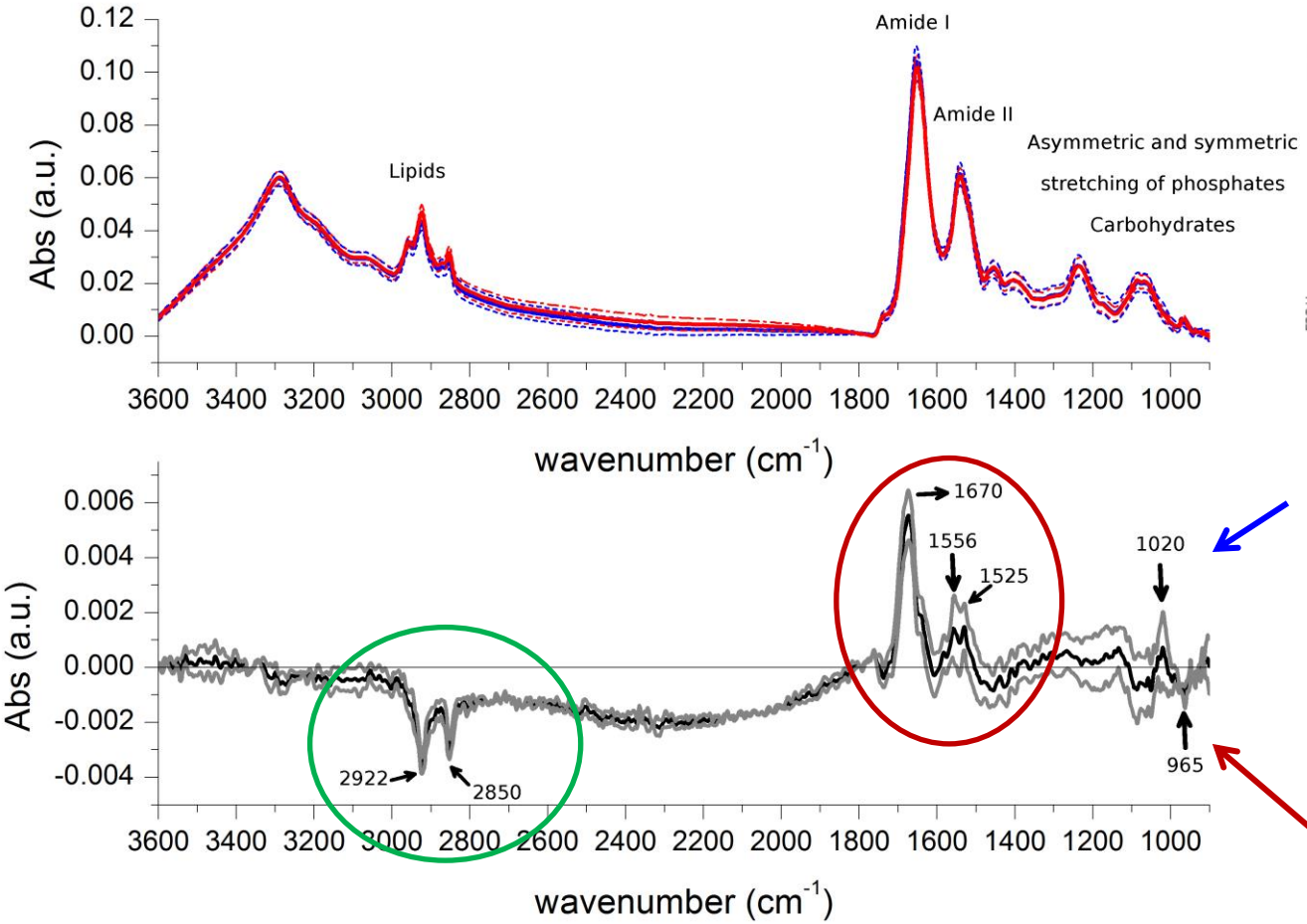

Same cell cycle distribution

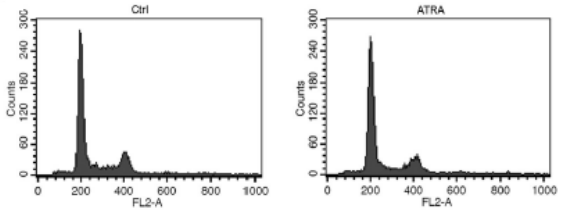

Same, minimal level of apoptosis

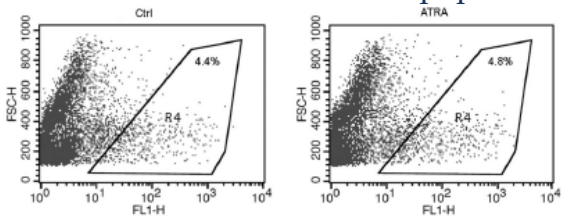

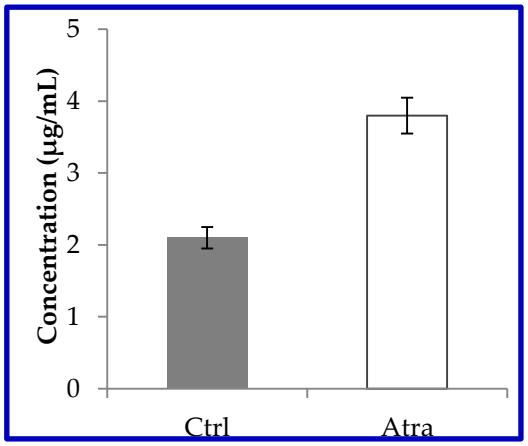

Different set of genes/proteins expressed by differentiated cells

Increased level of phosphorilated proteins in differentiated cells → Down-regulation of kinase inhibitors and high level of protein kinase in glioma CSCs

Higher glycogenated cells are characterized by lower lipid concentration

Increased lipid and glycogen levels (altered processes) → higher fluidity

Glycogen serves as supplemental energy substrate when glucose supply is insufficient

Elettra
Sincrotrone
Trieste

Stem cell differentiation as revealed by FTIRM

All the aforementioned differences are detected at single cell level by using a label-free, non-damaging and fast method.
To determine abundancy of stem cells and efficiency of ATRA-induced differentiation of glioma stem cell model NCH412K is possible.

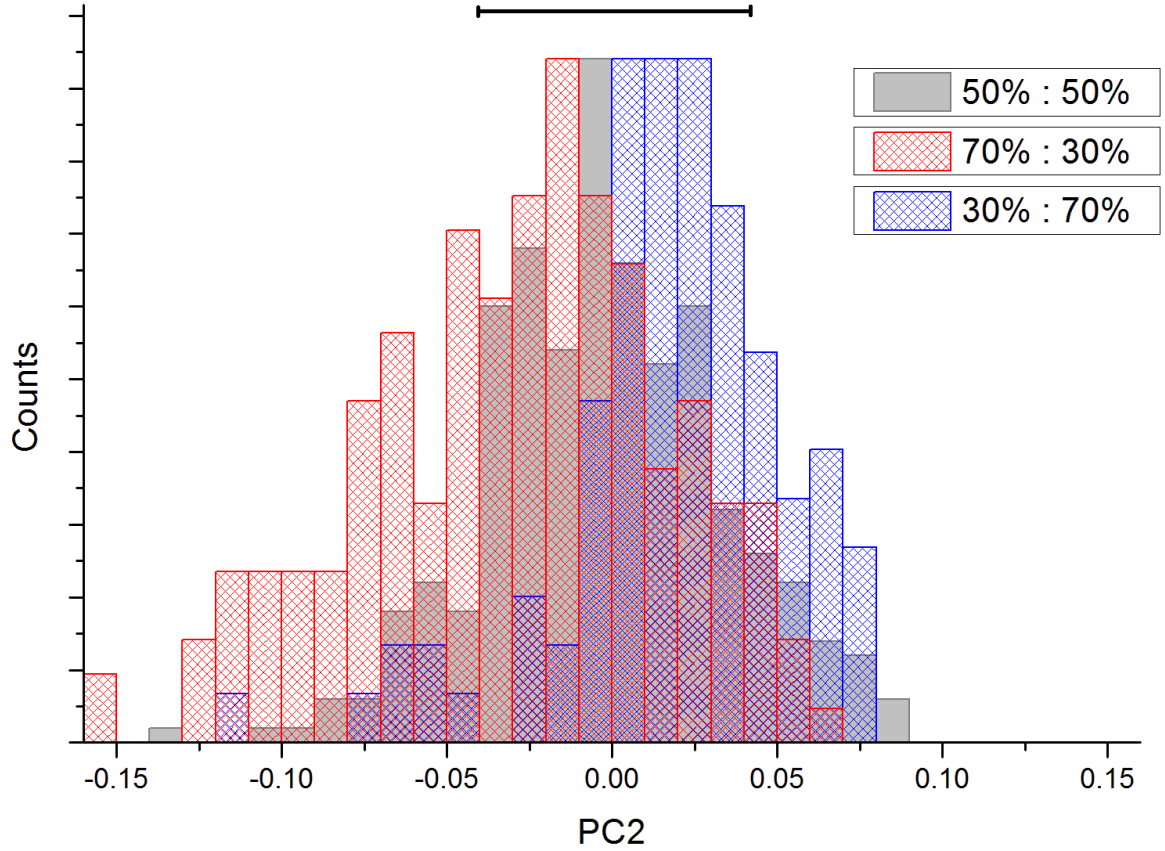

What's about primary cells? This is still an open question

Water: two sides of the same coin

"Water is

medi

er and

er"

Albert Szent-Gyor

dicine in 1937

With s

ins a

'nightmare

croscopy

Elettra Sincrotrone Trieste

FTIRM of live cells:

The physiological Conditions

Why

1- For fully exploiting the label-free capabilities of FTIRM
2- For collecting data of major biological relevance
3- For monitoring dynamic cellular processes

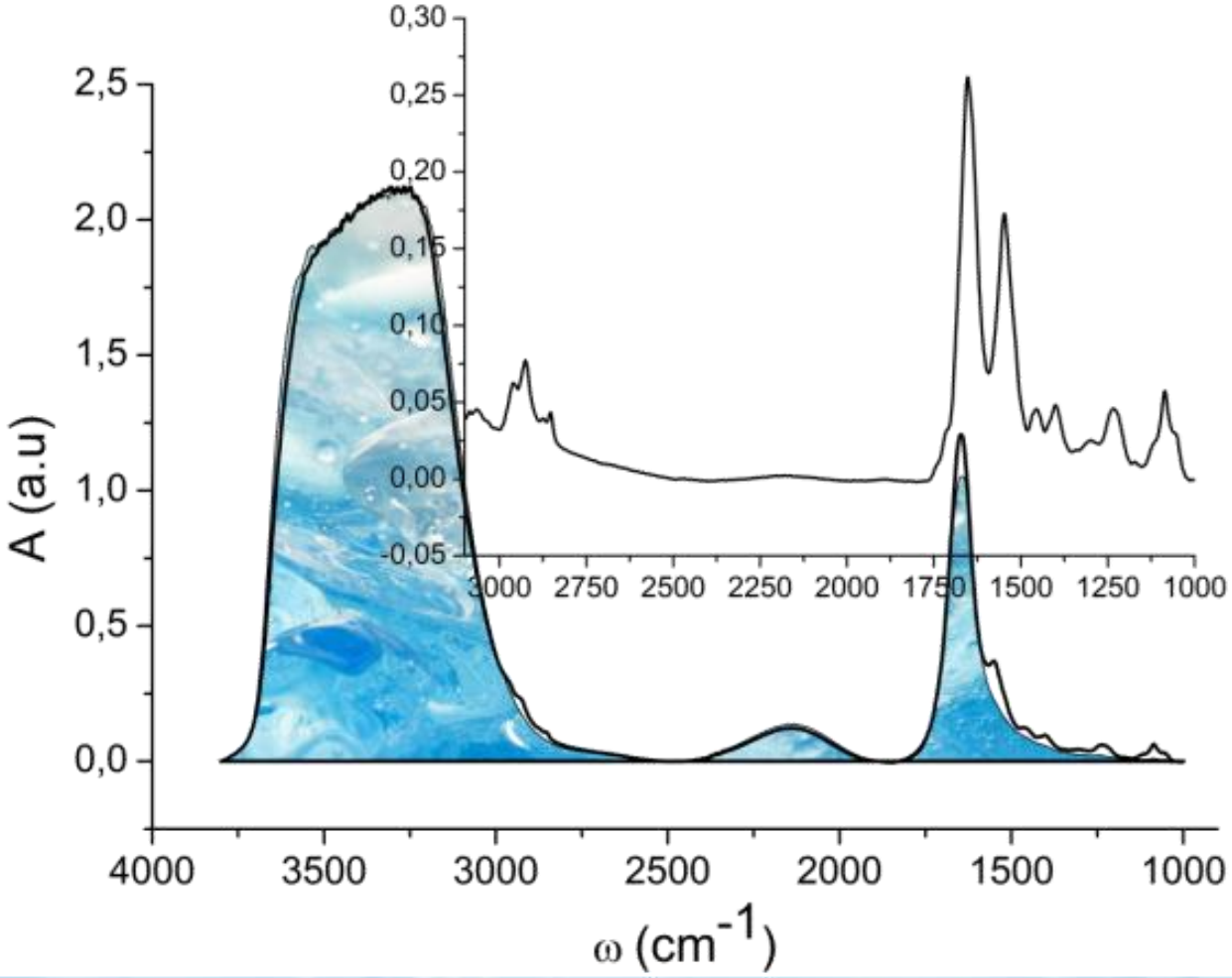

Cell Dry mass

~ 50% of proteins
~ 15% of carbohydrates
~ 15% of nucleic acids
~ 10% of lipids
~ 15% other molecules

Cellular water

~ 70% of the cell weight

Elettra
Sincrotrone
Trieste

Microtechnologies for IR-Live

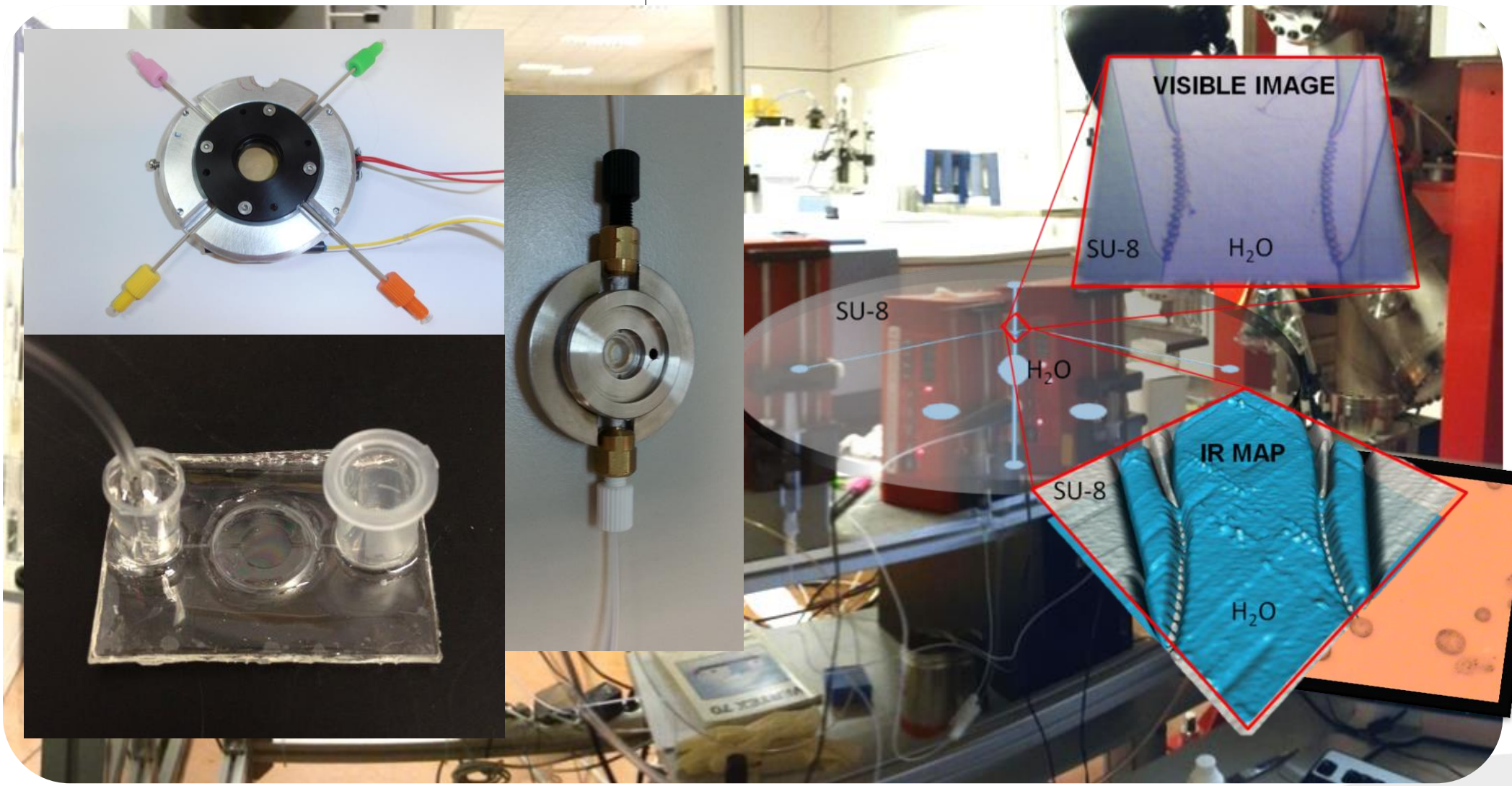

G. Birarda et al., **IR-Live: Fabrication of a low-cost plastic microfluidic device for infrared spectromicroscopy of living cells ,** *Lab Chip*, **2016**, Accepted Manuscript (**DOI:** 10.1039/C5LC01460C)

Mitri E., Birarda G., Vaccari L., Kenig S., Tormen M., Grenci G. **SU-8 bonding protocol for the fabrication of microfluidic devices dedicated to FTIR microspectroscopy of live cells .** *Lab on a Chip* **2014** *14(1)*, 210-8

Mitri E., Pozzato A., Coceano G., Cojoc D., Vaccari L., Tormen M., Grenci G. **Highly IR-transparent microfluidic chip with surface-modified BaF 2 optical windows for Infrared Microspectroscopy of living cells.** Microelectronic Engineering **2013** *107*, 6-9

Advantages of live cell analysis

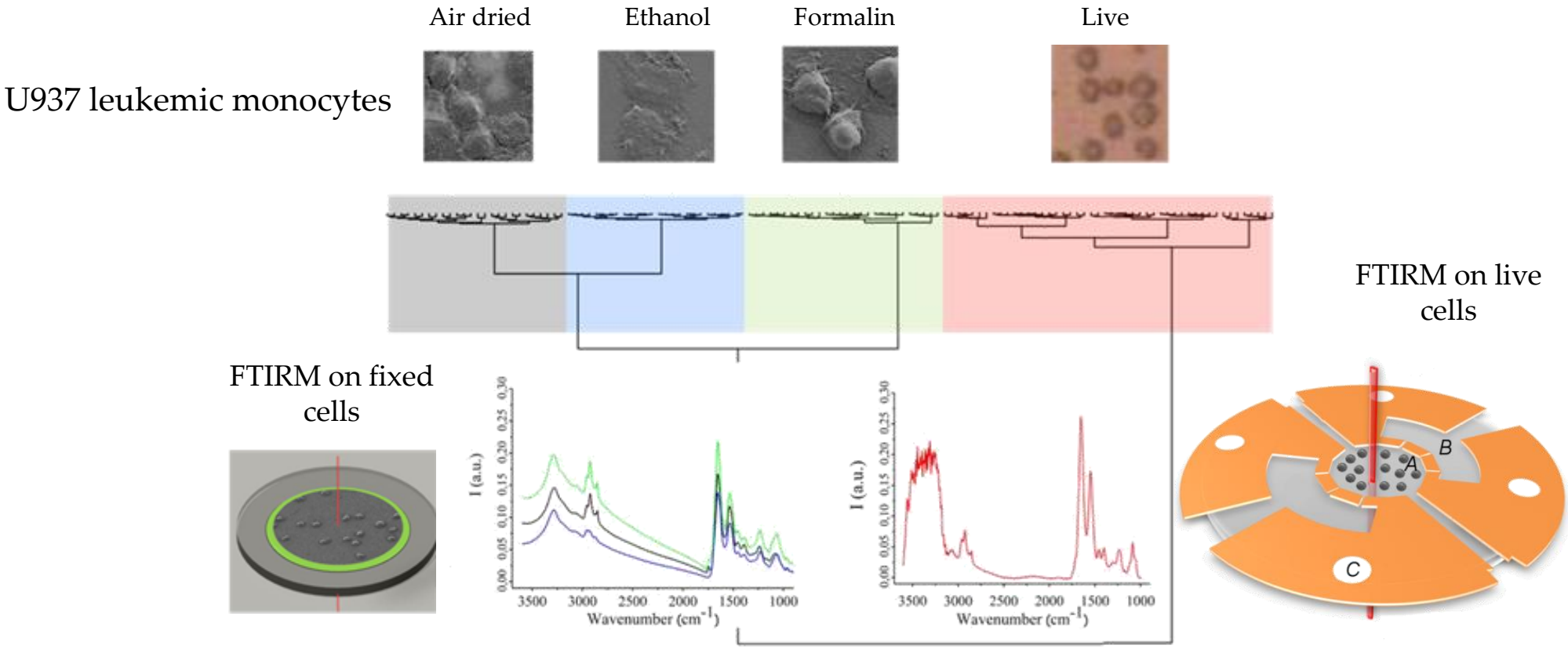

- Ethanol dramatically alters both membrane order (increased disorder) and composition. It also induces protein aggregation and precipitation, as well as a massif loss of cellular material
- Formalin well preserves both cellular membranes and protein secondary structure, similarly to unfixed air-dried cells. However, unfixed cells are not stable in time
- Nucleic acid structure is affected by both formalin and ethanol as well as by air-drying. Dehydration induces the B-DNA to A-DNA transition (1120 → 1240 cm^{-1}), limiting FTIRM diagnostic capabilities

Reliable spectroscopic assessment of nucleic acid content and structure can be done only under hydrated conditions

L. Vaccari, G. Birarda, L. Businaro, S. Pacor and G. Grenci. **Infrared Microspectroscopy of Living Cells in Microfluidic Devices (MD-IRMS): Toward a Powerful Label-Free Cell-Based Assay.** *Analytical Chemistry* **2012,** *84 (11),* 4768–4775

Cell life: Cell cycle analysis by FTIRM

Elettra Sincrotrone Trieste

Cell cycle stages

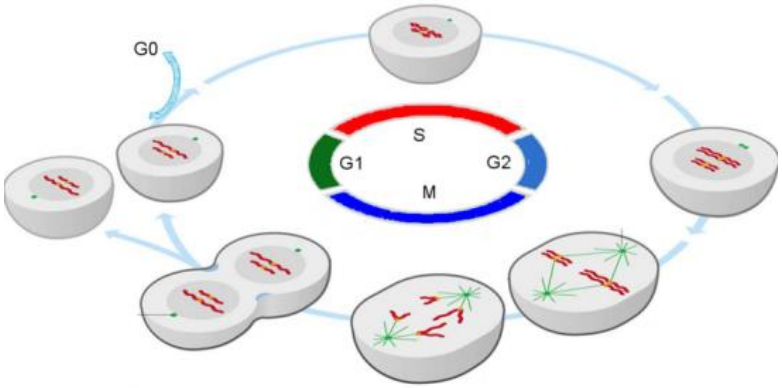

Cell growth

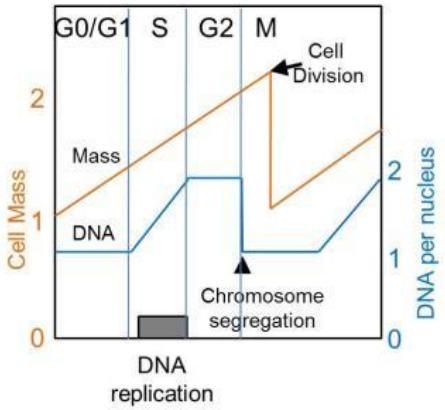

Cell cycle analysis by FC

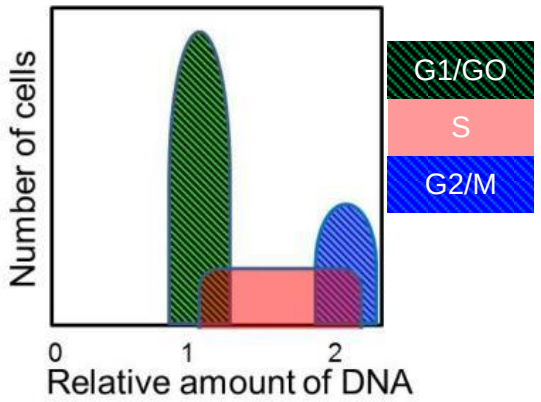

Experimental Design

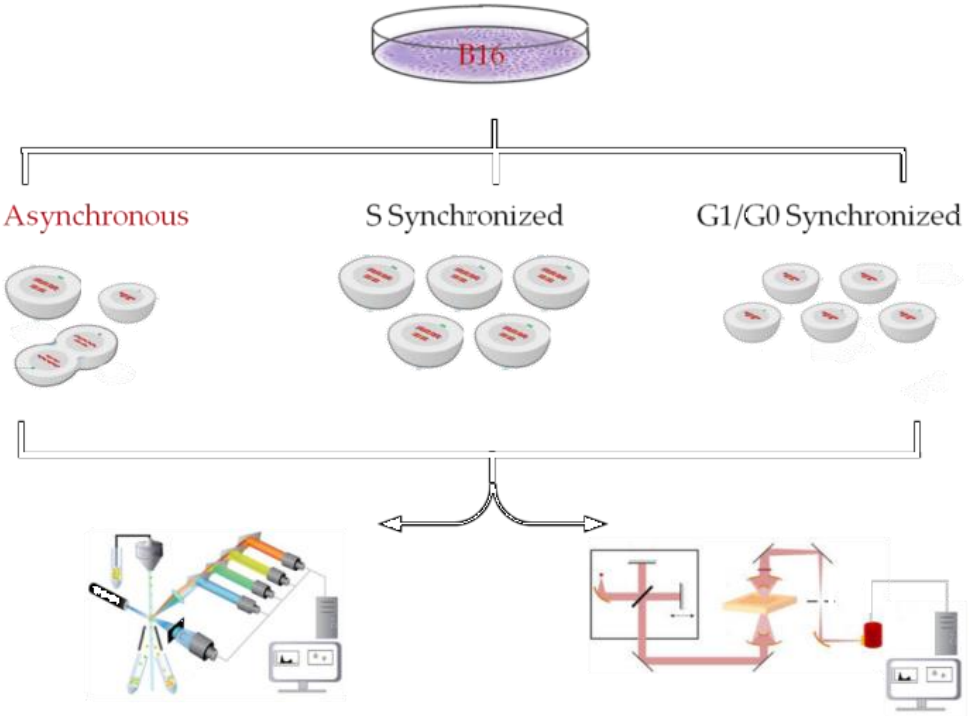

Elettra Sincrotrone Trieste

From PI-FC to FTIRM

FC Analysis

HCA on FTIRM

HCA Centroids

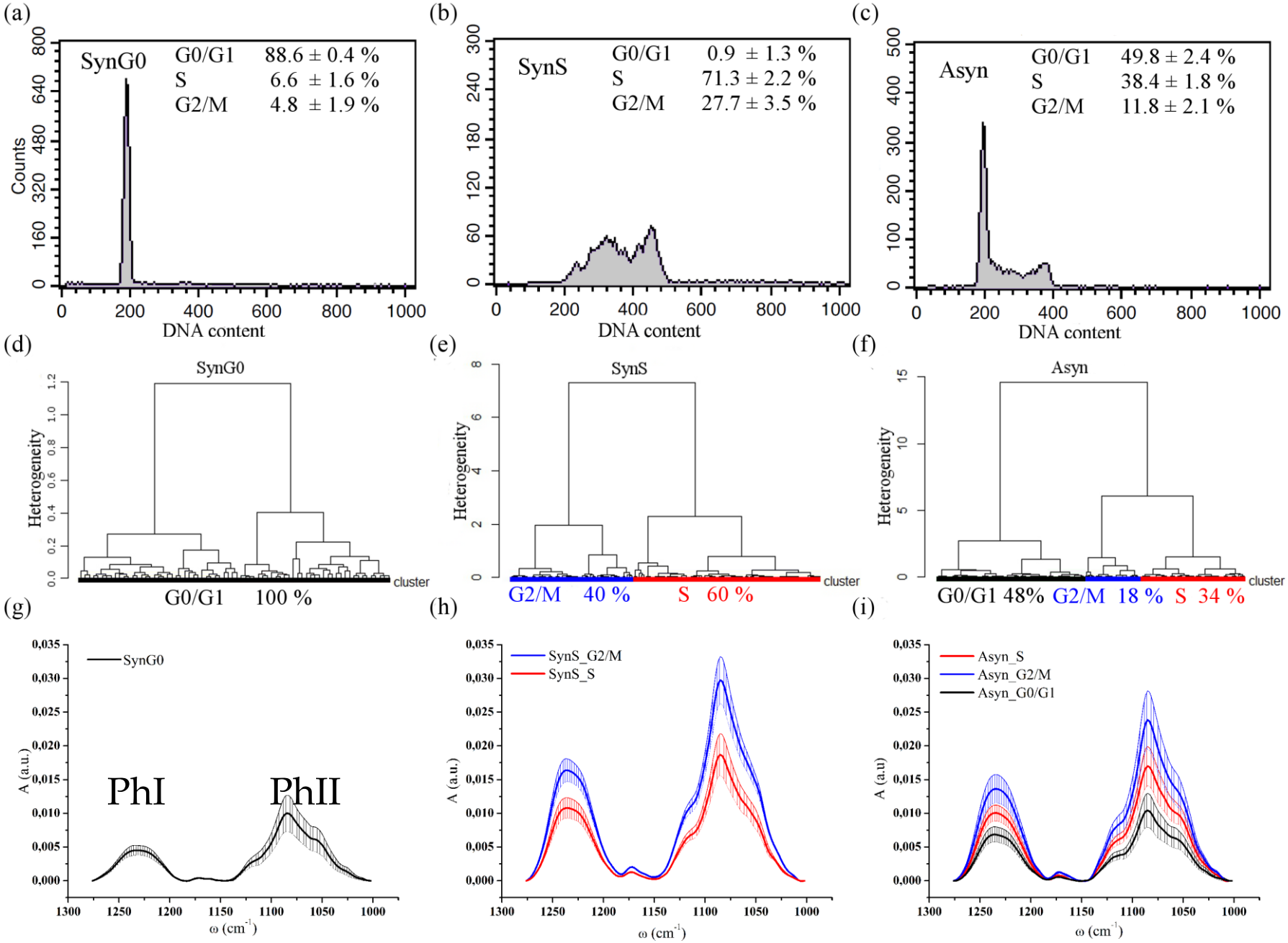

Elettra
Sincrotrone
Trieste

From PI-FC to FTIRM

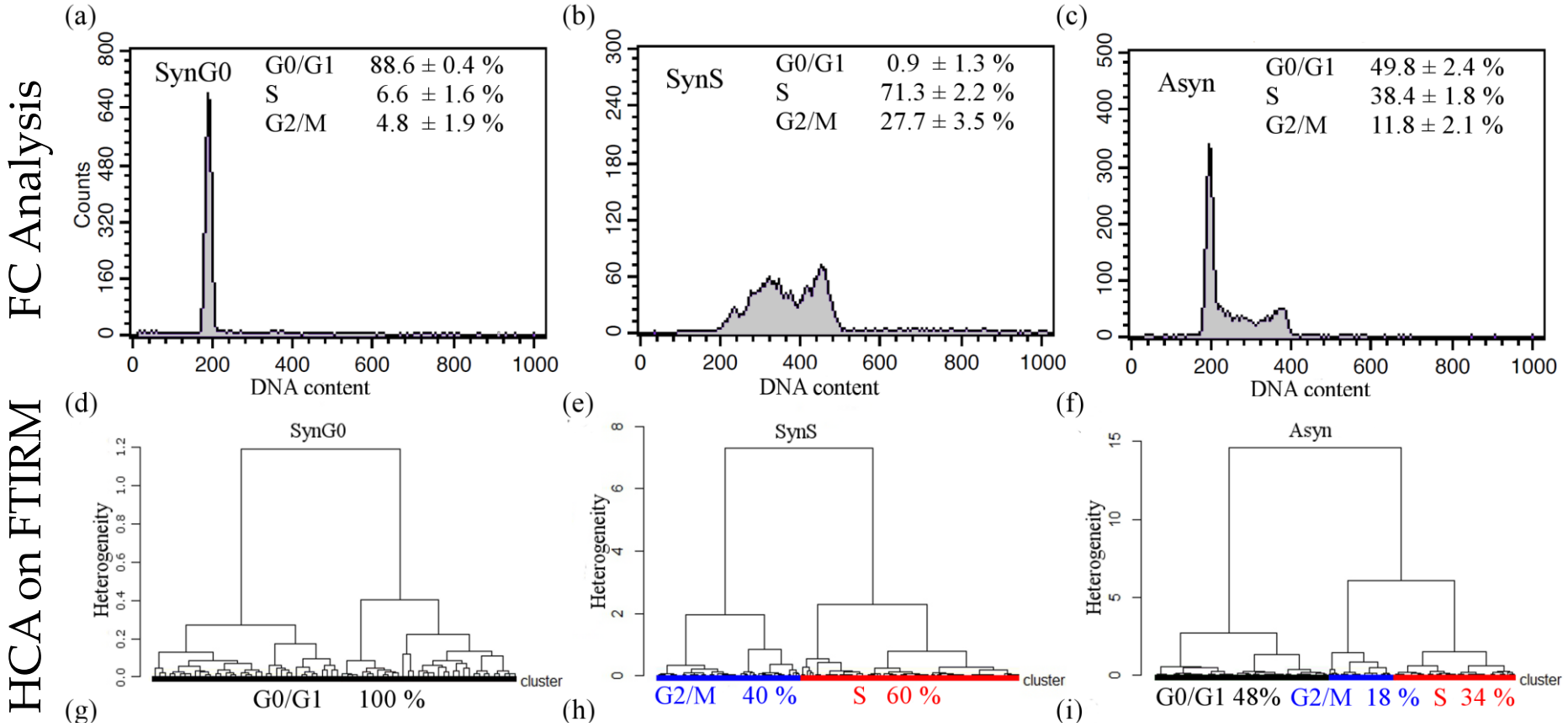

Discrimination between G1/G0, S and G2/M phases of the cell cycle is possible in-situ on live cells by FTIRM with a degree of accuracy comparable to PI-FC

Bedolla DE, Kenig S, Mitri E, Ferraris P, Marcello A, Grenci G, Vaccari L. **Determination of cell cycle phases in live B16 melanoma cells using IRMS.** Analyst **2013**, 138 (14), 4015–21

Elettra
Sincrotrone
Trieste

From PI-FC to FTIRM

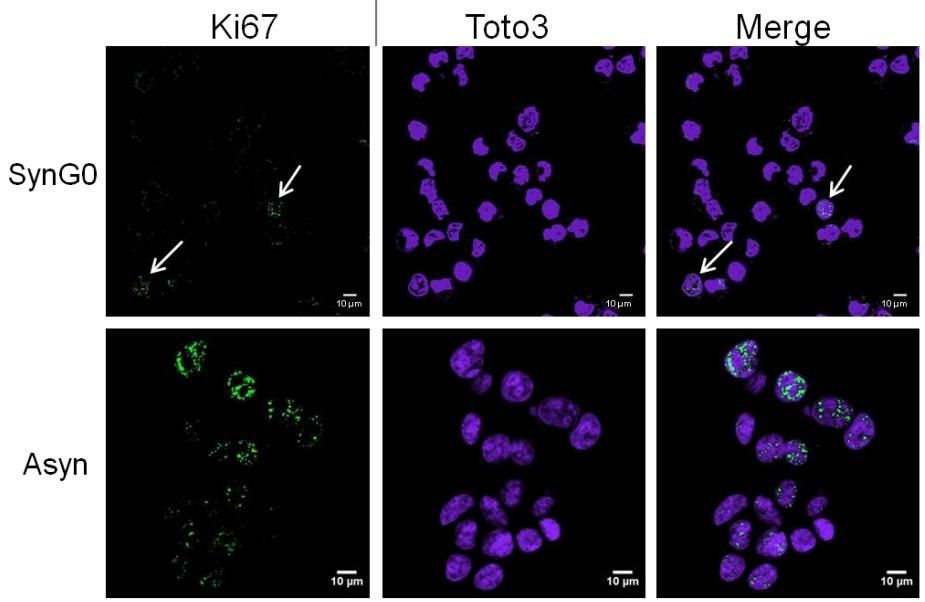

FTIRM can discriminate between progressive G1 and G0 quiescent cell cycle stages

$RNA/(RNA+DNA) \approx 0.5$ G1, S, G2, M

$RNA_{G0} \approx \frac{1}{2} RNA_{G1}$

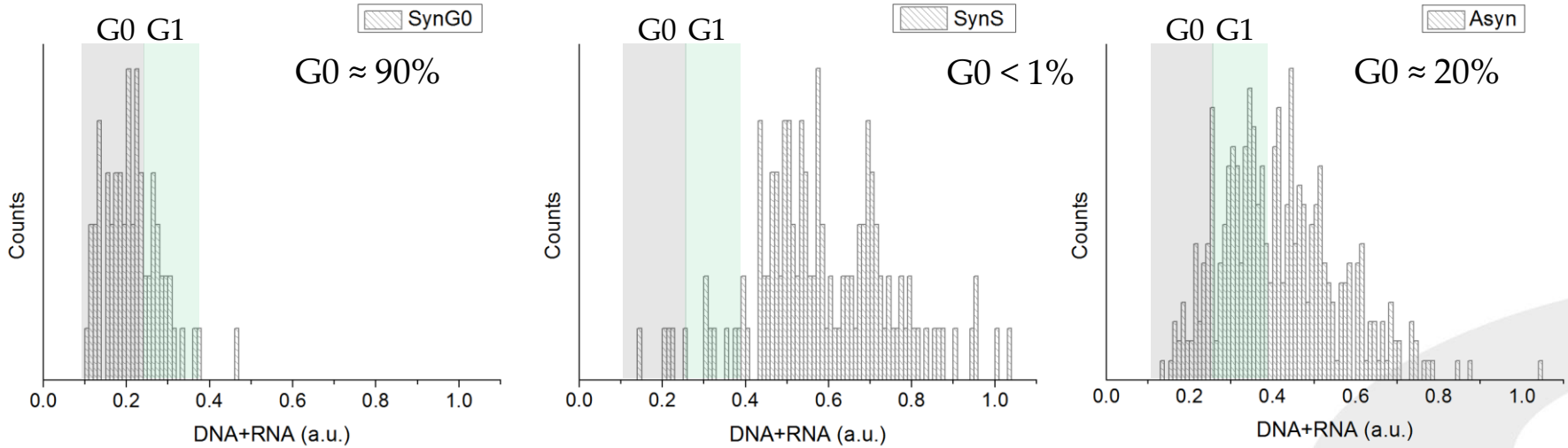

Diana E. Bedolla, Saša Kenig, Elisa Mitri, Paola Storici, Lisa Vaccari. **Further insights into the assessment of cell cycle phases by FTIR microspectroscopy.** *Vibrational Spectroscopy* **2014,** *75*, 127–35

Elettra
Sincrotrone
Trieste

In-cell RNA spectral features

The spectral features of a molecule in a cell can not be entirely described by the isolated molecule

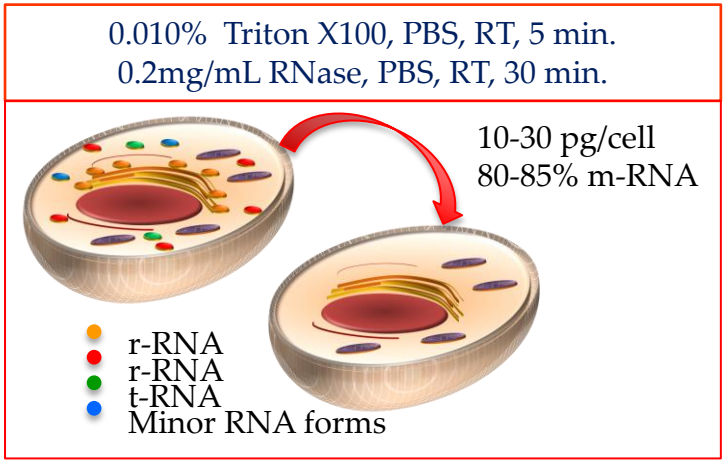

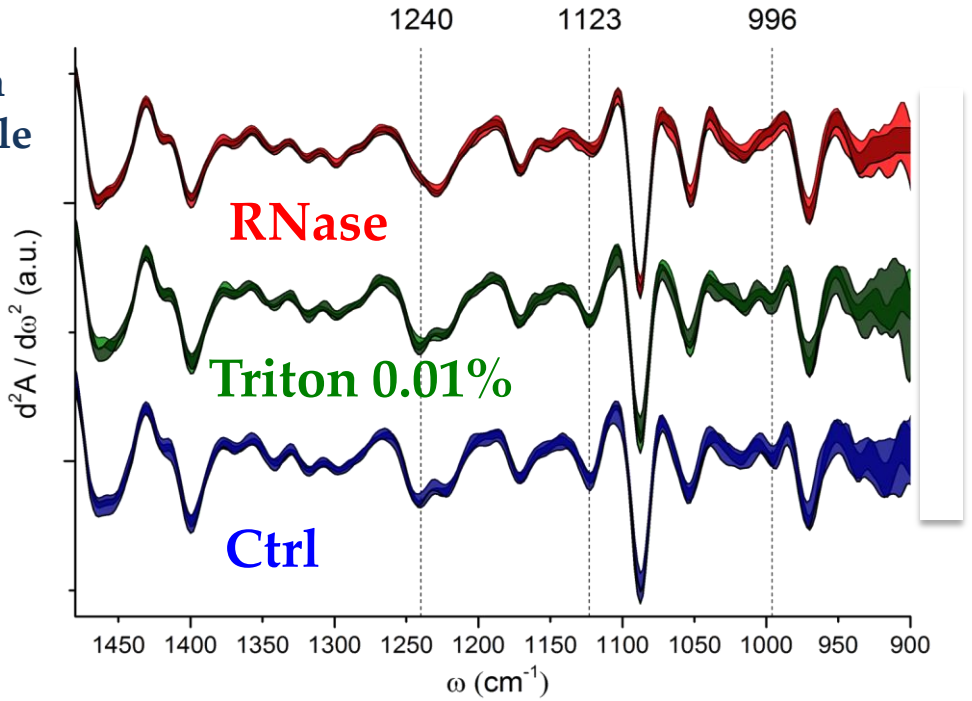

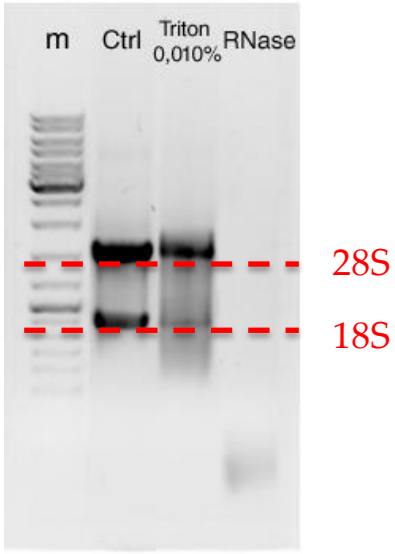

• Permeabilization at very low Triton concentrations does not affect the biochemical cellular composition

• Only three well defined spectral contributions <u>are affected</u> by RNase treatment, centered at & "classically" assigned to:

- ~ **1240** cm^{-1}: Asym. Stretch. of phosphodiester group of RNA + phospolipids + Amide III (<u>in which proportion?</u>)
- ~ **1123** cm^{-1}: Sym. Stretch. of phosphodiester group of RNA & Asym C-O Stretch. of Ribose
- ~ **996** cm^{-1}: Sym. C-O Stretch. of Ribose

Elettra
Sincrotrone
Trieste

From AO-FC to FTIRM

Results of FC with Acridine Orange

Acridine orange: Nucleic acid selective fluorescent dye
DNA probe: Exc: 502 nm Em: 525 (green)
RNA probe: Exc: 460nm; Em: 650 nm(red)

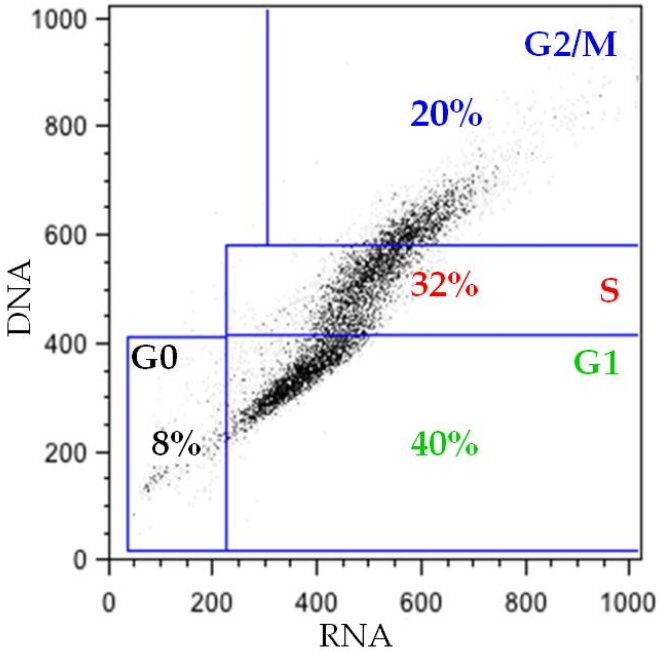

FTIRM Results

New method for baseline correction
New developed program for spectral band fitting

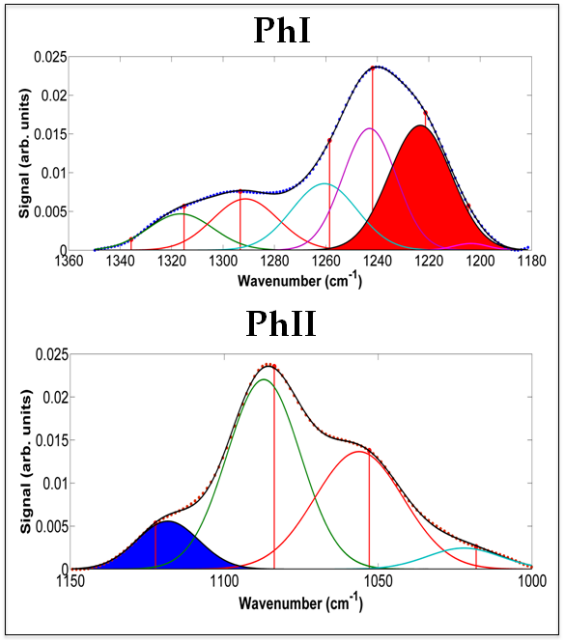

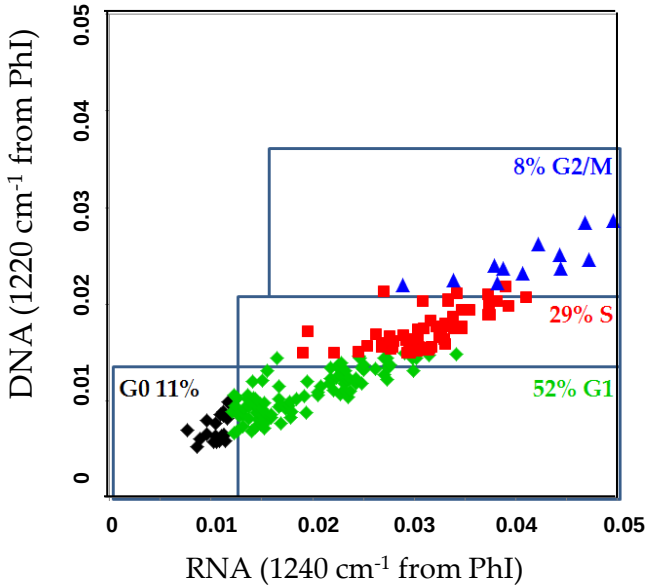

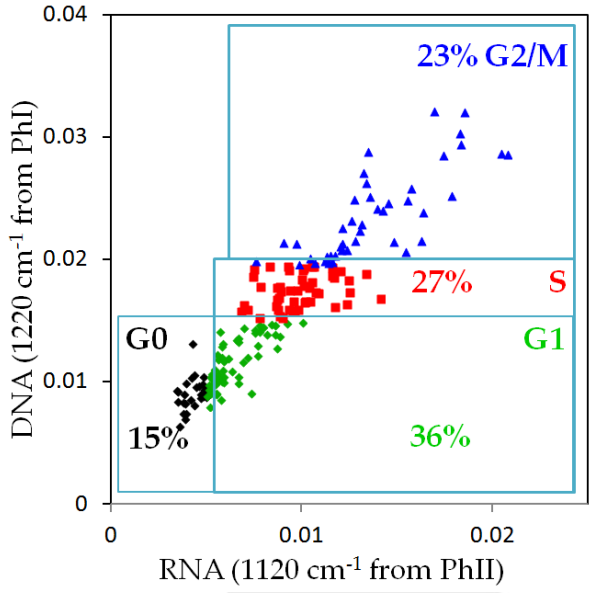

Elettra Sincrotrone Trieste

Real-time cellular dynamics

Heat Shock Response

Regular temperature

HSP proteins

Folded proteins

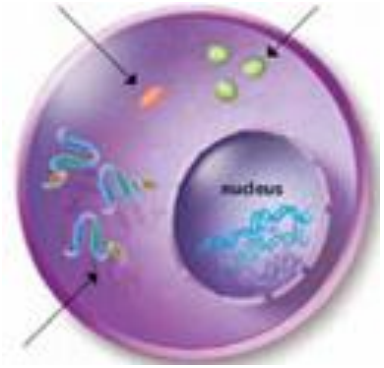

Inactive Heat-shock transcription factors (HSF)

Temperature increase

Misfolded proteins

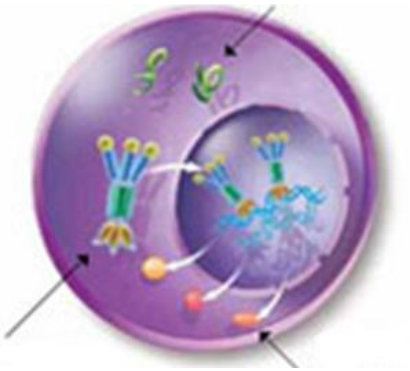

Active HSF

HSP bonded to Misfolded proteins

New HSP proteins

Native folding restoring

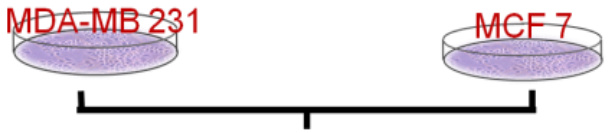

Cells were collected, pelleted, washed and resuspended in physiological solution

Experimental Design

IRMS measurements

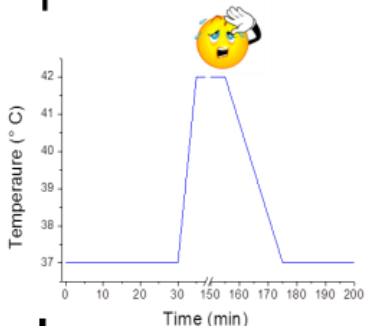

Mild	39.5±1° C
Severe	42.5±1° C
Deleterious	45.5±1° C

Elettra
Sincrotrone
Trieste

Initial State

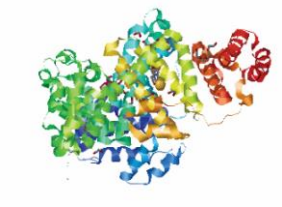

Initial state

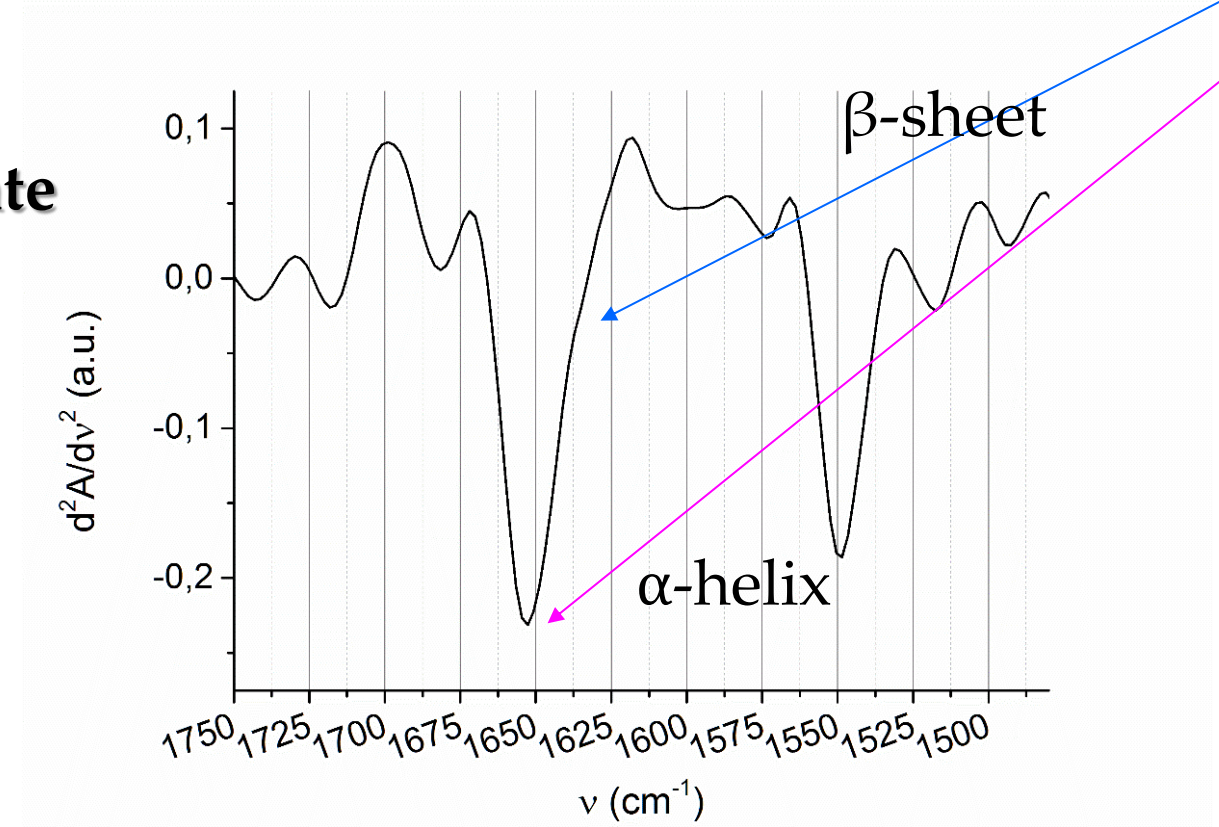

Elettra
Sincrotrone
Trieste

Immediate Response: 5-10 minutes

Initial state

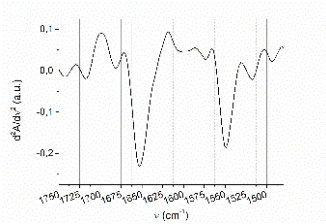

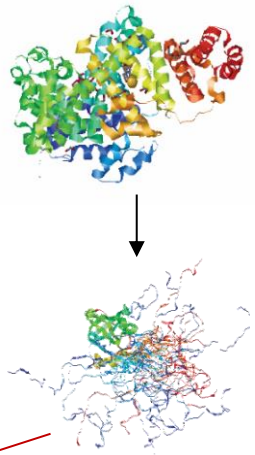

5 minutes

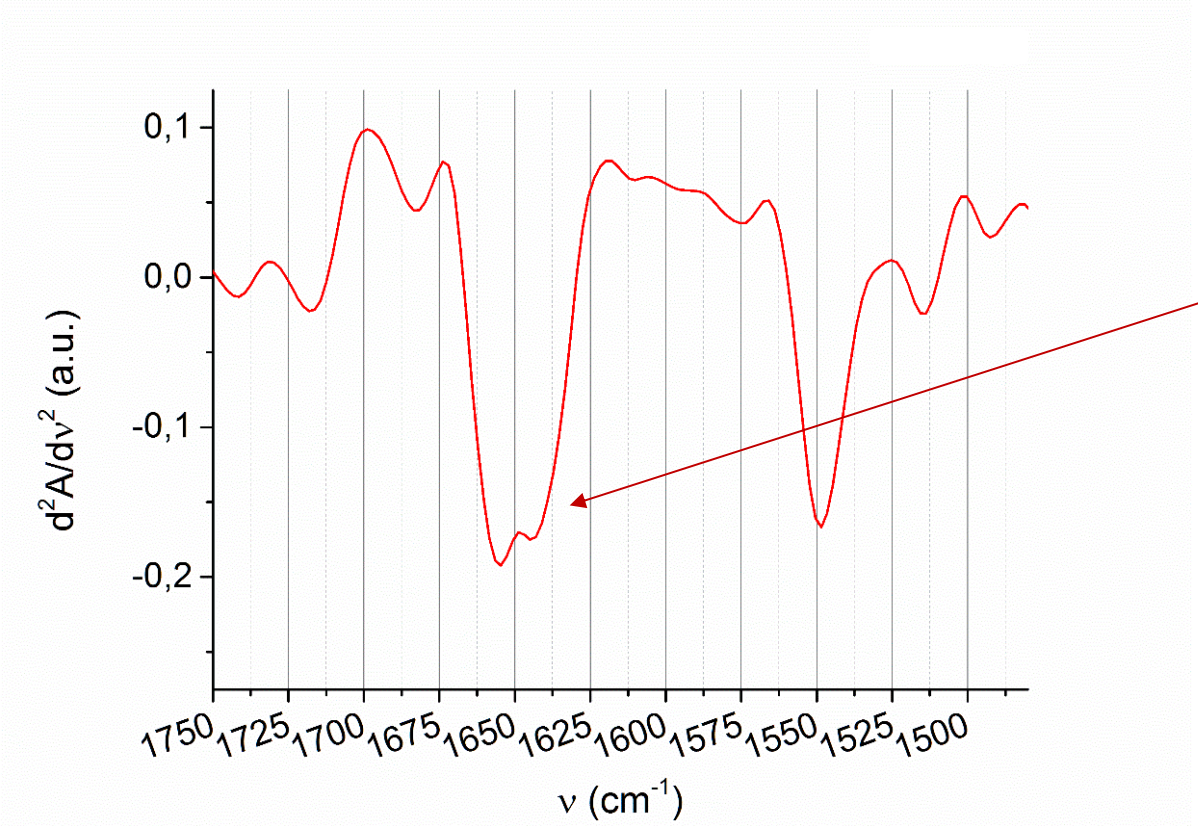

Elettra
Sincrotrone
Trieste

Immediate Response: 5-10 minutes

Initial state

5 min

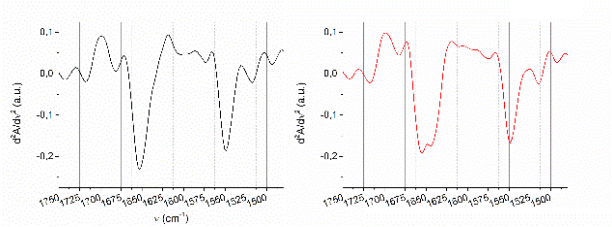

10 minutes

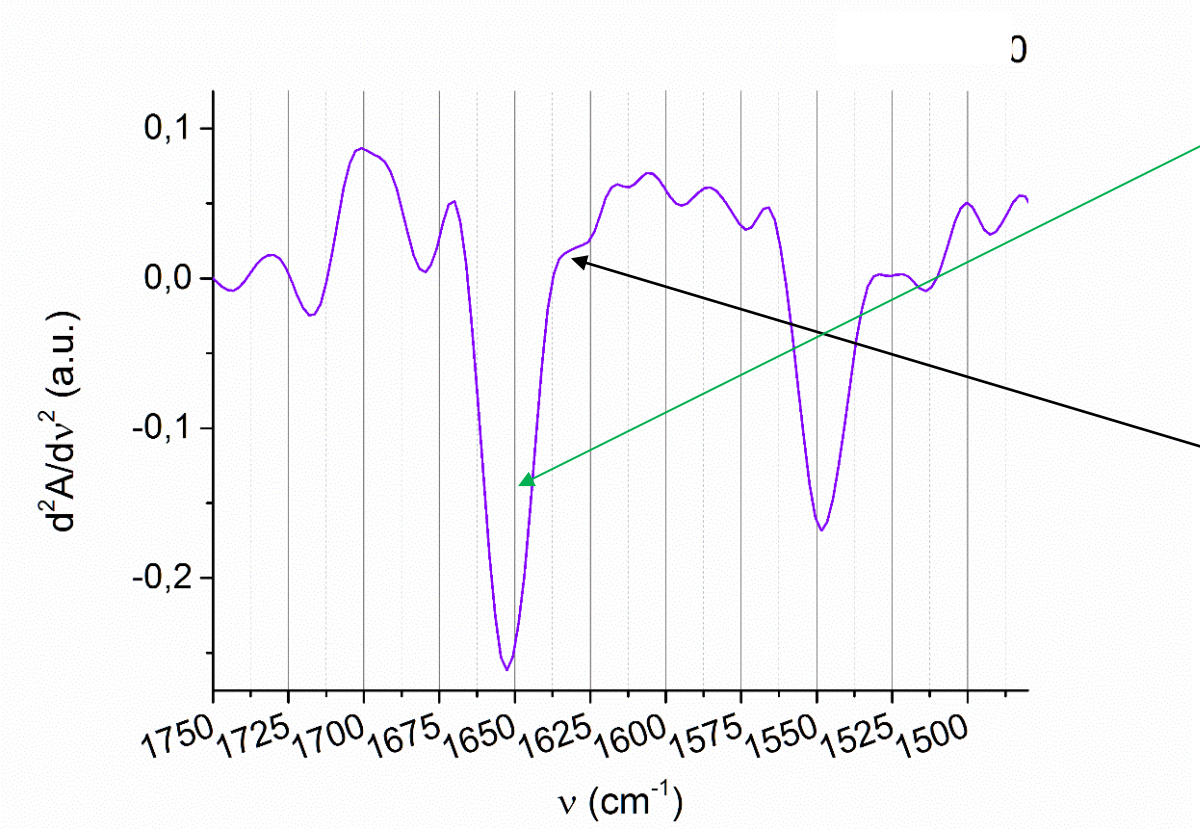

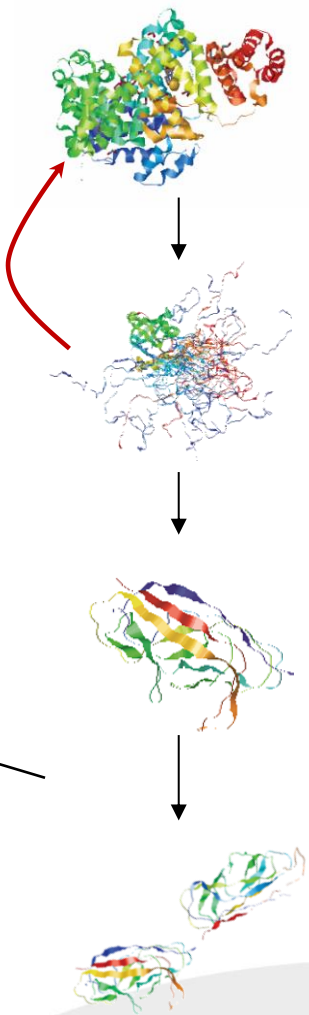

Elettra
Sincrotrone
Trieste

Early Response: 15-35 minutes

Initial state 5 min 10 min

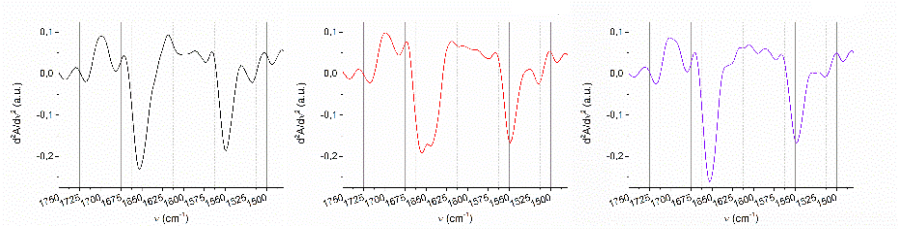

15-25 minutes

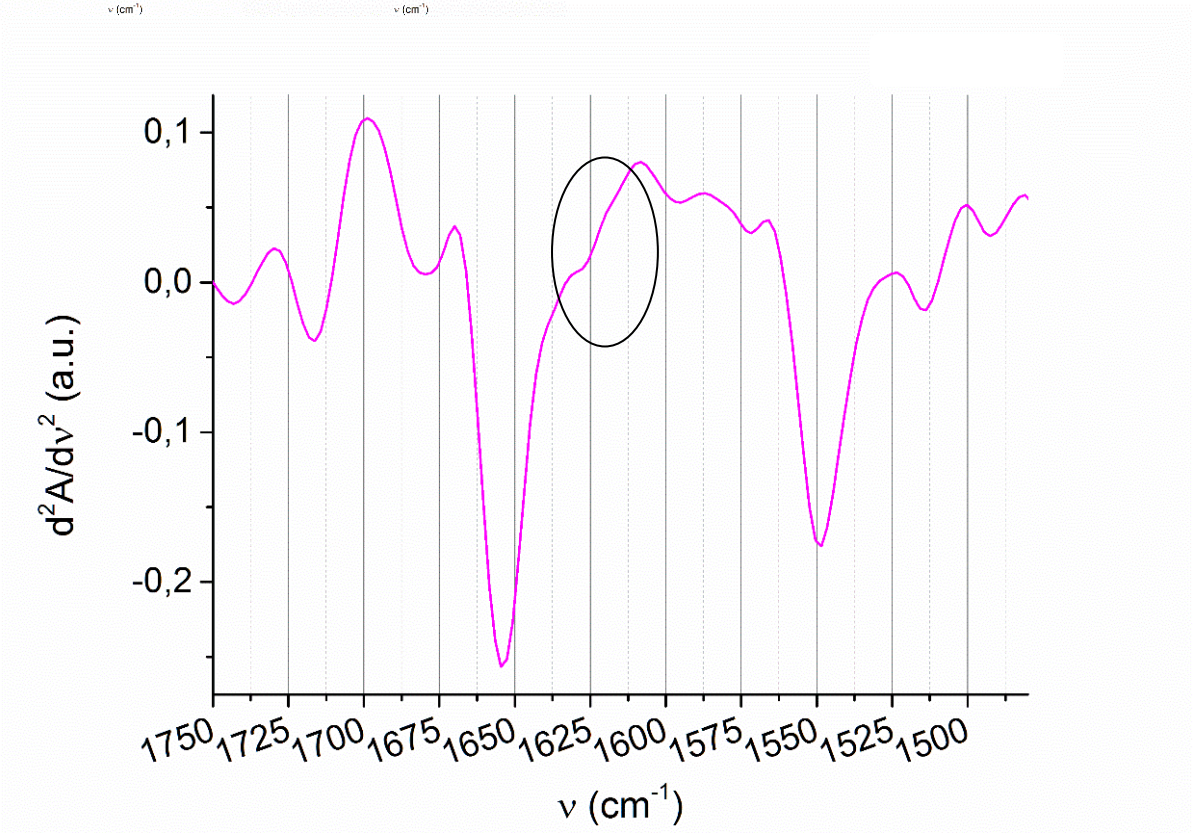

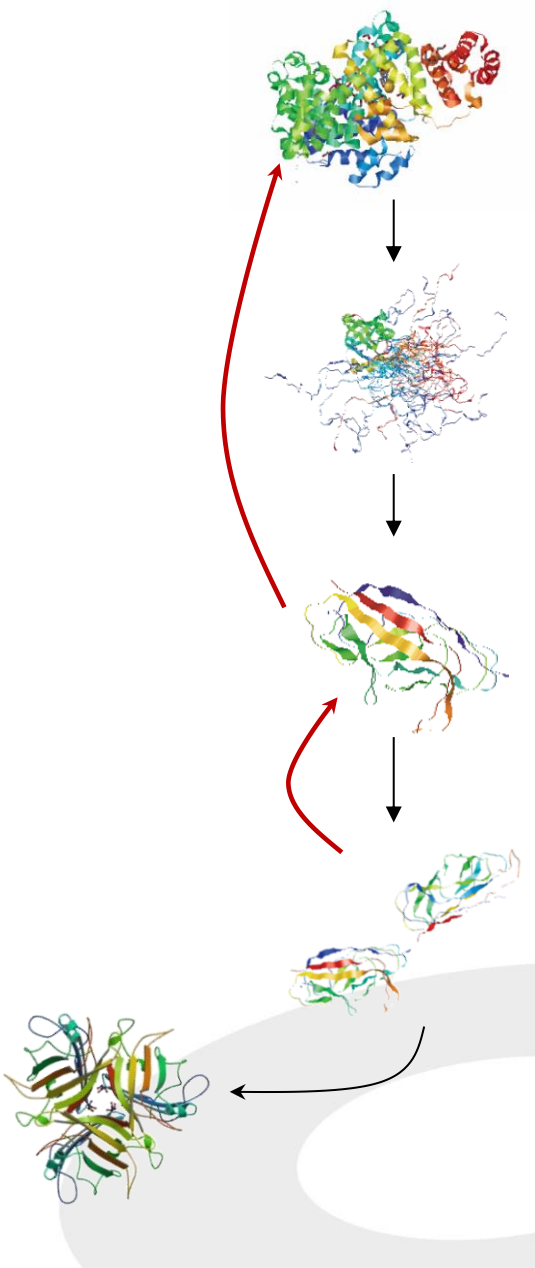

Elettra
Sincrotrone
Trieste

Early Response: 15-35 minutes

Initial state | 5 min | 10 min | 10-25 min

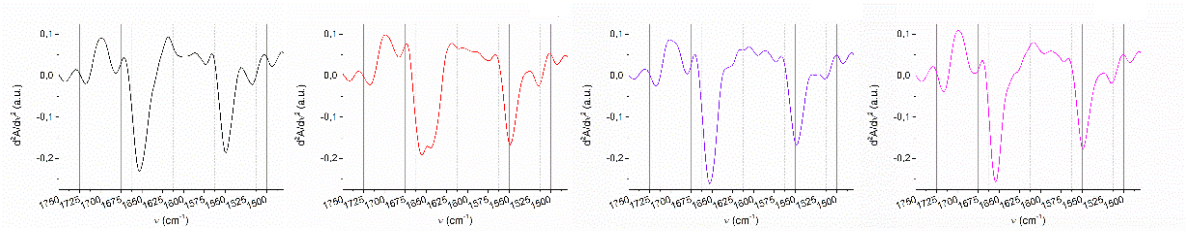

30 minutes

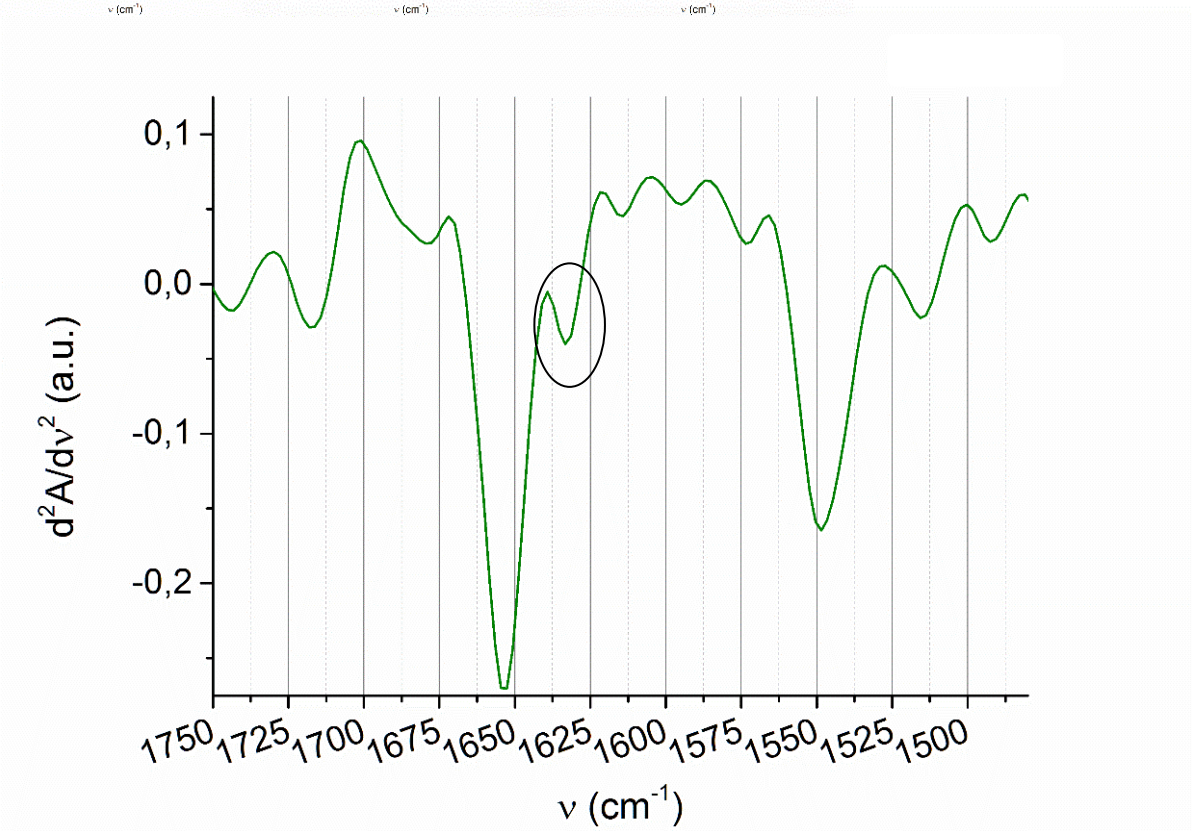

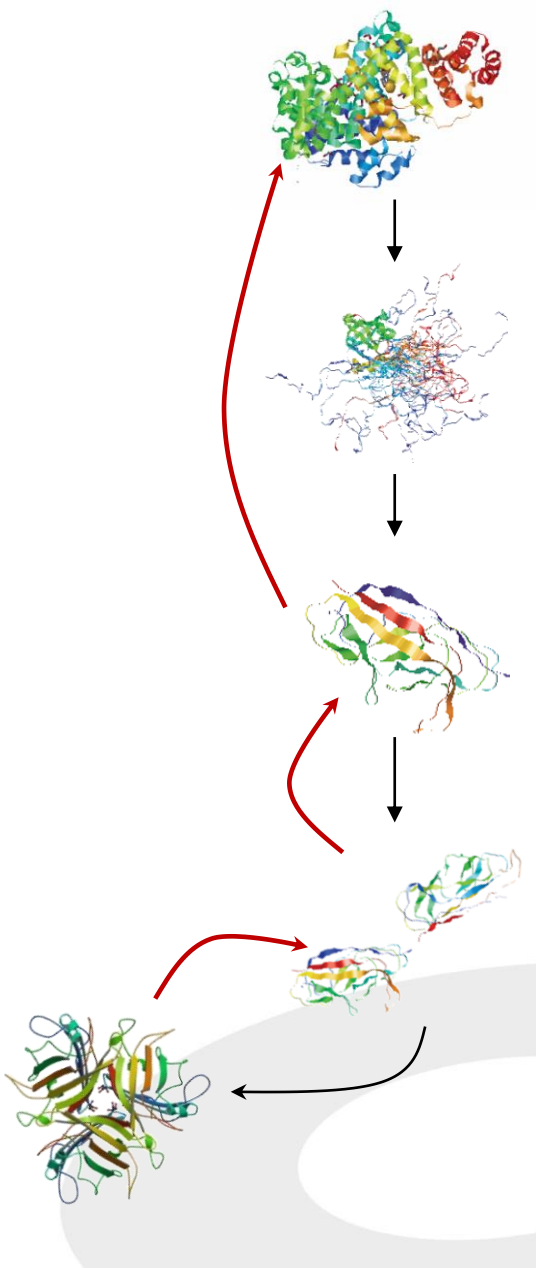

Elettra Sincrotrone Trieste

Late Response: 40-120 minutes

Initial state | 5 min | 10 min | 15-25 min | 30 min

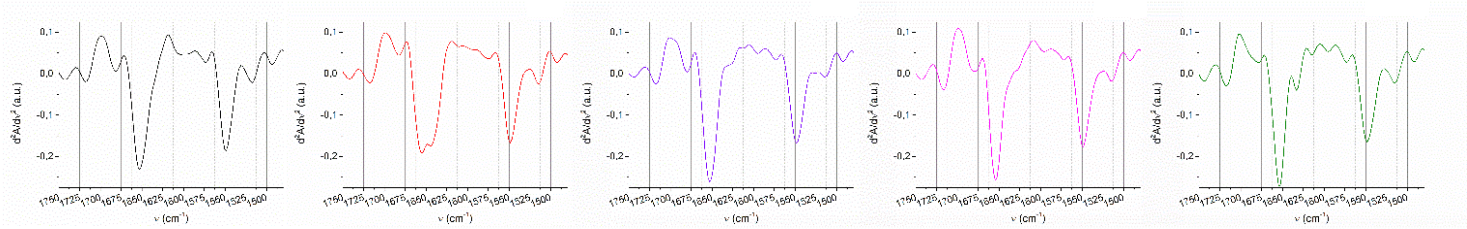

40 minutes

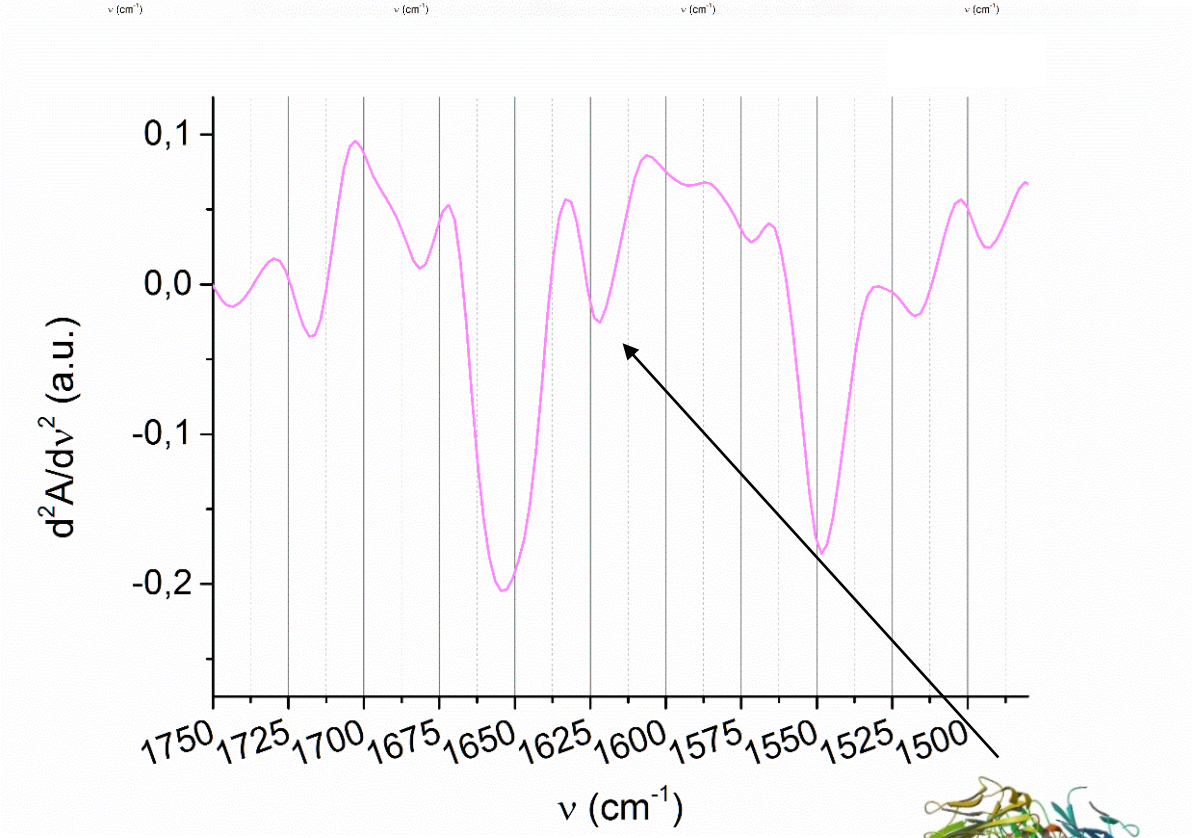

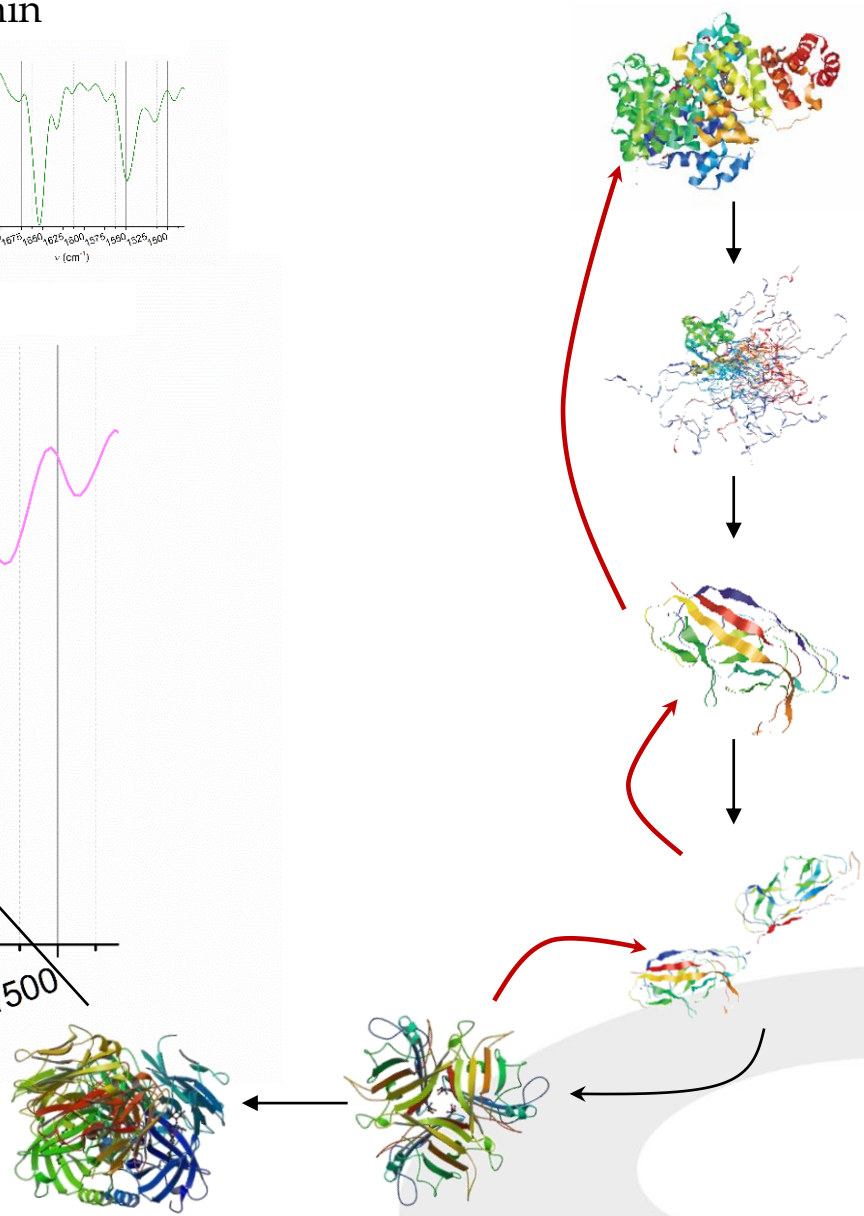

The final State: 130 minutes

Initial state | 5 min | 10 min | 15-25 min | 30 min | 40 min

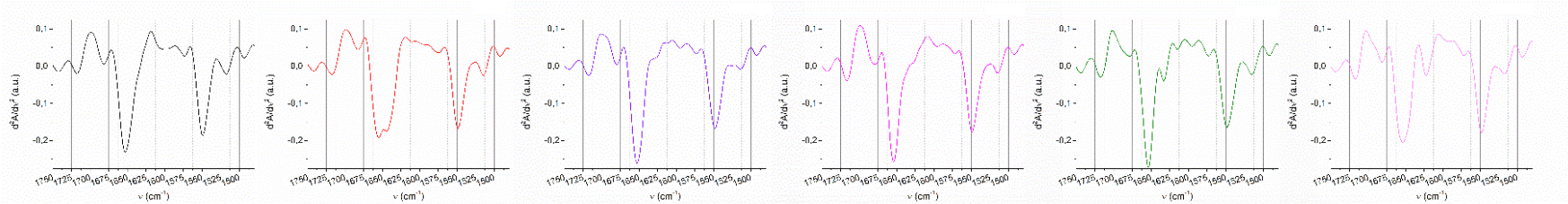

Final state

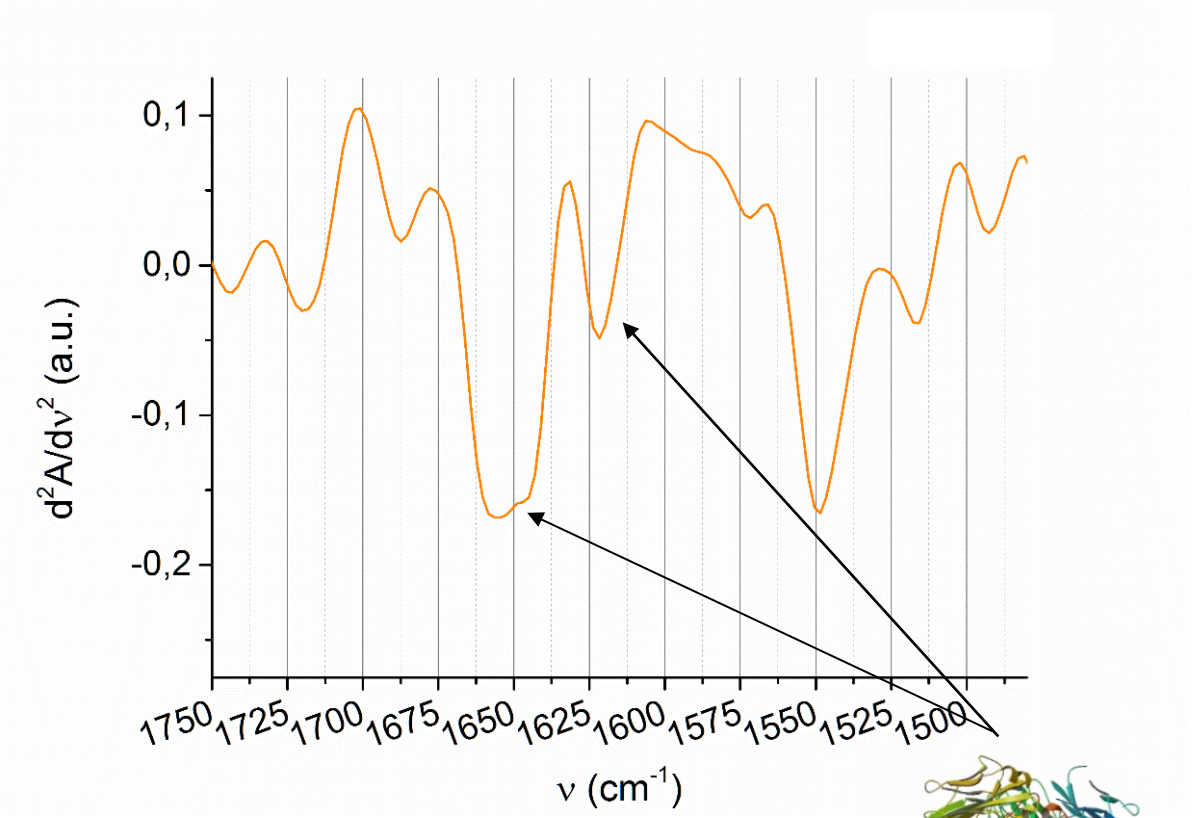

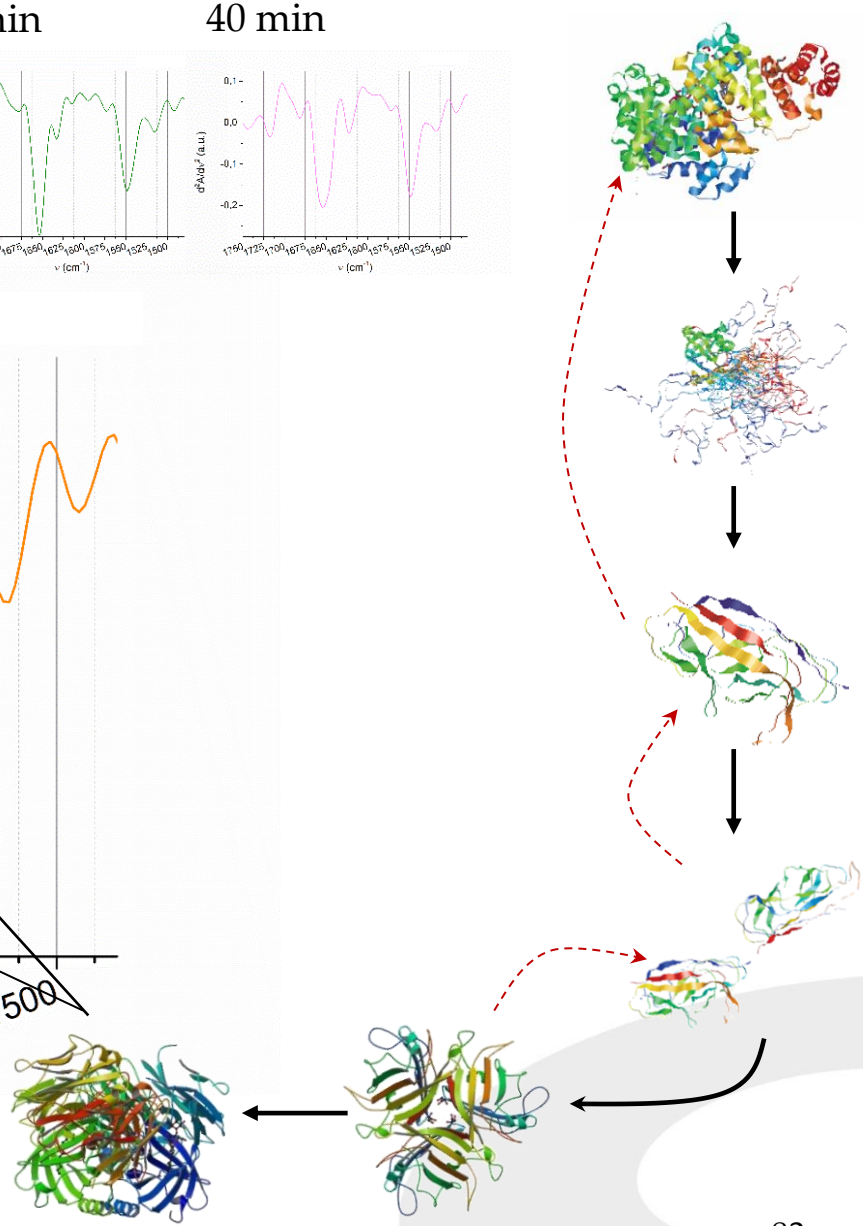

Elettra
Sincrotrone
Trieste

Time-Resolved FTIRM in Live Cells

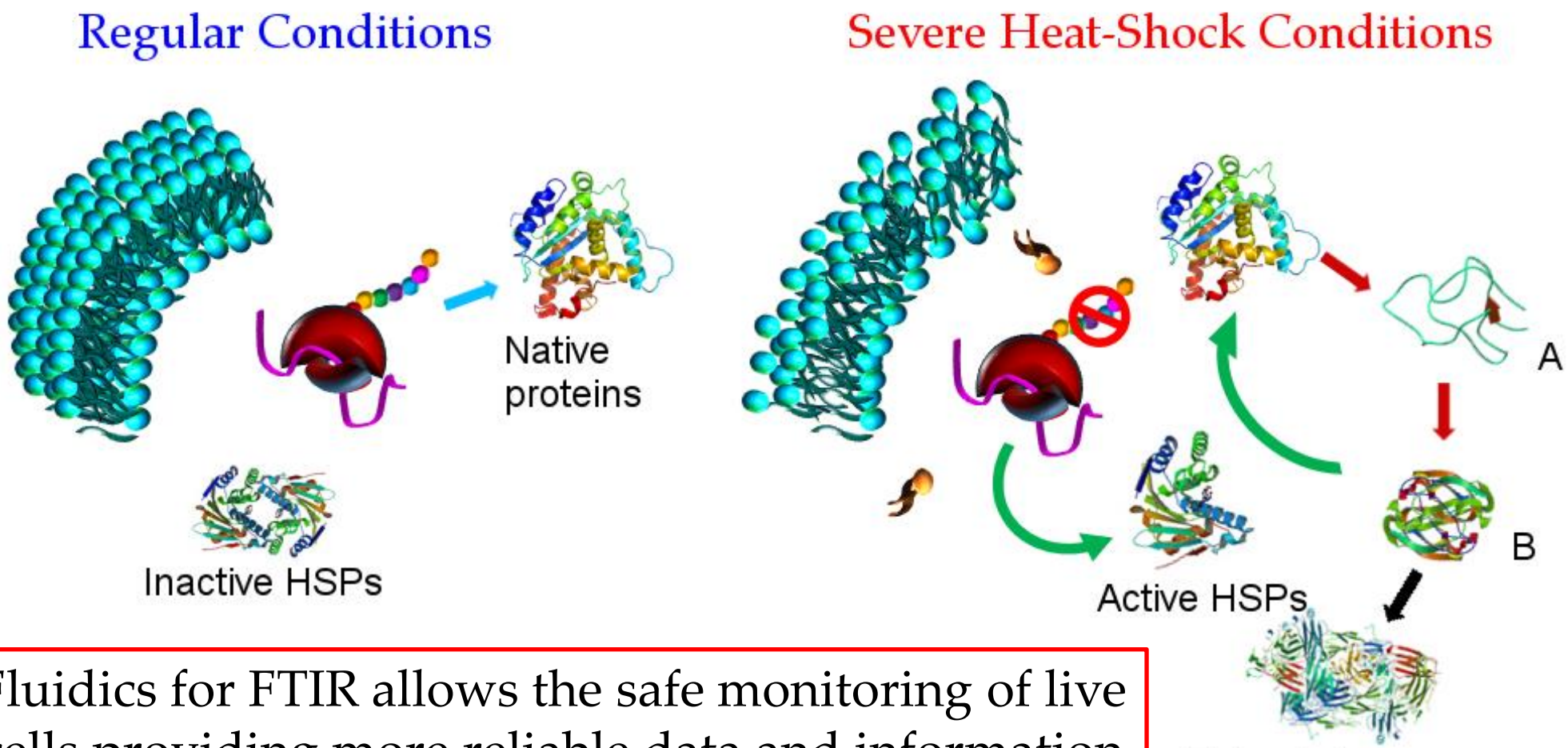

Fluidics for FTIR allows the safe monitoring of live cells providing more reliable data and information on the cellular dynamics

Elisa Mitri, Saša Kenig, Giovanna Coceano, Diana E. Bedolla, Massimo Tormen, Gianluca Grenci, and Lisa Vaccari. **Time-Resolved FT-IR Microspectroscopy of Protein Aggregation Induced by Heat-Shock in Live Cells.** *Analytical Chemistry*, 2015, **87(7)**: 3670-77

Where is the future of SR-FTIR?

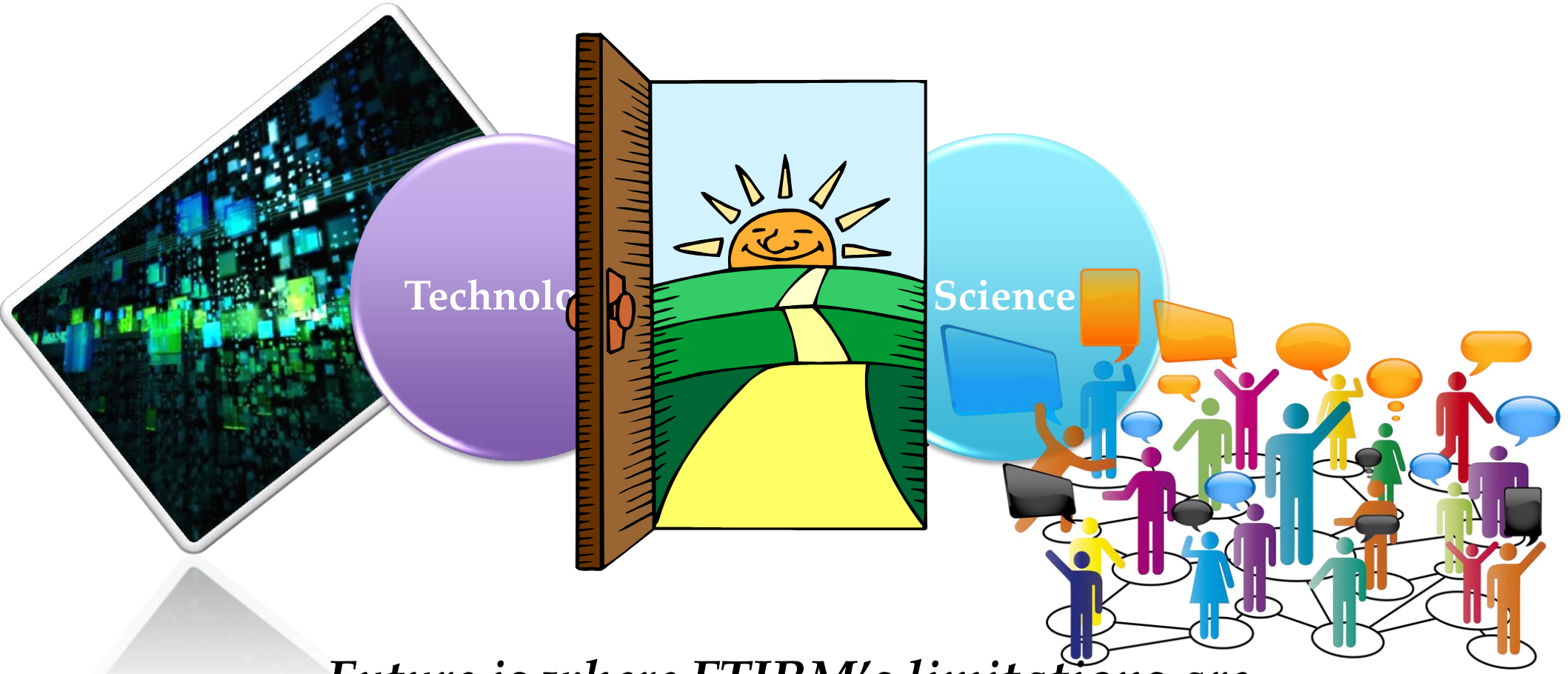

Future is where FTIRM's limitations are

- *Slow data acquisition*
- *Limited lateral resolution*
- *Limited sensitivity (micromolar regime)*

Elettra
Sincrotrone
Trieste

From FTIR Microscopy to FTIR Imaging

Speeding data acquisition by using 2D multiplex MIR detectors

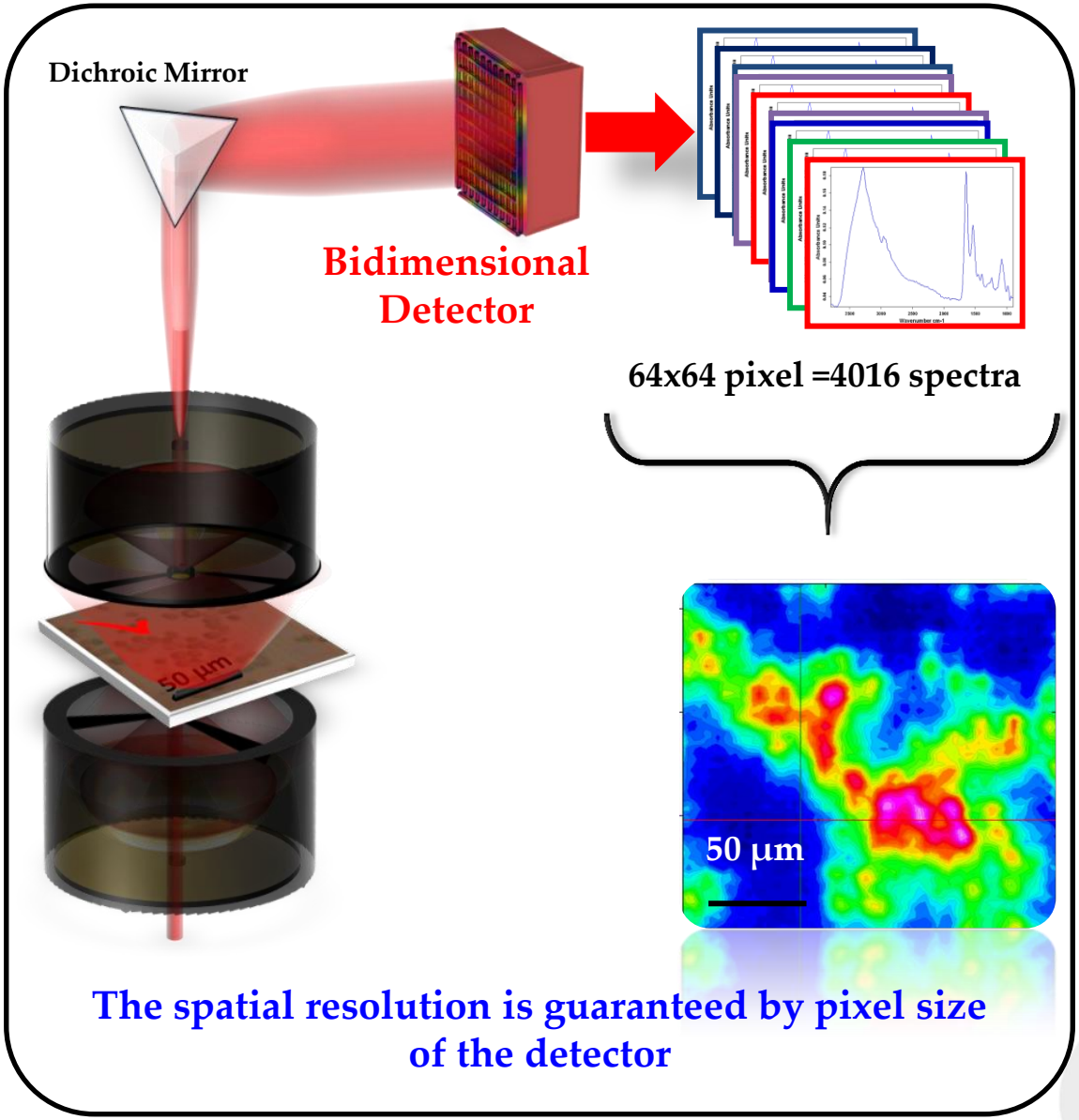

The spatial resolution is guaranteed by pixel size of the detector

Elettra
Sincrotrone
Trieste

From FTIR Microscopy to FTIR Imaging

IRENE (SRC, Wisconsin): a dedicated beamline

Wide horizontal extraction: 320X27 mrad (HXV)

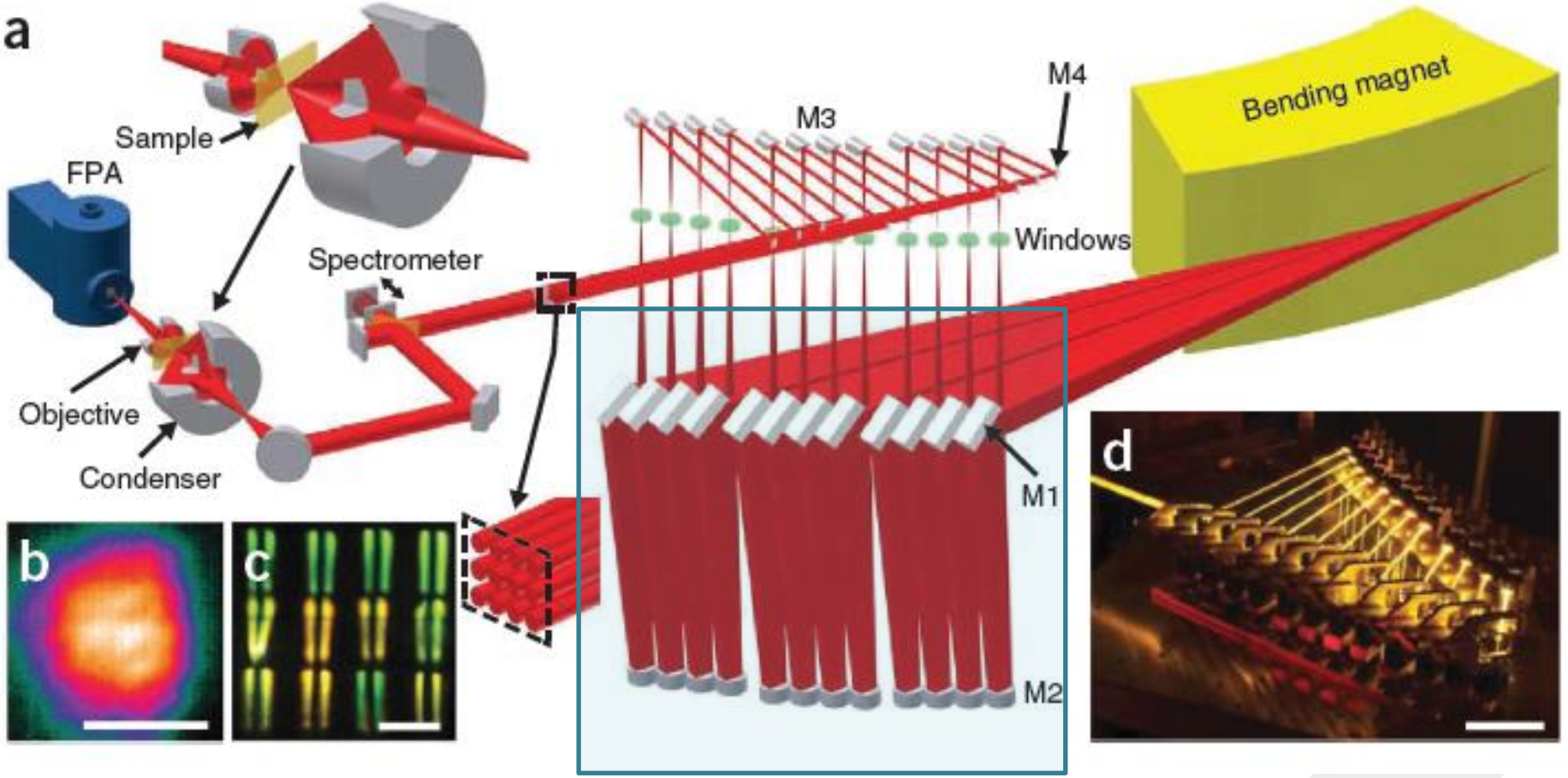

From M.J. Nasse *et al.*, *High-resolution Fourier-transform infrared chemical imaging with multiple synchrotron beams*, Nature Methods, 8:413 (2011)

Elettra
Sincrotrone
Trieste

From FTIR Microscopy to FTIR Imaging

FTIRI at U10 (NSLS, NewYork) with an external coupling box

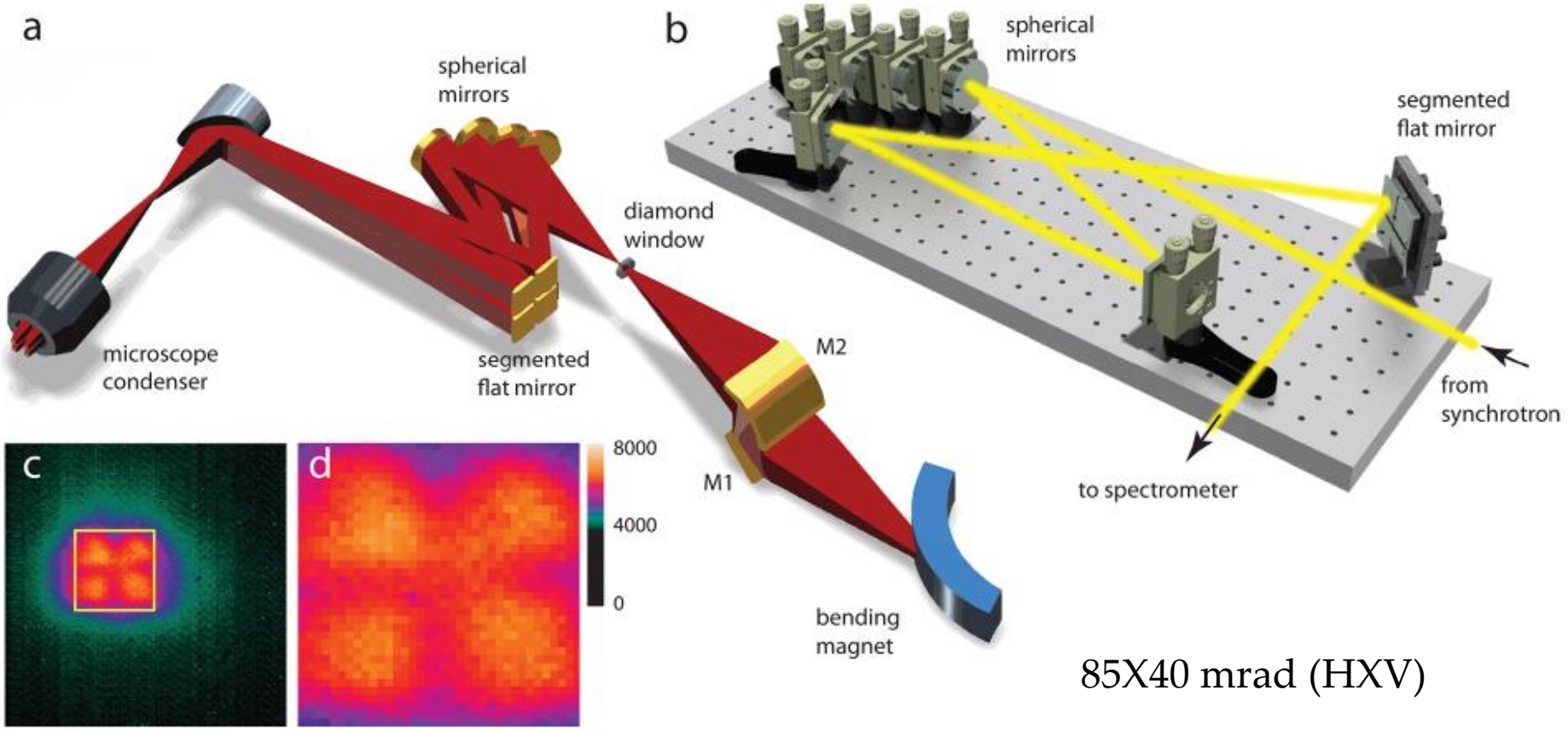

85X40 mrad (HXV)

From E. Stavitski et al., *Dynamic Full-Field Infrared Imaging with Multiple Synchrotron Beams*, Anal. Chem., 2013, 85 (7), pp 3599–3605

Elettra
Sincrotrone
Trieste

Potentialities of FTIR Imaging

- ~100 fold pixel area reduction (5μm → 0.5 μm) maintaining almost unaffected the spectral quality
- ~ 10 fold S/N gain
- ~ 10^2-10^3 data-acquisition time speeding
- Enhanced chemical contrast
- Improved sensitivity (in the femto-molar range)

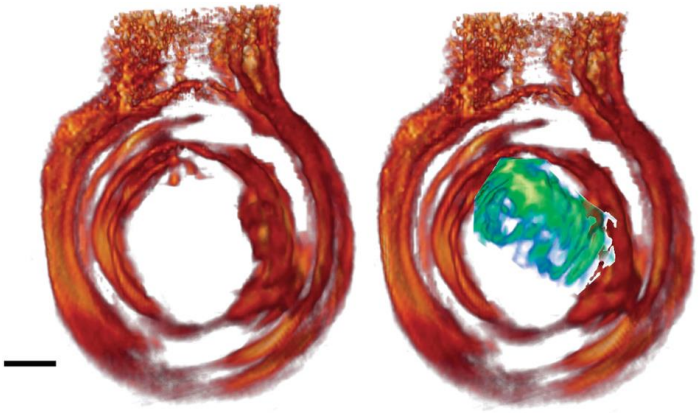

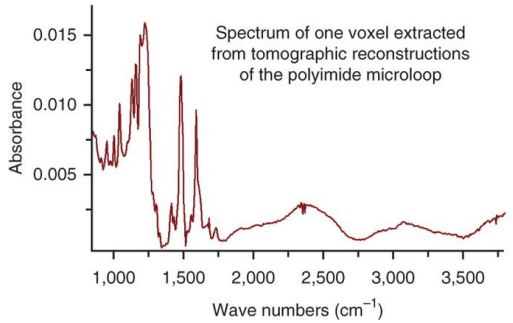

FTIR spectro-microtomography

From M. Martin et al., *3D spectral imaging with synchrotron Fourier transform infrared spectro-microtomography*, Nature Methods, 10: 861 (2013)

Elettra
Sincrotrone
Trieste

FTIR spectro-microtomography

From 2D

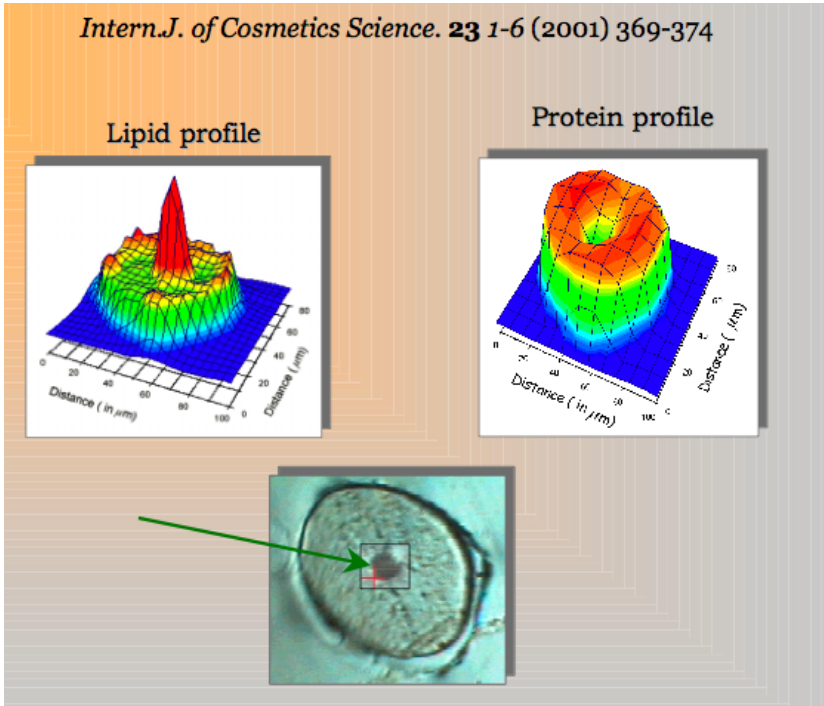

To 3D

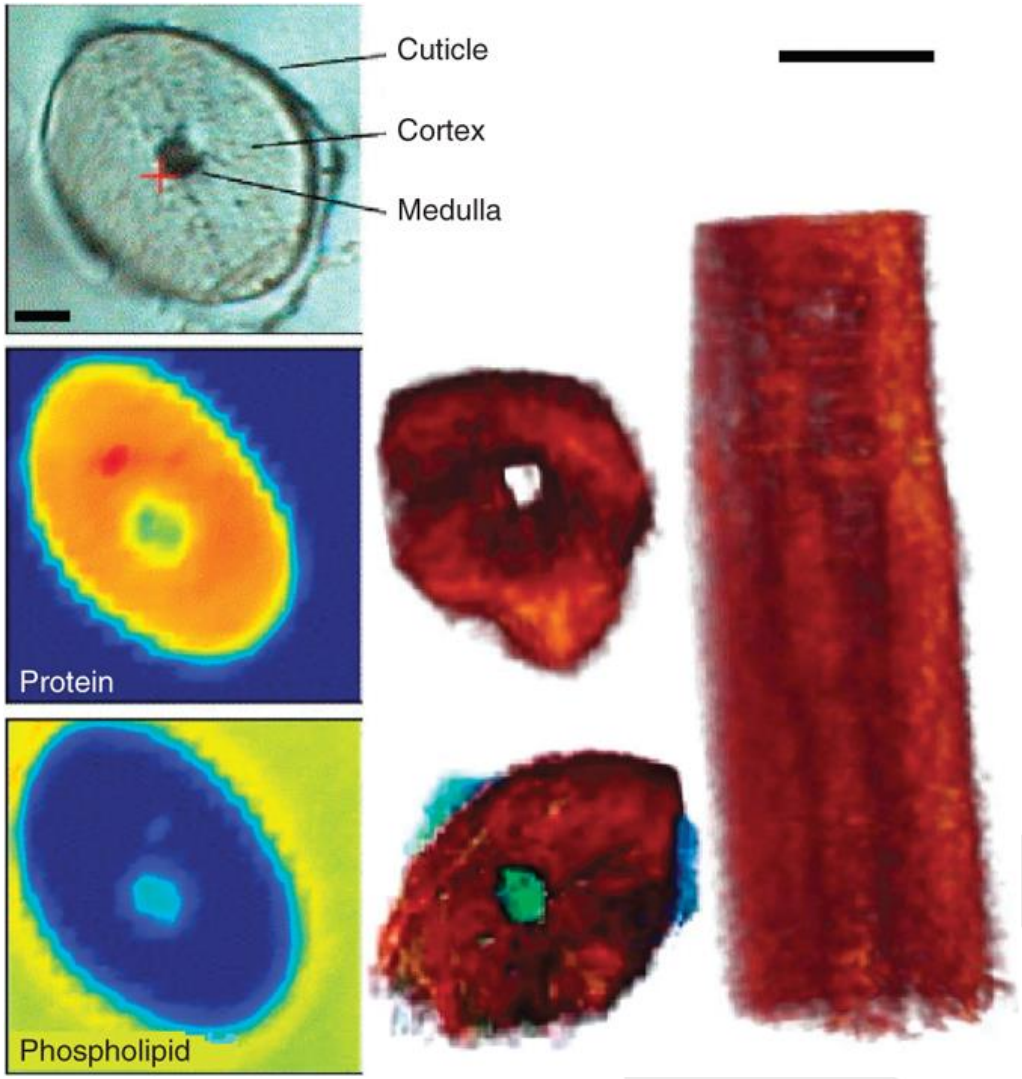

Elettra
Sincrotrone
Trieste

Vibrational characterization at the nanoscale

Understanding how natural systems are organized at the nanoscale and how this organization contributes to their function will improve human ability to interact with them and to build nano-organized synthetic platforms with improved functional efficiency

There is nowadays a large variety of tools for characterizing materials' morphology, structure and function at the nanoscale, while chemical composition analysis through far-field infrared microscopy yields information at a larger length scale

FUTURE of FTIR IS WHERE CHEMICAL SPECIATION MEETS MORPHOLOGICAL CHARACTERIZATION

Elettra Sincrotrone Trieste

Vibrational characterization at the nanoscale

Scattering-type Scanning Near-field Infrared Microscopy: s-SNIM

Fritz Keilmann and Rainer Hillenbrand

Optical oscillation modes of plasmon particles observed in direct space by phase-contrast near-field microscopy , Applied Physics B 73, 239 (2001)

Working principle

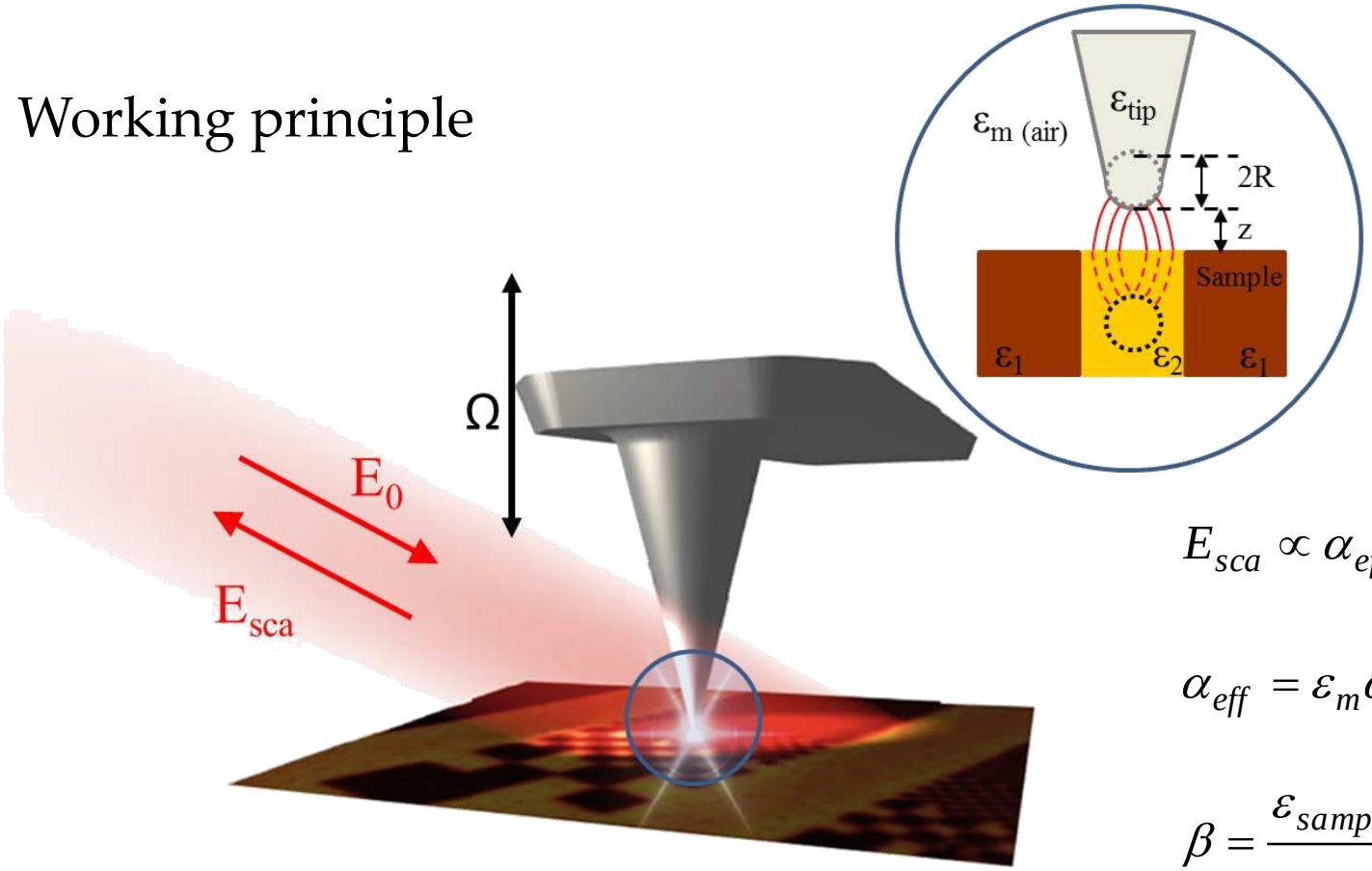

http://www.neaspec.com/products/near-field-illumination-units/

Lateral resolution

~

AFM tip radius

$$E_{sca} \propto \alpha_{eff} E_0 = s e^{i\varphi}$$

$$\alpha_{eff} = \varepsilon_m \alpha_{tip} (1+\beta)\left(1 - \frac{\alpha_{tip}\beta}{16\pi(z+R)^3}\right)^{-1}$$

$$\beta = \frac{\varepsilon_{sample} - 1\cdot\varepsilon_m}{\varepsilon_{sample} + 1\cdot\varepsilon_m}$$

Elettra Sincrotrone Trieste

Vibrational characterization at the nanoscale

Scattering-type Scanning Near-field Infrared Microscopy: s-SNIM

A sample affects the s-SNOM signal only through its dielectric value ε_s taken at the wavelength of illumination. This provides the basis to view s-SNOM as a nanospectroscopic tool, to measure the local dielectric function for identifying nanosystems according to their known (far-field) optical and infrared dielectric properties.

Working principle

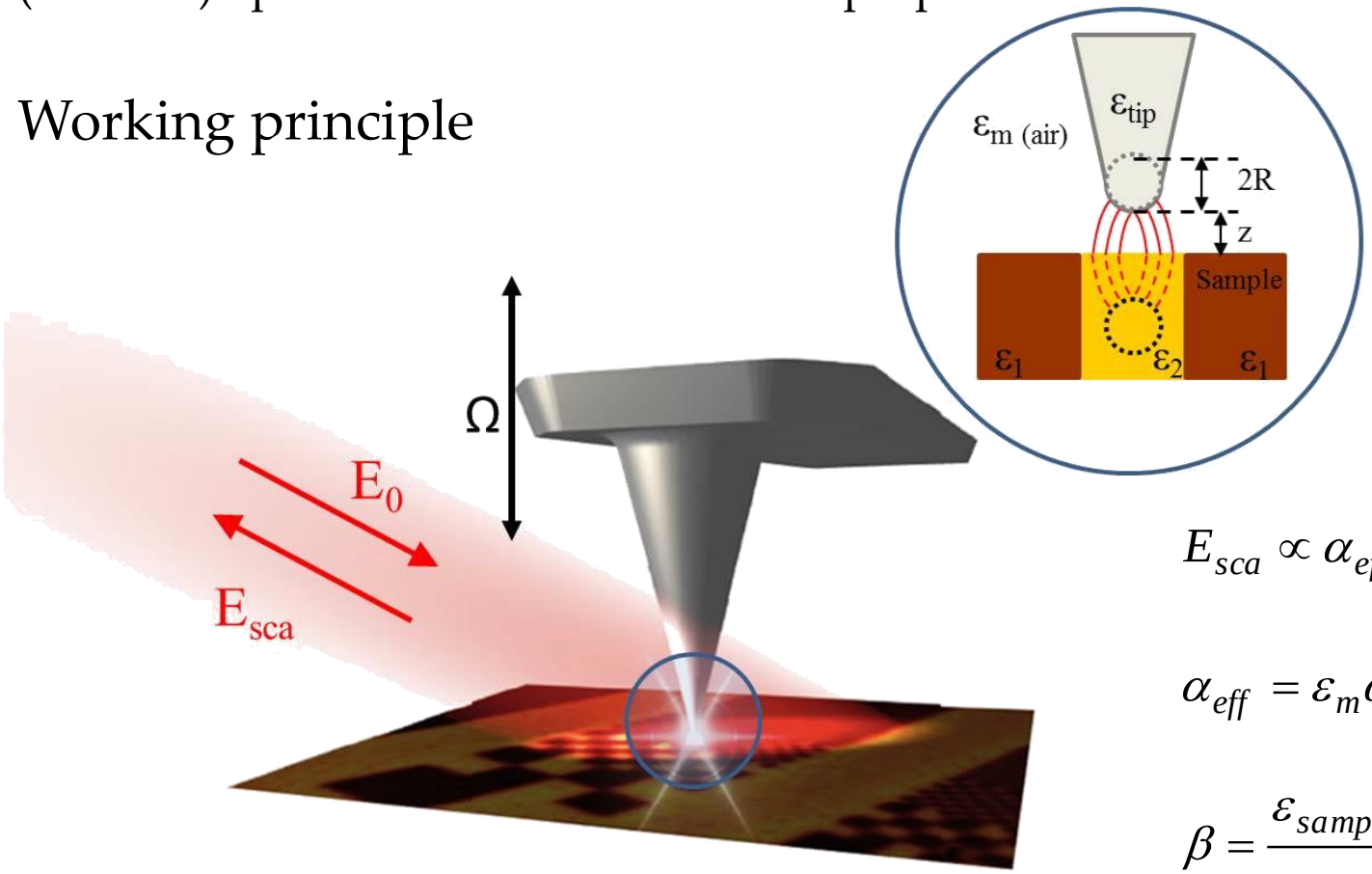

http://www.neaspec.com/products/near-field-illumination-units/

Lateral resolution ~ AFM tip radius

$$E_{sca} \propto \alpha_{eff} E_0 = s e^{i\varphi}$$

$$\alpha_{eff} = \varepsilon_m \alpha_{tip} (1+\beta)\left(1 - \frac{\alpha_{tip}\beta}{16\pi(z+R)^3}\right)^{-1}$$

$$\beta = \frac{\varepsilon_{sample} - 1\cdot\varepsilon_m}{\varepsilon_{sample} + 1\cdot\varepsilon_m}$$

Vibrational characterization at the nanoscale

$$E_{sca} \propto \alpha_{eff} E_0$$

$$\alpha_{eff} = se^{i\varphi}$$

Relative amplitude

Phase shift

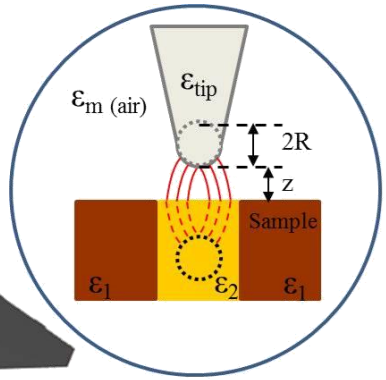

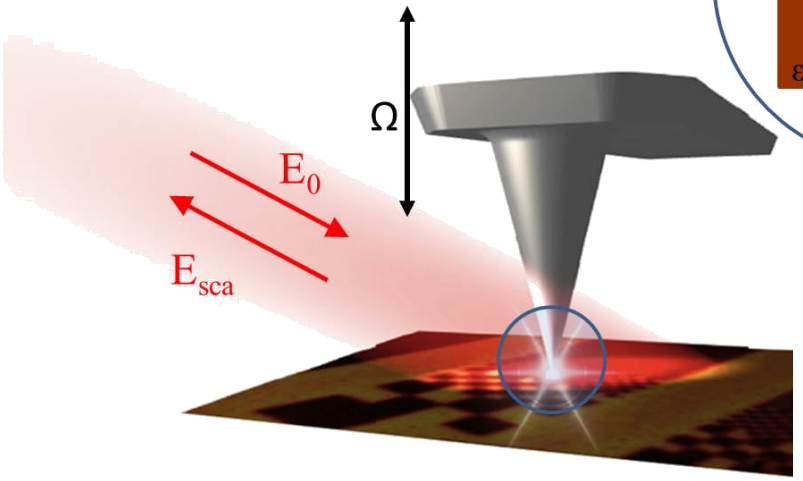

http://www.neaspec.com/products/near-field-illumination-units/

Wavelength 633 nm

Material Si: $\varepsilon_s = 15$

Tip Au: R=10 nm; $\varepsilon_s = -10+2i$

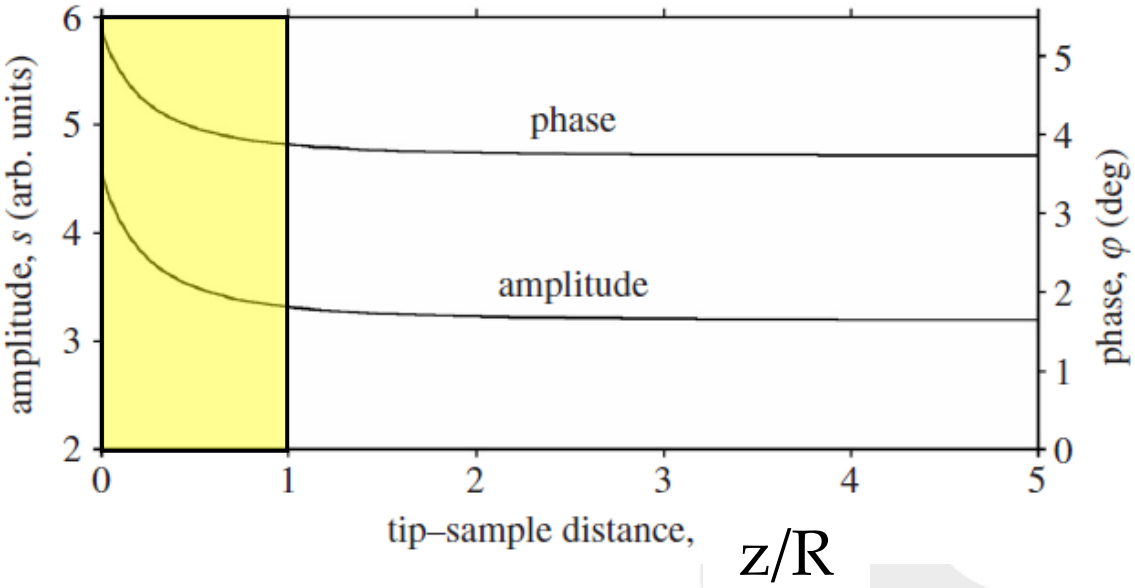

Elettra
Sincrotrone
Trieste

Vibrational characterization at the nanoscale

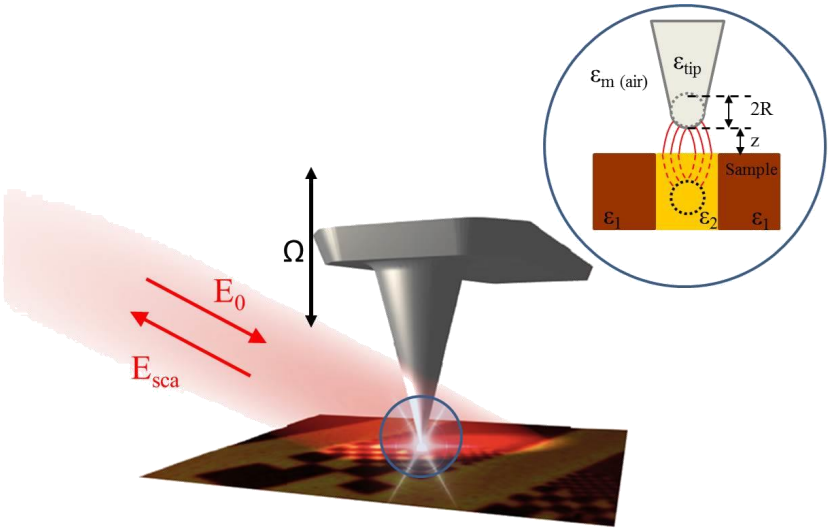

http://www.neaspec.com/products/near-field-illumination-units/

Measured signal
Background scattering + Near field scattering

Background scattering >> Near field scattering

Demodulation of the dectector signal at second of higher armonics of the oscillation frequency of the tip

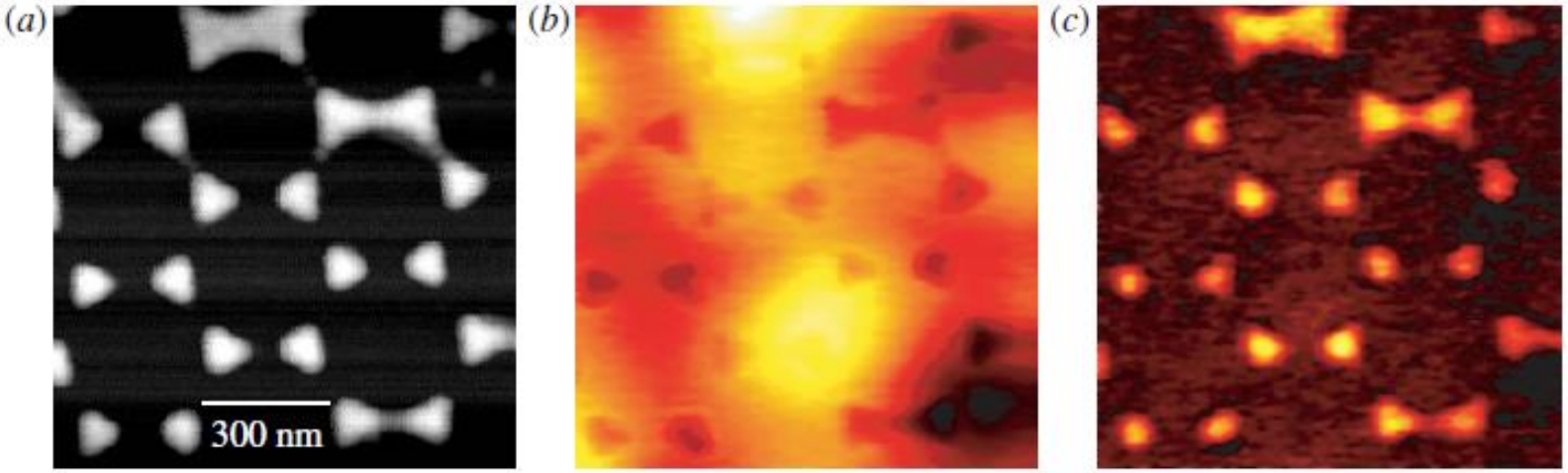

Figure 7. Experimental s-SNOM images of 20 nm high Au islands on Si. (*a*) Topography, (*b*) optical amplitude s_1 showing residual background scattering, and (*c*) optical amplitude s_3 showing pure near-field response.

Elettra Sincrotrone Trieste

Vibrational characterization at the nanoscale

From laser s-SNIM

Structural analysis and mapping of individual protein complexes by infrared nanospectroscopy resolution

Iban Amenabar et al., published in Nature Communications 4, Article number: 2890doi:10.1038/ncomms3890

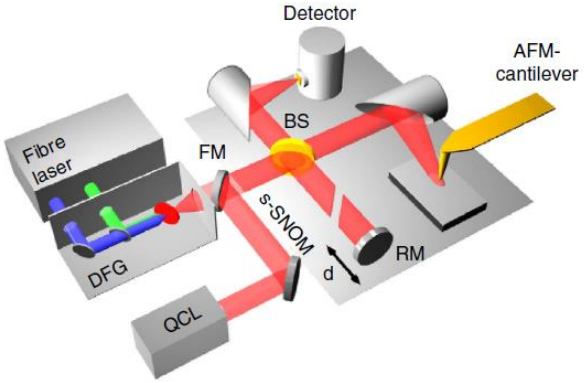

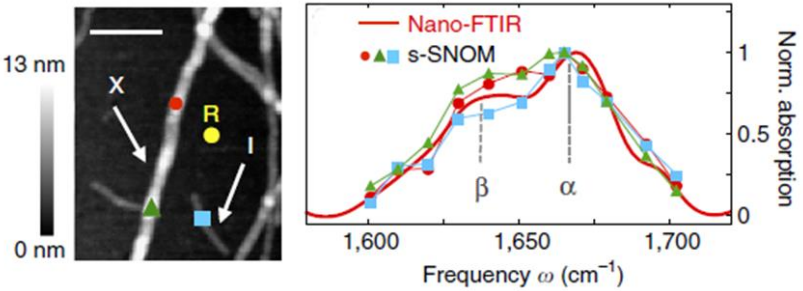

To broadband s-SNIM

Infrared-spectroscopic nanoimaging with a thermal source

F. Huth, M. Schnell, J. Wittborn, N. Ocelic & R. Hillenbrand, published in Nature Materials 10, 352–356 (2011)

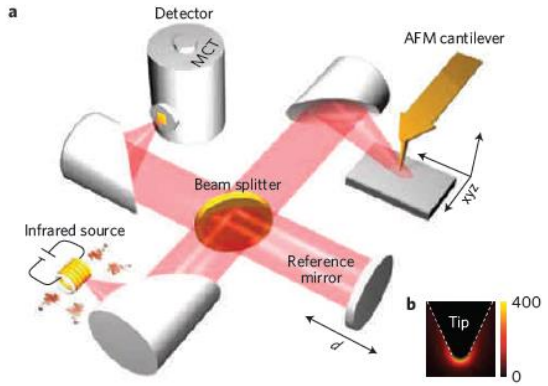

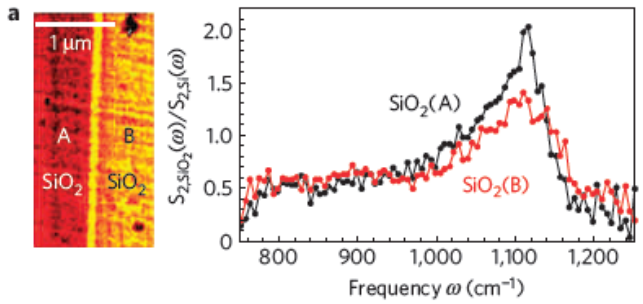

Broadband sources offer better spectral accuracy and more efficient data collection, improving recognition capabilities

Elettra Sincrotrone Trieste

Vibrational characterization at the nanoscale

From laser/conventional IR sources to IR-SR

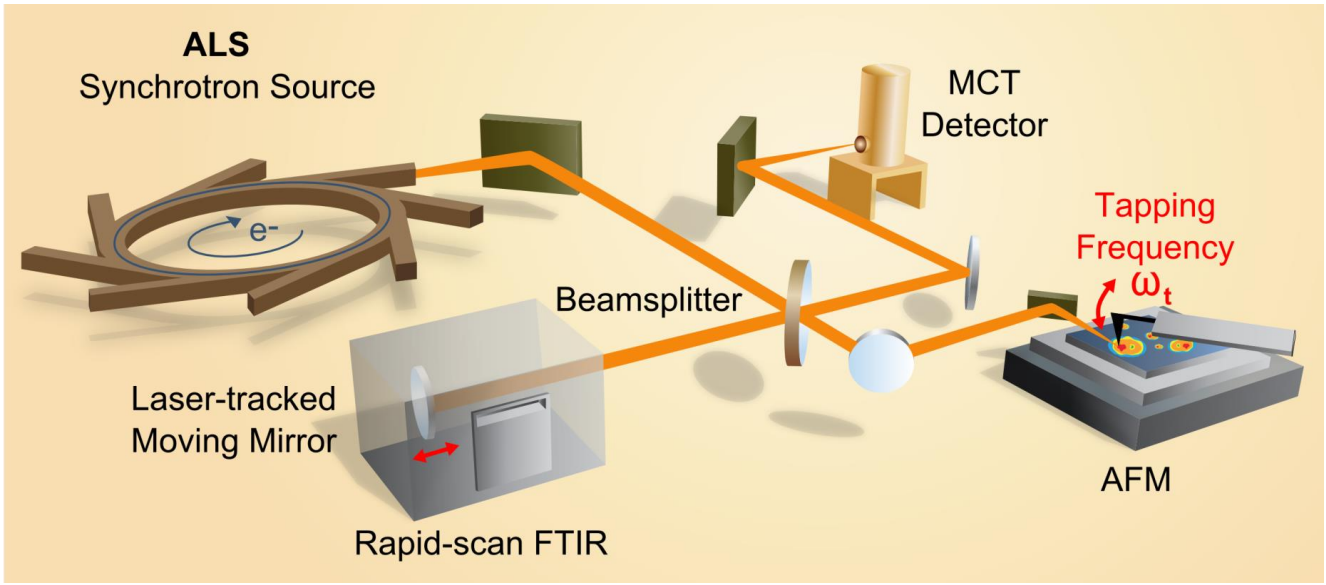

Hans A. Bechtel et al.,
Ultrabroadband infrared nanospectroscopic imaging
PNAS 111 (20) 7191-7196 (2014)

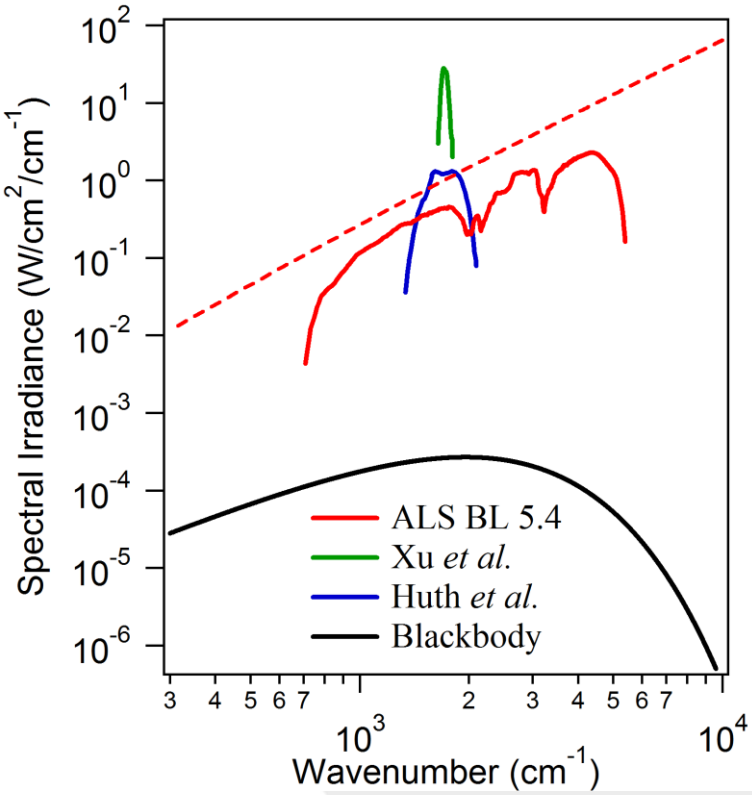

s-SNIM @ SR Facilities

- Advance Light Source
- ANKA
- Spring8
- Brazilian Synchrotron Light Laboratory
- Diamond

Elettra
Sincrotrone
Trieste

Structural characterization of functional proteins by ultrasensitive SR Collective Enhanced IR Absorption Microscopy (SR-CEIRA Microscopy)

Background

- FTIR spectroscopy is a very sensitive technique for the structural characterization of proteins in solution (natural environment)
  - It offers complementary information to CD, SAXS and NMR spectroscopy for proteins difficult to crystallize

Amide I deconvolution

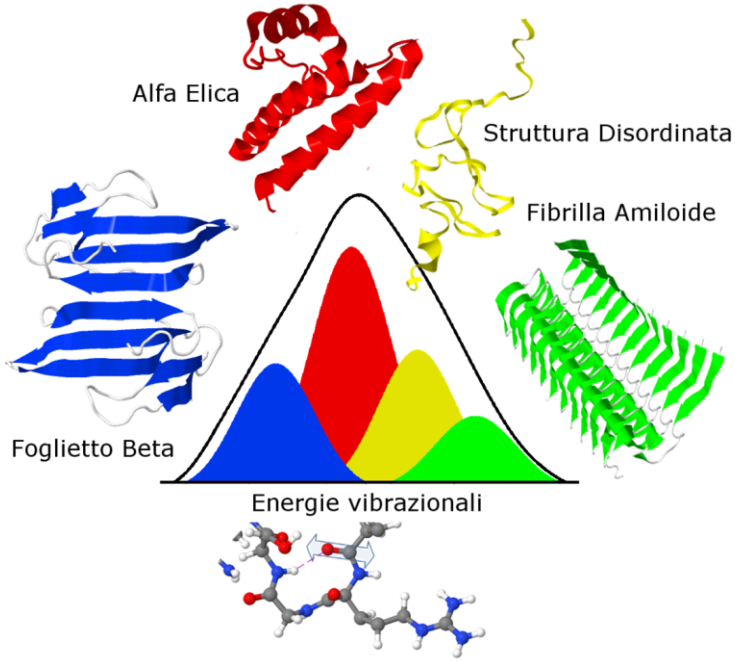

FTIR spectroscopy is sensitive to micromolar concentration at the best.

Elettra
Sincrotrone
Trieste

Structural characterization of functional proteins by ultrasensitive SR Collective Enhanced IR Absorption Microscopy (SR-CEIRA Microscopy)

Surface Enhanced IR Absorption spectroscopy (SEIRA) offers the possibility to defeat the sensitivity limits of FTIR spectroscopy

- SEIRA with randomly oriented substrates
  - Randomly oriented metallic substrate – E field enhancement up to 10-10^2
- SEIRA with single engineerized nanoantennas
  - Single metallic nanoantennas/nanogap - E field enhancement up to 10^3
- CEIRA with ordered arrays of nanoantennas - E field enhancement up to 10^4-10^5

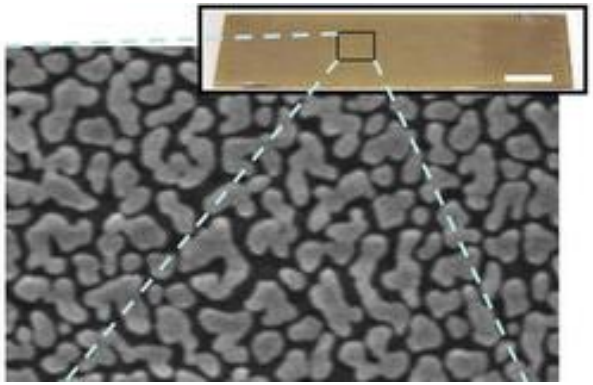

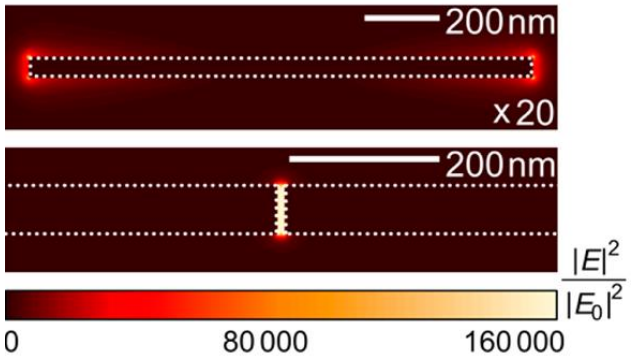

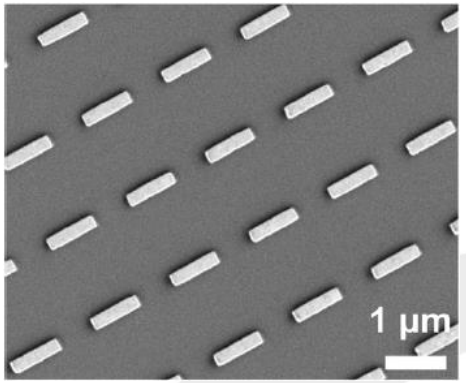

Elettra Sincrotrone Trieste

Structural characterization of functional proteins by ultrasensitive SR Collective Enhanced IR Absorption Microscopy (SR-CEIRA Microscopy)

The reasons for SR-CEIRA Microscopy

- **Increasing the intensity of the incoming electric field, the surface enhancement effect is maximized**

SR Brilliance

- **Not only Amide I band is interesting for structural characterization of proteins (despite largely used)**

SR broadband and Flexibility of fabrication approaches

ISTITUTO ITALIANO DI TECNOLOGIA

The project

Four spectral regions Regions Of Interest (ROIs) optimized for SR-CEIRA:
•Amide I (1695-1610 cm^{-1}) and Amide II (1590-1480 cm^{-1})
• Amide III band (~1350-1250 cm^{-1})
• Stretching modes of lateral aliphatic chains of aminoacids (3000-2800 cm^{-1})
•C-O-C and phosphate linkages, especially relevant for glyco- and phosphorilated-proteins), and (below 1200 cm^{-1})

Elettra Sincrotrone Trieste

Structural characterization of functional proteins by ultrasensitive SR Collective Enhanced IR Absorption Microscopy (SR-CEIRA Microscopy)

IRSR light polarized parallel to antennas

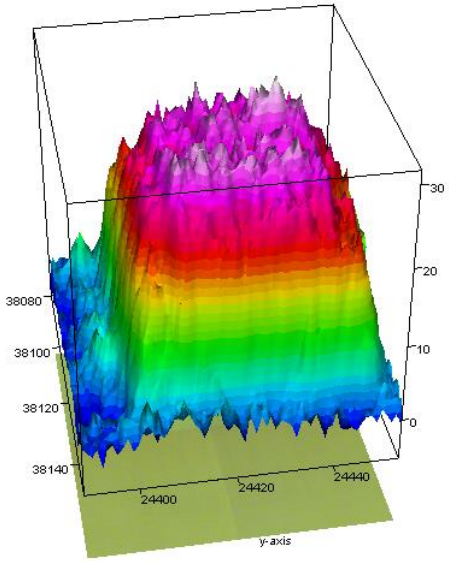

IRSR signal enhancement by CEIRA

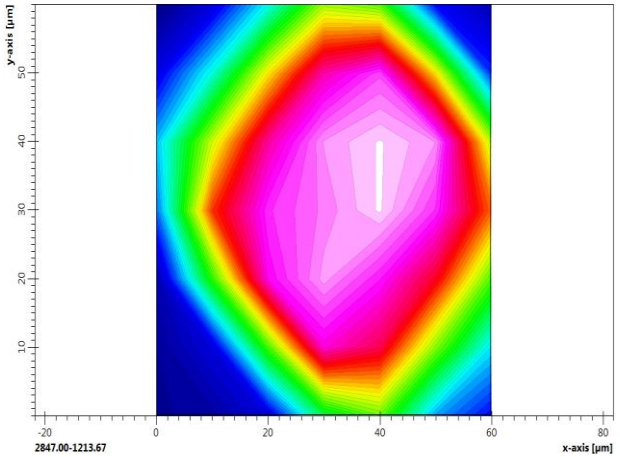

IRSR light polarized perpendicular to antennas

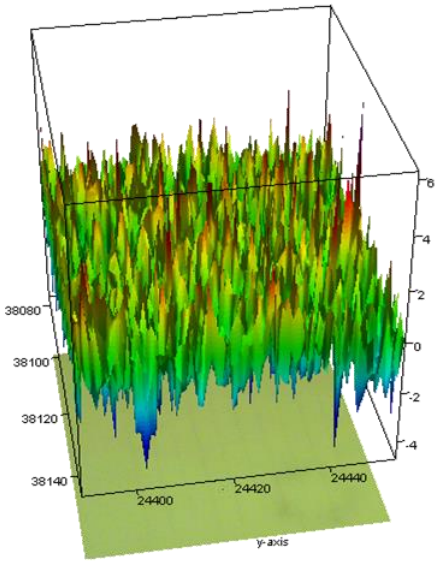

IRSR signal of a BSA monolayer enhanced by CEIRA

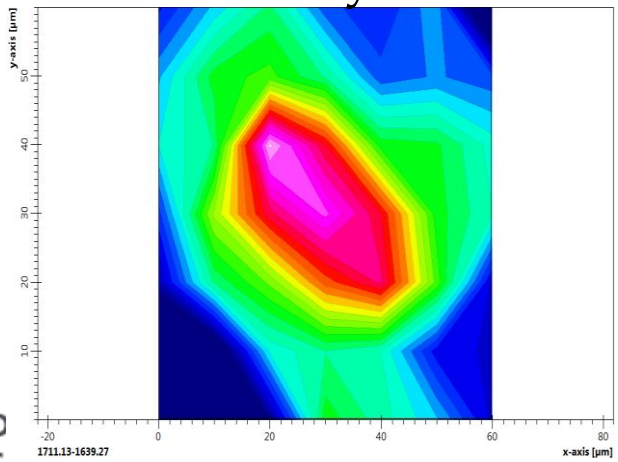

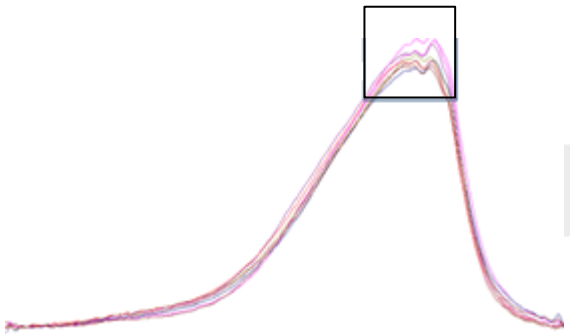

ISTITUTO ITALIANO DI TECNOLOGIA

www.elettra.eu